Zebrafish Modelling of Apoptosis and Inflammation in Aggressive B-cell Lymphoma

Ziyuan Chang

Doctor of Philosophy

The University of Edinburgh

2018

Acknowledgements

I would like to sincerely thank my principal supervisor Prof. Chris Gregory for his invaluable guidance, constant assistance and useful critique of my research work. Especially during my tough time, he gave me extra support and guidance without which this thesis would not be possible.

I am particularly grateful to my second supervisor, Dr. Yi Feng, for her continuous encouragement, insightful comments and constructive advice for this project as well as excellent technical teaching of zebrafish imaging. Much more than an excellent supervisor, she is also a dear and supporting friend.

I can barely find words to express my gratitude to Dr. John Pound who continues to be a valuable resource in guiding my project as it evolves. I truly appreciate his consistent attention, constant encouragement, reliable help, kind teaching and brilliant guidance.

Many thanks to Dr. Margaret Paterson for helping and teaching me in the separation and characterisation of EVs and taking care of my cells when I was on holiday. Special thanks to Dr. Catriona Ford for her instruction on western blotting; to Lynsey Melville for her help with immunohistochemistry; to Dr. Thomas Ramezani for instruction on gateway cloning.

I also wish to extend my warmest thanks to all the members in Inflammation and Cancer group, their precious friendship, encouragement and help make an amazing atmosphere.

And last, but not least, I would like to express my gratitude to my family and friends, for their unconditional love and support.

Statement of originality

I declare the work presented in this thesis has been performed by the candidate, Ziyuan Chang, unless stated otherwise. I declare that the text presented in this document is original and that no sources other than those mentioned in the text and its references have been used in creating it.

Neither this thesis nor the original work therein has been submitted for a degree.

Ziyuan Chang
(常子媛)

Abstract

Apoptosis is a well-orchestrated programmed cell death. In cancer biology the evasion of apoptosis has been considered as one of the key events for tumour development and paradoxically, studies also show that apoptosis has detrimental effects that may even promote cancer. High rates of apoptosis have been observed in many cancers and aggressive B cell lymphoma (prototypically Burkitt's lymphoma (BL)) present characteristic 'starry sky' appearance due to extensive apoptotic tumour cells engulfed by infiltrating tumour-associated macrophages (TAM). Previous work using a murine BL cell model has shown that constitutive apoptosis promotes both angiogenesis and the accumulation of pro-tumour TAMs. However, the detailed cellular and molecular mechanisms underlying how apoptosis fosters this pro-tumour growth microenvironment are still not fully understood, especially the role of apoptosis during early steps of tumour initiation. The aim of this project is to establish an *in vivo* model system to dissect the mechanisms as to how apoptotic B lymphoma cells enhance angiogenesis and how apoptotic B lymphoma cells interact with cells within the host microenvironment to promote tumour progression.

Zebrafish (*Danio Rerio*), a small tropical fresh water fish, has become increasingly popular as a biomedical research model organism. Not only is it amenable for genetic manipulation, but also due to its transparency in the larval stages, is one of the most important models for *in vivo* live imaging studies. Therefore efforts were made to establish a novel transgenic B lymphoma model in zebrafish. Complementary to the transgenic model, I also established a Xenograft model using a B lymphoma cell line BL2 and its apoptosis resistant derivative BL2-bcl2 cell lines.

Using a Tol2 based transgenesis system and zebrafish promoter for IgM heavy chain, I have generated transgenic zebrafish with either constitutive B cells expressing oncogenic cmyc, Tg (*IgM1::cmyc-eGFP*), or a tamoxifen

inducible version, Tg(*IgM1::CreERT2/IgM::lox-H2BmCherry-lox-cmyc-eGFP*) which allows induction of oncogenic *cmyc* expression in B-cells with precise temporal control. Unfortunately, neither of these models developed B cell lymphoma, and fish appear to be generally healthy. Although flow cytometic analysis showed normal expression of the transgene in Tg(*IgM::lox-H2BmCherry-lox-cmyc-eGFP*), further analysis of the constitutive model failed to detect any CMYC expressing eGFP positive B-cells in the head-kidney. Therefore, unexpectedly IgM driven cmyc expression in zebrafish might drive B-cell death instead of B-cell malignancy. This is in contrast to the mouse B lymphoma model.

More work is needed in choosing a suitable promoter and/or oncogene combination to generate a transgenic zebrafish B lymphoma model.

Xenograft models using zebrafish larvae provided an additional opportunity to study interaction between tumour cell and cells within the tumour microenvironment. Available transgenic reporter zebrafish strains labelling various cell lineages facilitate *in vivo* imaging of host cellular responses to B lymphoma cells. In order to identify putative roles that apoptotic tumour cells might play in the tumour microenvironment, I have established a reliable and consistent xenograft protocol to graft tumour cells into yolk sack of 2 days post fertilization (dpf) zebrafish larvae. Consistent with previous observations in mice, BL2 (an apoptotic prone lymphoma cell line) cells survive better than their apoptotic resistant derivative BL2-bcl2 (over-expressing bcl2 in BL2 cells). However, the overall longest survival time is no more than 4 days post grafting even with BL2 cells. A possible explanation for this could be lack of some key B cell survival factors in zebrafish larvae, as normally mature B cells do not develop until two weeks post fertilization. The mouse models of BL indicate that TAMs have been attracted by apoptotic BL cells and accumulate at the BL microenvironment. To evaluate whether macrophages modulated by apoptotic cells promote BL survival in the zebrafish model, human monocyte-derived macrophages were activated by either apoptotic

BL2 cells or IFN-γ / lipopolysaccharide (LPS) and co-injected with BL2 cells into zebrafish. Results showed that macrophages activated by apoptotic BL2 cells, but not IFN-γ /LPS, enhanced the survival of BL2 cells.

In the next part I further investigated how apoptotic BL2 cells might modulate macrophages and the tumour microenvironment. Extracellular vesicles (EVs) are small membrane-bounded vesicles whose molecular profile is regulated by their cellular origin and the types of stimuli. EVs have been shown to be critical messengers in tumor progression and metastasis. The study of apoptosis-induced EVs (Apo-EVs) is sparse. I hypothesised that EVs released by apoptotic cells might mediate their pro-tumourigenesis properties. I used a recently developed novel protocol in my laboratory to isolate Apo-EVs from BL2 cells. EVs from apoptosis resistant BL2-bcl2 cells (non-Apo-EVs) were used as a control. I show here for the first time that Apo-EVs are pro-angiogenic *in vivo*. Further analysis of the secretome from apoptotic BL2 cells as well as their Apo-EVs indicates that soluble protein component(s) mediate the pro-angiogenic function. Combining macrophage reporter fish Tg(*mpeg1::mCherry*) with TNFα reporter Tg(*tnfα::eGFP*), I show that Apo-EVs promote macrophage activation but not TNFα *in vivo*.

In conclusion, this project suggests that apoptotic tumour cells execute their pro-oncogenic functions by modulating macrophage activation, enhancing tumour angiogenesis, possibly through releasing Apo-EVs. Apo-EVs are recognized as a key player in fostering a pro-tumour growth microenvironment. Thus a further understanding of how apoptotic cells exert their tumour promoting roles will help us to optimise cancer therapy by maximizing tumour cell death while minimizing unwanted pro-tumorigenic effects. The models established during this project may be used to identify factors that are key to the survival and growth of B lymphoma.

Lay Abstract

Apoptosis is a form of cell suicide that was first described by Pathology Professor A.R.Currie in Aberdeen for tumour cells, but is now recognised to occur in normal cell development as well. In cancer where cell proliferation exceeds cell death causing the accumulation of transformed cells, it is considered to have a positive role for health. However, in several cancers, studies showed that apoptosis can promote tumour growth. For example, in Burkitt's lymphoma (BL), a type of aggressive B cell lymphoma, extensive apoptotic tumours are engulfed by macrophages (leukocytes that eat dead cells) and these apoptotic cells enhance tumour vessel growth. How these apoptotic tumour cells interact with macrophages and enhance tumour blood vessel growth are the main questions that this project is addressed to.

This project aimed to establish an in vivo animal system offering the opportunity to directly observe tumour growth events. A small tropical fresh water fish, zebrafish (*Danio Rerio*) was chosen due to its transparency in the larval stage and amenability for genetic manipulation.

I have generated genetically modified (GM) zebrafish whose B cells express a cancer gene called *cmyc* constitutively or temporally. Unfortunately, neither of these models developed B cell lymphoma, and fish appear to be generally healthy. These models indicated that other factors are needed to initiate B cell lymphoma as in the human.

I have also generated xenograft (foreign tissue grafts) by transplantation of human tumour cells into zebrafish. BL2 cells (an apoptotic prone lymphoma cell line) can survive better than their apoptosis-inhibited counterparts in zebrafish. However, BL2 cells cannot live longer than 4 days in zebrafish. To see what are the potential elements in the tumour that help tumour cell survive, macrophages, were co-injected with BL2 into zebrafish. Interestingly, macrophages that were co-cultured with apoptotic BL2 cells could help BL2 cells survive. As macrophages are highly plastic cells with a spectrum of

functional activities, apoptotic tumour cells seem to modulate them into a pro-tumour type. To see what are the other ways that apoptotic tumour cells modulate the tumour microenvironment, small membrane-bounded vesicles (EVs) released from apoptotic tumour cells were separated and injected into zebrafish and they showed an ability to promote tumour vessel growth. Furthermore, these apoptosis-induced EVs also showed an ability to modulate macrophages.

In conclusion, this project suggests that apoptotic tumour cells can modulate the tumour microenvironment to promote tumour growth by enhancing tumour vessel growth, changing macrophage function and they may achieve these by releasing EVs. A further understanding of apoptosis in cancer may help us to optimise anti-cancer therapy by maximizing tumour cell death while minimizing unwanted pro-tumorigenic effects

Table of Contents

List of abbreviation

ABC-like	activated B-cell like
AID	activation-induced cytidine deaminase
ANG-2	Angiopoietin-2
Apaf-1	apoptosis protease-activating factor-1
ATP	adenosine triphosphate
AV	axial vein
AxV	annexin V
BAI-1	brain-specific angiogenesis inhibitor 1
BCL-2	B-cell lymphoma-2
BCR	B-cell receptors
bFGF	basic FGF
BL	Burkitt's lymphoma
BMDMs	bone marrow-derived macrophages
CDK	cyclin-dependent kinase
CHT	caudal hematopoietic tissue
CML	chronic myeloid leukemia
COX-2	cycloxygenase-2
cryo-EM	cryo-electron microscopy
CSR	class switch recombination
CX3CR1	chemokine (CX3-C motif) receptor 1
DA	dorsal aorta
dATP	deoxyadenosine triphosphate
DISC	death-inducing signaling complex
DLBCL	Diffuse large B-cell lymphoma
dpf	days post-fertilization
DSBs	DNA double strand breaks
EBV	Epstein-Barr virus
ECM	extracellular matrix
eGFP	enhanced green fluorescent protein
Evs	extracellular vesicles
FACS	Fluorescence Activated Cell Sorting
FADD	Fas-associated death domain protein
FGF	fibroblast growth factor
fli1	friend leukemia integration 1 transcription factor
FLT1	VEGF receptor VEGFR1
Gas6	growth arrest-specific gene 6
GC	germinal centre
GCB-like	germinal centre B-cell like
GTPases	guanosine triphosphatases

H&E	haematoxylin and eosin
HGBL	High-grade B-cell lymphomas
Histone3	phosphor-histone-3
HIV	human immunodeficiency virus
hpf	hours post-fertilization
HSCs	hematopoietic stem cells
HUVEC	human umbilical vein endothelial cell
ICAD	Inhibitor of Caspase Activated DNAse
ICAM-3	intercellular adhesion molecule 3
ICM	intermediate cell mass
IFN-γ	interferon gamma
Ig	immunoglobulin
IgM1	major immunoglobulin M
IHC	Immunohistochemistry
IL-6	interleukin-6
IL-8	interleukin-8
LDL	low-density lipoprotein
LPC	lysophosphatidylcholine
LPS	lipopolysaccharide
Mab	monoclonal antibody
MAM	metastasis-associated macrophages
mfap4	microfibrillar-associated protein 4
MFG-E8	milk fat globule epidermal growth factor
miRNA	micro-RNAs
MMPs	metalloproteases
MOI	multiplicity of infection
MOMP	mitochondrial outer membrane permeabilisation
mpeg1	macrophage-expressed gene 1
mRNA	messenger RNA
MVs	microvesicles
NF-κB	nuclear factor of κB
NHEJ	non-homologous end joining
NOS	not otherwise specified
NTA	Nanoparticle Tracking Analysis
PDGF	platelet-derived growth factor
PFA	Paraformaldehyde
PGF	placenta growth factor
PI	propidium iodide
PMDM	peripheral monocyte derived macrophages
Pros S	Protein S
PS	phosphatidylserine

PTU	1-phenyl-2-thiourea
PVP40	Polyvinylpyrrolidone
RAG1	recombinase-activating genes 1
RAG2	recombinase-activating genes 2
RBI	rostral blood island
ROS	reactive oxygen species
RT	room temperature
S1P	Sphingosine-1-phosphate
SCL	stem cell leukemia
sHEL	soluble hen egg lysosyme
SHM	somatic hypermutation
SIV	sub-intestinal vessels
Stau	staurosporine
SYK	spleen tyrosine kinase
T-ALL	T cell acute lymphoblastic leukemia
TAMs	tumour-associated macrophages
TEM	transmission electron microscopy
TGF	transforming growth factor
TIM-4	T cell immunoglobulin mucin 4
TME	tumour microenvironment
TNF	tumour necrosis factor
TRAIL	tumour necrosis factor-related apoptosis-inducing ligand
Tulp-1	tubby-like protein 1
UTP	uridine triphosphate
UV	ultraviolet
VavP	Vav gene regulatory sequences
VEGF	vascular endothelial growth factor
WHO	World Health Organization Classification
YS	yolk sac

Chapter 1 Introduction

1.1 B cell lymphoma

1.1.1 General characteristics

About 20 new cases of lymphoma are diagnosed per 100,000 people every year in the western world and approximately 95% of them are of B- cell origin (Fisher and Fisher, 2004). Aggressive B cell lymphoma consists of precursor B-cell lymphoblastic leukaemia/lymphomas and peripheral B-cell lymphomas according the 4th edition of the World Health Organization Classification (WHO) of Haematopoietic and Lymphatic Tissues (Swerdlow et al., 2016).

Diffuse large B-cell lymphoma (DLBCL) forms the majority of peripheral B-cell lymphomas that also includes Blastic (blastoid/pleomorphic) mantle cell lymphoma, Burkitt's lymphoma (BL) and High-grade B-cell lymphomas (HGBL) (Ott, 2017). DLBCL, not otherwise specified (NOS) are mainly nodal tumours exhibiting diffuse infiltration by medium-sized to large lymphocytes and do not conform to a specific subtype and/or variant. They can be sub-categorised either by molecular subtype into germinal centre B-cell like (GCB-like) or activated B-cell like (ABC-like) or by morphology into centroblastic, immunoblastic and anaplastic (Alizadeh et al., 2000, Rosenwald et al., 2002).

BL is a highly aggressive mature B-cell neoplasm that makes up 40 % of non- Hodgkin lymphomas in individuals under the age of 20. It defines three clinical variants: endemic, sporadic, and human immunodeficiency virus (HIV)-associated type. The endemic form is normally associated with Epstein-Barr virus (EBV) infection and commonly affects young children in Africa (Molyneux et al., 2012). The sporadic type is less geographically defined and common in children between 3 and 12 years of age and about 30% of them are EBV-positive (Molyneux et al., 2012). Compared to the frequency in children and young adults, BL is rare in adults and mainly

associated with HIV (Aldoss et al., 2008). BL constitutes 1% to 2% of all non-HIV adult lymphomas in Western Europe and the United States and accounts for 30% to 40% of HIV-associated non-Hodgkin lymphomas (Jaffe ES, 2001, Gabarre et al., 2001). BL is characterised by high rates of proliferation and apoptosis. The phagocytosis of apoptotic cells by macrophages leads to a "starry sky" appearance of haematoxylin and eosin (H&E) staining of histological sections of BL (Ford et al., 2015).

The update of the WHO classification of 2016 introduced a new concept of HGBL to partly replace the previously so-called 'grey zone' lymphomas which show features intermediate between DLBCL and BL (Ott, 2017). HGBL comprises of two types: one harbours *myc* translocations and a *bcl2* and/or a *bcl6* rearrangement (HGBL Double Hit), the other lacks a double or triple hit constellation (HGBL, NOS) (Ott, 2017).

1.1.2 Mechanism and treatment

The common mechanisms underlying the pathogenesis of human B cell lymphoma include aberrant intracellular signalling, interrupted transcriptional and epigenetic regulation, and immune evasion (Ondrejka and Hsi, 2015, Shaffer et al., 2012).

The molecular mechanisms employed by B cells for antibody diversification during V(D)J recombination, somatic hypermutation (SHM) and class switch recombination (CSR) all involve programmed DNA damage and thereby makes them susceptible to chromosomal translocations and oncogenic mutations (Nussenzweig and Nussenzweig, 2010, Lieber, 2016).

Genomic translocations require DNA double strand breaks (DSBs) on separate chromosomes, proximity of broken ends and rearrangement between non-homologous chromosomes. DSBs during V(D)J recombination by recombinase-activating genes 1 and 2 (*rag1* and *rag2*) in developing lymphocytes allows random rearrangement of H and L chains to generate the

B-cell receptors (BCR) (Lieber et al., 2006). These DSBs are repaired by non-homologous end joining (Nussenzweig and Nussenzweig, 2010). In mature B cells, DSBs also occur during SHM and CSR inside the germinal centre (GC) in response to antigen encounter and they are initiated by the enzyme activation-induced cytidine deaminase (AID), a single strand DNA deaminase that mutates cytidine residues to uracyl (Di Noia and Neuberger, 2007, Chaudhuri et al., 2007). AID functions at S regions and leads to CSR which changes the Ig isotype involving the Ig C region only whereas at V regions causes SHM that is responsible for BCR diversity (Robbiani et al., 2008). In addition to non-homologous end joining (NHEJ), base-excision repair, mismatch repair and other mechanisms are necessary for accurate DSBs repair (Zhang et al., 2010). Dysregulation of repair pathways may facilitate B cell malignancy (Shaffer et al., 2002).

Most B cell lymphoma require BCR expression as for normal B cell development (Shaffer et al., 2012). The BCR is formed by two identical heavy chain and two identical light chain immunoglobulin (Ig) polypeptides that are covalently linked by disulphide bridges. The type of B cell lymphoma is closely related to its proposed normal B-cell counterpart. The specific structures of BCR at distinct stages can be used to indicate the cellular origin of B cell lymphomas and related studies showing that most types of B-cell lymphoma are derived from GC or post-GC B cells (Kuppers et al., 1999, Stevenson et al., 2001).

Chromosome translocation represents a hallmark of a plethora of aggressive B cell lymphomas (Kuppers and Dalla-Favera, 2001). Malignancy is caused by hijacking of normal B-cell signalling pathways to confer a survival or proliferative advantage. There are three main mechanisms through which this occurs.

Firstly, translocating *cis*-regulatory transcriptional elements to the neighbourhood of a proto-oncogene and induced enhanced expression of the

oncogene. In terms of B cell lymphoma, these translocations often involve Ig loci. A prototypical example is BL where the profound oncogenic role of *myc (*also known as *cmyc)* and its translocation was initially identified. BL result from the translocation of the *myc* proto-oncogene from 8q14 to immunoglobulin heavy-chain (Ig H) region (14q32) (80% of cases), or to the kappa light-chain gene (2p11) (15% of cases), or to the lambda-chain gene (22q11) leading to constitutive activation and subsequent accumulation of MYC (Hecht and Aster, 2000, Kuppers, 2005). The over-expression of MYC in BL is mainly caused by the translocation of *myc* that thereby deregulates and promotes cellular transformation through its effects on various cellular processes including proliferation, metabolism, differentiation and apoptosis. A small group (5–10% of phenotypically classical BL) may be fostered by deregulation of specific microRNA (Leucci et al., 2008). Deregulation of MYC is present in many other B cell cancers, such as plasmablastic lymphomas, multiple myeloma, rare mature B-cell lymphomas, transformed B-cell lymphomas and rare TdT-positive precursor B-cell lymphoblastic leukaemias/lymphomas. *Myc* translocation is also found in 5-10% of DLBCL and approximately 60% of these cases bear simultaneous rearrangements of *bcl2* or/and *bcl6* (Ott et al., 2013). GCB-type and ABC-type DLBCL present different incidences of *myc* rearrangement. Rearrangement of *myc* is present in up to 50% of grey zone' lymphomas (Ott et al., 2013). Secondly, the oncogenic activity is initiated by the expression of a chimeric protein produced by the fusion of two genes. For example, the *bcr-abl* fusion gene encodes a protein with deregulated kinase activity that has been detected in chronic myeloid leukaemia (CML) (Shaffer et al., 2012). Thirdly, chromosomal translocations can also cause structural and functional alterations in microRNAs that has been found in many cancers (Calin and Croce, 2007, Robbiani et al., 2009).

Other transforming mechanisms, such as the anti-apoptotic nuclear factor of κB (NF-κB) pathway, *ras* signalling pathways, BCR-derived survival signalling, oncogenic mutations in *myd88* are also involved in B cell

malignancy and perhaps the constitutive activation of the NF-κB signalling lies at the centre of these converged pathways by which B cell malignancies escape cell death (Kuppers, 2005, Gaidano et al., 1991, Martin-Subero et al., 2002, Dierlamm et al., 1999, Shaffer et al., 2012). NF-κB is a family of transcription factors that are formed by homo- and hetero-dimerization of the subunits p65 (encoded by *rela*), RelB, c-Rel, p50 (encoded by *nfkb1*), and p52 (encoded by *nfkb2*). NF-κB pathways can be activated by either classical or alternative mechanisms to initiate an anti-apoptotic transcriptional module, including the BCL2 family members BCL-XL and A1, c-FLIP, c-IAP1, c-IAP2, and other molecules (Grumont et al., 1999, Grumont et al., 1998, Gyrd-Hansen et al., 2008, Gyrd-Hansen and Meier, 2010). The activation of NF-κB pathway and constitutive expression of various NF-κB target genes is a hallmark of ABC-like DLBCL (Davis et al., 2001).

Certain viruses may also be related to B cell transformation. EBV has been found in 40% of cases of classical Hodgkin's lymphoma and almost all endemic BL (Young and Rickinson, 2004). Herpes virus 8, a member of the herpes-virus family, is associated with the pathogenesis of primary effusion lymphomas (Cannon and Cesarman, 2000).

Treatment of B cell lymphoma depends on the type and clinical stage of cancer. Currently, Rituximab, a chimaeric monoclonal antibody (MAb) for CD20, chemotherapy, and radiation have been widely used for the treatment of B cell lymphoma (Dotan et al., 2010). Combination of cyclophosphamide, doxorubicin, vincristine, and prednisone with Rituximab significantly improves the outcome for some patients (Hiddemann et al., 2005).

1.1.3 Transgenic murine models of B cell lymphoma

As reciprocal chromosomal translocations of the immunoglobulin loci and a proto-oncogene is a hallmark of many types of aggressive B cell lymphoma, murine transgenic models of B cell lymphoma are established by the strategy

of translocation of the oncogene to a site downstream of a B-cell specific enhancer or promoter region (Kuppers and Dalla-Favera, 2001).

Brief introduction of myc and its roles in cancer

Cmyc (also called *myc* here) belongs to a family of encoding transcription factors, which also includes *nmyc* and *lmyc* genes. These three genes are expressed differently during development and among them *myc* has drawn intense interest (Meyer and Penn, 2008, Zimmerman and Alt, 1990, Brodeur et al., 1984).

By binding the carboxy-terminal basic-helix–loop–helix–zipper domain of MAX, the formation of MYC–MAX heterodimers activates many genes through binding enhancer box sequence of 5′-CACGTG-3′which is a universal occurring DNA-binding motif in the human genome (Luscher, 2001). Recent data also demonstrate that MYC–MAX heterodimers may also suppress gene expression (Staller et al., 2001, Herold et al., 2002). It is widely accepted that *myc* activity mainly relies on the deregulated and constitutive activation of its various target genes through its regulation of transcription. The wide array of transcriptional targets of *myc* indicates its complicated and broad biological functions.

Myc has revealed its role in various cellular outcomes including modulating the cell cycle and differentiation (for example, active MYC promotes G0/G1 to S phase progression, regulates the function of cyclin-dependent kinase (CDK) inhibitors), promotes cell growth (increase cell metabolism and protein synthesis), increases genomic instability (gene amplification, chromosomal instability) (Roussel et al., 1991, Oster et al., 2002, Facchini and Penn, 1998, de Alboran et al., 2001, Trumpp et al., 2001, Obaya et al., 1999, Li and Dang, 1999, Schmidt, 2004, Felsher and Bishop, 1999b). Since the late 1990s, *myc* has been found to promote angiogenesis (Ngo et al., 2000, Dews et al., 2006, Watnick et al., 2013, Soucek et al., 2007).

In 1992, Gerard Evan and his colleagues revealed an intriguing finding that despite its well-known role in cell proliferation, *myc* induces substantial apoptosis in Rat-1 fibroblasts (Evan et al., 1992). Since then, several studies demonstrate that the over-expression of MYC can sensitise cells to undergo apoptosis (Pelengaris et al., 2002a, Pelengaris et al., 2002b, Shi et al., 1992, Meyer et al., 2006). Direct evidence for the crucial role of *myc* in apoptosis was that *myc* -null cells are resistant to many apoptotic stimuli (Soucie et al., 2001).

There is also indirect evidence that apoptosis suppresses the role of *myc* by revealing the close collaboration between *myc* and pathways underlying apoptosis. For example, over-expression of anti-apoptotic proteins such as BCL2 or BCL-XL, or loss of the tumour suppressors ARF or p53 have shown strong correlation with *myc* in several mouse models (Strasser et al., 1990, Adams et al., 1985, Blyth et al., 1995, Elson et al., 1995, Jacobs et al., 1999, Eischen et al., 1999). The possible mechanisms underlying *myc* induced apoptosis include the direct regulation of cell cycle and indirect actions caused by DNA damage. Specifically, *myc* activates the pro-apoptotic molecule BAX by either direct chromatin remodelling of BAX or through activation of the p53 via ARF, leading to transcription of BAX. In an *in vitro* setting, MYC seems to accumulate reactive oxygen species (ROS) via E2F1-mediated inhibition of NF-κB and whether the cell commits to apoptosis or growth arrest is likely to depend on the cell type (Tanaka et al., 2002, Vafa et al., 2002). Apparently, the interactions that are associated with MYC and apoptosis are complex and depend on the cell type as well as the tissue location and the involvement of additional mutations in other pro- and anti-apoptotic genes.

A very recent study shows that MYC is a key regulator of the proliferation program of T and B lymphocytes (Heinzel et al., 2017). Heinzel et al. reveal that MYC expression is tightly controlled by the signals received

quantitatively, which controls the extent of lymphocyte proliferation, at least in this mouse system *in vitro*.

In terms of tumour biology, deregulated MYC expression is usually associated with aggressive, poorly differentiated tumours as well as poor prognosis. Many studies illustrate the pervasive role of *myc* in the genesis of tumours. Several transgenic mouse models demonstrate that deregulated expression of MYC is sufficient to initiate tumourigenesis (Adams et al., 1985, Morton and Sansom, 2013). However, in each of these models, the time delay before the onset of tumours and the accelerated rates of tumour formation with the existence of other genetic alterations indicates that other co-operative mutagenic alterations are required to enable tumour formation. The transgenic mice bearing both abnormal *myc* and *bcl2* carry higher potential for lymphomagenesis compared with mice with ectopic MYC expression only (Strasser et al., 1990, Adams et al., 1985). Mouse models also show that *myc* acts in synergy with *p53* and *arf* to enhance lymphomagenesis (Blyth et al., 1995, Elson et al., 1995, Tago et al., 2015). The exact mechanisms underlying these are still unknown and the most plausible explanation is that MYC induced apoptosis is inhibited.

In inducible transgenic models where mice have ectopic MYC expression in a spatio-temporal manner tumours in T cells, B cells, liver and bone can be regulated and indicate the importance of *myc* in tumour maintenance (Felsher and Bishop, 1999a, Morton and Sansom, 2013).

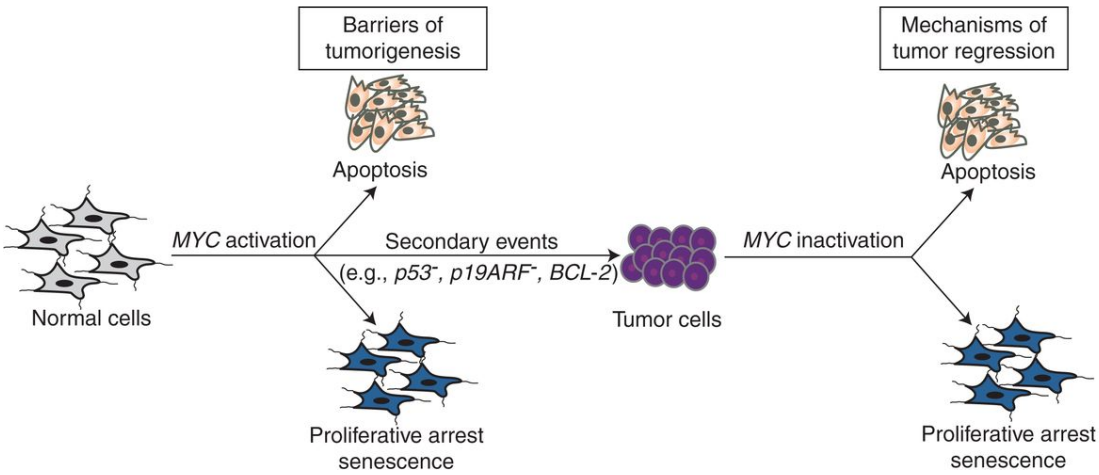

Figure 1.1 *Myc*-induced tumour initiation and maintenance

Myc induces tumourigenesis by orchestrating with several tumor-suppressing checkpoint mechanisms, including proliferative arrest, apoptosis, and/or senescence. The suppression of MYC was shown to sustain tumour regression (adopted from (Gabay et al., 2014)).

In addition to cell-autonomous function underling *myc* oncogenesis, *myc* may also regulate immune surveillance pathways to foster tumourigenesis (Gabay et al., 2014, Grivennikov et al., 2010, Rooney et al., 1985). MYC suppression provokes tumour regression with reduced kinetics in an immunocompromised RAG1-/- host (deficient for B and T cells) or a CD4-/- host (deficient for CD4+ T-helper cells) (Rakhra et al., 2010).

Mouse B cell lymphoma models

Due to the evident critical roles of *myc* in B cell lymphoma, there are several transgenic murine models mimicking human B cell lymphoma by manipulating *myc*.

In the Eμ- *myc* model, generated by linking the *myc* gene to the Igh enhancer (Eμ), two principal tumour phenotypes develop, one resembling BL which arises during an early time window and another form resembling DLBCL which develops after day 400 (Kitaguchi et al., 2009, Sander et al., 2012, Adams et al., 1985). Introducing retroviruses expressing the *ras* oncogene into this model leads to an accelerated lymphomagenesis (Kitaguchi et al.,

2009). By crossing the Eμ-*myc* mice with transgenic mice bearing a BCR specific for hen egg lysozyme, the BCR was shown to cooperate with the over-expression of MYC to produce more aggressive lymphomas of mature B cell origin in the Eμ-*myc* /BCR^{HEL} mice (Junttila and de Sauvage, 2013). This supports the notion that BCR-derived survival signaling can facilitate the evolution of B cell lymphoma.

The introduction of a transgene encoding soluble hen egg lysosyme (sHEL) in Eμ-*myc*/BCR^{HEL} mouse leads to development of more aggressive tumors composed of activated mature post–GC–like B cells, closely resembling BL. The disruption of BCR signaling in both Eμ-*myc*/BCR^{HEL} mouse and Eμ-*myc*/BCR^{HEL}/sHEL mice indicates the importance of BCR expression for tumour maintenance and development (Young et al., 2009). One of the BCR-derived signal effectors is spleen tyrosine kinase (SYK), a non-receptor tyrosine kinase. Activation of SYK can support cell survival and proliferation by pathways involving the cooperation of NF-κB, PI3K, NF-AT, MAP kinase, and RAS signaling (Rowley et al., 1995, Dal Porto et al., 2004). SYK exhibited a role for survival of non-Hodgkin lymphoma-like tumours in the Eμ-*myc*/BCR^{HEL}/sHEL mouse and suggests it to be an attractive therapeutic target (Carter et al., 2018).

Although human follicular lymphomas over-express the anti-apoptotic oncogene *bcl2* by chromosomal translocation of *bcl2* under the control of Ig H, transgenic mice (Eμ-*bcl2*) expressing BCL2 by Eμ do not develop follicular lymphoma. VavP-*bcl2* mice bearing a *bcl2* transgene controlled by *Vav* gene regulatory sequences (VavP), engineered to over-express BCL2 in cells of all hematopoietic lineages develop follicular lymphoma when mice are older than 10 months and this may be promoted by the prolonged GC reactions dependent on CD4 T-cell help (Egle et al., 2004).

More recent studies have indicated that at least two pathways-MYC and PI3K-are required to establish the full BL phenotype and next generation

sequencing results reveal mutations in *tcf3* or *id3* genes which are crucial in the PI3K pathway (Sander et al., 2012, Davis et al., 2001, Rowley et al., 1995).

Other mechanisms underlying the cell proliferation also show oncogenic potential. For example, transgenic mice (Eμ-*brd2*) with lymphoid-restricted overexpression of a nuclear-localized transcription factor kinase, double bromodomain protein bromodomain-containing 2 (BRD2) develop splenic B-cell lymphoma (Greenwald et al., 2004). Constitutive expression of BRD2 increases cell proliferation through the transcription of *cyclin A* (Greenwald et al., 2004).

1.2 Tumour microenvironment

It is widely accepted that a tumour, rather than being a collection of homogeneous deviant cells, is actually a community comprising malignant cells together with stromal components including macrophages, fibroblasts, epithelial cells, endothelial cells (both blood and lymphatic), neutrophils, T cells, B cells and mast cells (Hanahan and Weinberg, 2000).

The interactions among these cells including tumour cell-stromal cells and stromal cells-stromal cells provide a tumour microenvironment (TME) to favour tumour growth. The concept that TME is evolving with the cancer cell and both continuously participate in the process of tumourigenesis is now acknowledged. The presence of infiltrating immune cells, angiogenic endothelial cells, cancer-associated fibroblasts, as well as a variety of cytokines, chemokines, growth factors, and proteinases is crucial for tumour cell proliferation, invasion and metastasis. The TEM is also involved in cancer recurrence and resistance to chemotherapy (Junttila and de Sauvage, 2013).

Among these cancer-promoting stromal elements, the macrophages are an intensively studied candidate and the relatively newly emerging candidate, the extracellular vesicles (EVs) will be discussed in detail (Carter et al., 2018).

1.2.1 Macrophages

Macrophages are professional phagocytes and are widely present in cancers. The accumulation of macrophages is achieved by monocyte recruitment as well as tissue macrophage proliferation (Jenkins et al., 2011, Mantovani et al., 2011, Hashimoto et al., 2013). Recent studies show that the resident macrophages emanated from yolk sac-derived progenitors and the macrophages responsible for the pathogenesis seem to arise from circulating bone marrow derived monocytes (Lavin et al., 2015, Noy and Pollard, 2014).

The phenotypic plasticity of macrophages allows them to execute various functions by acquiring a spectrum of phenotypes depending on environmental signals (Lewis and Pollard, 2006, Hanahan and Coussens, 2012, Sica et al., 2008, Mosser and Edwards, 2008, Qian and Pollard, 2010).

A relatively large body of work has even devoted to understanding the exact mechanisms of macrophage activation and polarisation and remains to be fully understood. Traditionally macrophages could be classified as either classically activated, also known as M1, or alternatively activated, M2. According to established definitions, the M1 activation state is induced by interferon gamma (IFN-γ) and lipopolysaccharide (LPS) stimulation, and M2 is activated by IL-4 and IL-13 (Mantovani et al., 2002). M1 classically activated macrophages express high levels of IL12 and IL23 and exert pro-inflammatory, anti-proliferative and cytotoxic functions by producing effector molecules, such as ROS/RNS and inflammatory cytokines, participating as inducers and effector cells in Th1 responses. The M2 macrophages express high levels of IL10 and scavenger receptors, such as CD163 and CD 206. They clear debris, promote wound healing, angiogenesis, tissue remodelling and repair (Kreider et al., 2007, Mantovani et al., 2002). However, the

macrophage M1 and M2 phenotype classification is an oversimplification and does not accurately represent the full spectrum of macrophages activation states.

The term, tumour-associated macrophages (TAMs), describes the macrophages that accumulate in both primary and secondary tumours. They are activated by signals such as lymphotactin, IL10 and antibodies in the TME and normally resemble alternatively activated macrophages (Sica et al., 2008, Wynn et al., 2013). High infiltration of TAMs has been associated with poor prognosis in over 80% of human tumours, with the notable exception of colorectal adenocarcinoma (Tsutsui et al., 2005, Cavnar et al., 2017)

As an abundant component of solid and haematological tumours, TAMs are thought to contribute to tumour growth at various stages including angiogenesis, invasion and metastasis by promoting an anti-inflammatory, immune-suppression, pro-tumourigenesis microenvironment (Martinez et al., 2009, Qian and Pollard, 2010, Cook and Hagemann, 2013, Hanahan and Coussens, 2012). Indeed, many clinical observations and macrophage depletion experiments in animal models have shown the trophic role of TAM in tumour angiogenesis.

Angiogenesis is the process of blood vessel formation from existing vessels which is distinguished from the process called vasculogenesis defining the de novo formation of vessels dependent on angioblasts (Carmeliet and Jain, 2000). Angiogenesis is tightly regulated by several signalling molecules such as vascular endothelial growth factor (VEGF), fibroblast growth factor (FGF), basic FGF (bFGF), platelet-derived growth factor (PDGF), placenta growth factor (PGF), transforming growth factor (TGF)-α, TGF-β, hepatocyte growth factor or scatter factor (HGF or SF), tumour necrosis factor-α (TNFα), angiogenin, interleukin-8 (IL-8), as well as angiopoietins (Gacche and Meshram, 2014, Yancopoulos et al., 2000). The receptors on endothelial cells sense the correspondent molecules and start the angiogenic process

involving sprouting, branching, artery and vein differentiation and lumen formation (Ferrara et al., 2003). There are two potential mechanisms underlying angiogenic vessel formation: sprouting and intussusceptive angiogenesis. Sprouting angiogenesis is the predominant mechanism and has been well described. This starts with the migration of endothelial cells at the leading edge, named 'tip' cells, with the help of metalloproteases (MMPs) degrading of surrounding extracellular matrix (ECM). It is followed by the extension of filopodia which lead to the duplication of 'stalk' cells to create the lumen of the forming vessel (Gerhardt et al., 2003). Intussusceptive angiogenesis, firstly introduced by Caduff et al., in 1986 and then renamed by Burri and Tarek in 1990, is a rare alternative form of angiogenesis which has yet to be observed in zebrafish (Caduff et al., 1986, Burri and Tarek, 1990, Schuermann et al., 2014, Makanya et al., 2009). Intussusceptive angiogenesis defines the process where an existing vessel divides into two by vessel intraluminal growth rather than endothelial cell proliferation (Caduff et al., 1986, Burri and Tarek, 1990, Hlushchuk et al., 2011).

Tumour angiogenesis - the generation of a pro-tumour vascular system from pre-existing blood vessels - is essential for tumour growth beyond a microscopic size of 1 to 2 mm^3 and also is considered to serve as a route for tumour metastasis (Arnold, 1985, Fox et al., 1996, McDonnell et al., 2000). In the tumour microenvironment, the balance between endogenous angiogenesis inhibitors and stimuli is disturbed by various signals including growth factors, proteases and ECM components. These signals are produced by neoplastic cells themselves as well as several stromal cell types including fibroblasts, smooth muscle cells/pericytes and macrophages, which are recruited by tumour cells, in close proximity to the blood vessels (Watnick, 2012, Ribatti and Crivellato, 2012).

It is well documented that tumours are infiltrated by immune cells which in turn are dependent on angiogenesis (Ribatti and Crivellato, 2009). Most, if not all types of immune cells elicit their angiogenesis-modulating functions

through the production and release of a large spectrum of pro-angiogenic mediators including angiogenic factors, extracellular matrix proteins, adhesion receptors, and proteolytic enzymes (Ribatti and Crivellato, 2009, Tazzyman et al., 2009). Among all inducers or regulators of angiogenesis, either cells or cell products, the macrophage is considered a major protagonist. Commitment of macrophage to a pro-angiogenic phenotype gives rise to pro-angiogenic cytokines and growth factors including VEGF, TNFα, IL-8 and FGF-2 and CSF-1/M-CSF as well as enzymes, such as MMP-2, -7, -9, -12, and cycloxygenase-2 (COX-2) (Sunderkotter et al., 1991, Lewis et al., 1995, Klimp et al., 2001). Normally TNFα is considered as a key feature of M1 macrophages and has been associated with higher endothelial permeability in a 3D tumour-endothelial intravasation microfluidic-based model (Zervantonakis et al., 2012). In a transgenic zebrafish model (Tg(*mpeg1::mCherry/tnfα::eGFP*)) genetically engineered to exhibit mCherry-labeled macrophages and eGFP-labelled TNFα, RT-qPCR on Fluorescence Activated Cell Sorting (FACS)-sorted TNFα+ and TNFα- macrophages showed that they, respectively, expressed M1 and M2 mammalian markers. Furthermore, fate tracing of TNFα+ macrophages during the time-course of inflammation caused by wounds or bacterial infection demonstrated that M1 macrophages progressively converted into M2-like phenotype during the resolution step (Nguyen-Chi et al., 2015).

TAMs are attracted to the hypoxic niche in TEM and polarised to a M2 type producing VEGF (Newman and Hughes, 2012). TAMs function as the "bridge cells" to promote vascular anastomosis and sprouting (Lewis and Pollard, 2006). Furthermore, a sub-population of monocytes/macrophages expressing the angiopoietin receptor Tie-2 is a critical inducer of angiogenesis (De Palma et al., 2005). Angiopoietin-2 (ANG-2)/TIE-2 signalling in TEMs upregulates proangiogenic genes and augments their inherent proangiogenic functions (Coffelt et al., 2010). Macrophages also secrete WNT whose receptors include FZD1, FZD2, FZD4, FZD5, FZD6, FZD7, FZD9, FZD10, LRP5, LRP6 are widely expressed in endothelial cells

(Goodwin et al., 2006, Favre et al., 2003, Mao et al., 2000). Wnt1, Wnt3a and Wnt5a have been related to two key events in angiogenesis, endothelial cell proliferation as well as migration in some situations (Masckauchan et al., 2005, Cheng et al., 2008, Newman and Hughes, 2012). WNT5a may also be involved in regulating TIE-2 expression in macrophages (Masckauchan et al., 2006).

Lymphangiogenesis and angiogenesis are closely related but unlike angiogenesis, not all solid tumours induce intratumoural lymphangiogenesis. Certain types of solid tumour including breast cancer, colorectal cancer, and head and neck cancer develop lymphatic vessels and the exact function of lymphangiogenesis in promoting tumour growth has yet to be fully understood (Al-Rawi et al., 2005, Cao, 2005). The most well recognised role of lymphangiogenesis is as an important conduit for the metastatic spread of human cancer (Al-Rawi et al., 2005). There is a growing appreciation that the VEGF-C/ VEGF-D/VEGFR-3 signalling system is a key regulator of tumour lymphangiogenesis (Yonemura et al., 2005, Adams and Alitalo, 2007).

The mechanisms underlying the close relationship between TAMs and metastasis lies in epithelial-to-mesenchymal transition and promotion of tumour cell extravasation to the circulation. TAMs also facilitate the extravasation, survival, and persistent growth of metastatic cells and provide premetastatic niches (Lewis et al., 2016). The requirement for CCR2+VEGFR1+Ly6C-F4/80+ metastasis-associated macrophages (MAM) was demonstrated in lung cancer (Colegio et al., 2014). The involvement of VEGF receptor VEGFR1 on MAMs also facilitates metastasis in breast cancer (Qian et al., 2015).

Their immunosuppressive function is another dominant feature of TAMs in the TME. TAMs can directly express molecules such as IL10, TGFb, activated STAT3, and arginase-1 or through the suppression of NK cells and T cells to enhance immune escape (Ruffell and Coussens, 2015, Lewis and Pollard, 2006). The subfamily of receptor protein tyrosines-Tyro3, Axl, and

Mer, as key pleiotropic inhibitors of the immune system, has revealed crucial functions in immune regulation of cancer development and been positively associated with cancer (Rothlin et al., 2015, Paolino and Penninger, 2016). The ligands of Tyro3, Axl, and Mer include growth arrest-specific gene 6 (Gas6), Protein S (Pros 1), Tubby, tubby-like protein 1 (Tulp-1) and Galectin-3 (Stitt et al., 1995, Caberoy et al., 2010, Caberoy et al., 2012). Although signalling pathways of Tyro3, Axl, and Mer have been shown to exert a crucial pro-oncogenic role in the initiation and progression of human cancers and their roles in immune-regulation have been extensively revealed, their direct immune regulation in TEM has yet to be further explored (Rothlin et al., 2007, Whitman et al., 2014, Ben-Batalla et al., 2013). The first study indicating the anti-tumour immunity of Tyro3, Axl, and Mer signally pathway used Gas-6-deficient mice where the tumour proliferation and metastasis were significantly impaired in different experimental cancer models by inhibition of Gas6 in hematopoietic cells (Loges et al., 2010). This study also showed that tumour cells educated infiltrated TAMs to produce Gas6 and may serve as an additional mechanism by which tumour cells modulate TEM for their own benefit (Loges et al., 2010). In the Mer-deficient mice, several cancers including breast cancer, melanoma and colon cancer exhibited prolonged latency and decreased metastasis (Cook et al., 2013). Furthermore, Mer-deficient leukocytes confer tumor resistance to *Mer+/+* mice and their anti-tumour role was confirmed by bone marrow transplants (Cook et al., 2013). NK cells have recently been shown to be recruited through Tyro3, Axl, and Mer signaling pathways leading to anti-metastasis functions in TEM (Paolino et al., 2014).

1.2.2 Extracellular vesicles (EVs)

The term extracellular vesicles (EVs) is used to describe a highly heterogeneous group of cell-derived membranous structures (van Niel et al., 2018). Although the nomenclature in the literature remains rather vague: many different names are used to refer to their origin (e.g. from prostate gland epithelial cells: prostasomes, from tumour cells: oncosomes), size

(prefix micro or nano: microvesicles, nanovesicles) and proposed functions (calcifying matrix vesicles, argosomes, tolerosomes) (Gould and Raposo, 2013). EVs may be broadly classified into exosomes and microvesicles (MVs) based on current knowledge of their cellular origin (Raposo and Stoorvogel, 2013, Akers et al., 2013, Todorova et al., 2017, van Niel et al., 2018).

Exosomes (40 to 120nm in diameter) are intraluminal vesicles of endocytic origin formed by inward budding of endosomal membrane and secreted upon fusion of multivesicular endosomes with the cell surface (Harding et al., 1984, Pan et al., 1985). Their endocytic origin enriches them with endosome-associated proteins such as Rab GTPases, SNAREs, Annexins, and flotillin as well as some membrane protein such as CD63, CD81, and CD9 (Shao et al., 2018). Initially exosomes were reported to be released by B lymphocytes and dendritic cells and mainly involved in immune regulation (Raposo et al., 1996, Zitvogel et al., 1998). Now exosomes are considered to be secreted by various cell types and have been widely implicated in intercellular communication (Colombo et al., 2014). MVs (50 to 1000nm in diameter) are formed by direct outward budding from the plasma membrane and subsequent release into the extracellular space (Tricarico et al., 2017, Colombo et al., 2014). The components of MVs are selectively enriched with protein and nucleic acid cargos and closely related to the cell types, physiological context and a wide variety of extracellular stimuli (Tricarico et al., 2017).

Of note, the reported morphology and the functional properties of EVs are based on methods of isolation and analysis. EVs appear as artefactual cup-shaped morphology probably caused by the processing of conventional transmission electron microscopy (TEM) and they are demonstrated as round structures enclosed by double-leaflet membranes by cryo-electron microscopy (cryo-EM) (Shao et al., 2018, Conde-Vancells et al., 2008). Although it is widely acknowledged that, the biogenesis of EVs is highly regulated and finely tuned, which equips EVs with particular bioactive

molecules including proteins, lipids, DNA, mRNA and miRNA (Colombo et al., 2014). The current available techniques for separating EVs result in a heterogeneous population of vesicles of unknown origin and the limited characterisation protocols precludes a clear attribution of a particular function to the different types of secreted vesicles and may account for the contradictions in different studies (Willms et al., 2016).

Abundant clinical observations show that release of EVs is increased in cancer and many studies suggest their complex role in pathogenesis ever since their biological significance was appreciated (Inal et al., 2012, Whiteside, 2005, Carter et al., 2018). EVs have shown the potential to carry biomarkers for cancer diagnosis and prognosis (Soekmadji et al., 2017a, Song et al., 2017, Matsuzaki and Ochiya, 2017). EVs can also facilitate immune escape and cause drug resistance in some cancers (Samuel et al., 2017, Soekmadji et al., 2017b, Czernek and Duchler, 2017).

EVs contains various cargoes, such as DNA, mRNA, microRNA, growth factors, adhesion proteins, lipids, tissue factors and protease inhibitors, based upon their cell origin and biogenesis pathways (Inal et al., 2012, Redzic et al., 2013, Collier et al., 2013, Bern, 2017, Chen et al., 2014, Williams et al., 2014, Zomer et al., 2010). Considering their small size and ability to carry selective cargo it seems likely that EVs spread the effects of their parental cells to distal sites (Vader et al., 2014, Pap et al., 2009). In ovarian cancer, EVs from malignant cancers selectively packaged MMP1 mRNA and enhanced the destruction of the peritoneal mesothelium barrier (Yokoi et al., 2017). Moreover the MMP1 mRNA transferred into mesothelial cells causes increased apoptosis of recipient cells(Yokoi et al., 2017). Galectins are enriched in EVs from different cancers, which may be important for the uptake of EVs by recipient cells (Escrevente et al., 2011, Mathivanan et al., 2010, Batista et al., 2011, Welton et al., 2010, Choi et al., 2011, Barres et al., 2010). EVs also show an ability to regulate the phenotype of macrophages in colorectal cancer (Shinohara et al., 2017).

Among their various activities in tumours, the involvement of EVs in angiogenesis has been drawing increasing attention. EV-associated Delta-like 4 was transferred from tumour cells and may induce angiogenic sprouting by altering the Notch signaling pathway (Noguera-Troise et al., 2006, Sheldon et al., 2010). In addition to delivering angiogeneic molecules, much evidence indicates that miRNA plays an important role in the EV-induced tumour angiogenesis. Hypoxia-cued EVs from multiple myeloma cells were shown to accelerate angiogenesis by targeting the FIH-1/HIF-1 signalling pathway via miR-135b (Umezu et al., 2014). EVs from lung cancer cells appeared to promote angiogenesis through miR-23a/PTEN (phosphatase and tensin homologue on chromosome ten) pathway and their effect was enhanced when the cells were X-ray treated (Zheng et al., 2017). EVs released from cancer cells were shown to contain miR-9 and activate the JAK/STAT pathway leading to endothelial cell migration and tumour angiogenesis (Zhuang et al., 2012).

Hypoxia drives the release of EVs to induce angiogenesis (Wang et al., 2014). PH also appears to be a regulator of the lipid composition of EV (Parolini et al., 2009). Besides these exogenous stimuli, endogenous factors such as TSAP6 (cellular stress-regulated protein) shown to enhance EVs production (Yu et al., 2006), oncogene *erbb2/her2* altered the cargo of EVs in favour of oncogenic effects (Amorim et al., 2014) . Abundant studies show that the molecular signature characteristic of their cell of origin is highly modulated by the stimulus suggesting that activation regulates the non-uniform distribution of various contents compared to the parental cells and to be closely associated with function.

Apoptosis and endothelial cell sprouting are closely associated (Li et al., 2014). While intensive investigation has targeted the role of EVs in cancer, apoptosis induced EVs remained less explored. Tumour cells release more EVs during apoptosis. These EVs are released at different stage of apoptosis compared to apoptotic bodies and exhibit different size profiles. We define

the EVs from apoptotic tumour cells whose productions are proportional to the degree of apoptosis as Apo-EVs. The most obvious way to distinguish Apo-EVs and apoptotic bodies is dependent on their sizes: Apo-EVs being less than 1 micron and apoptotic bodies ranging from 1 to several microns in diameter (Atkin-Smith and Poon, 2017, Gregory and Paterson, 2018). Obviously, this difference in size is insufficient for a clear distinction and the components of EVs are also used as comparison standards with EVs containing integral plasma membrane proteins, enzyme systems and RNAs while apoptotic bodies harbour organelles and nuclear components including DNA and histones (Gregory and Paterson, 2018). Apo-EVs were shown to contain higher levels of B cell surface markers (CD19 and CD20), apoptosis associated proteins, DNA and RNA than EVs from viable tumour cells (Patience, 2016). Furthermore, the presence of matrix metalloproteinases, MMP2 and MMP12 in Apo-EVs indicates a role in angiogenesis (Patience, 2016). Apo-EVs possess pro-angiogenic properties in the in vitro human umbilical vein endothelial cell (HUVEC) angiogenesis assay (Patience, 2016). As mentioned before, the separation and characterisation methods are crucial for EV study. The most widely used method for the isolation of EV is differential ultracentrifugation and this is indeed the main principle for the protocol used for the Apo-EVs separation in previous studies by our group. The limitations of separation protocols of EVs through differential ultracentrifugation include the contamination by many factors, such as cells and disruption of the membrane structure of EVs.

1.3 Apoptosis

1.3.1 Characteristics and mechanisms

The term, apoptosis was introduced by Kerr et al. to describe a controlled way of cell death morphologically characterised by nuclear fragmentation, chromatin condensation, cell shrinkage, cytoplasmic acidophilia and release of apoptotic bodies by budding (Kerr et al., 1972, Kerr, 2002). This form of programmed cell death plays vital roles in normal development and

homeostasis including normal cell turn over, immune reactions (Green, 2011). Dysregulation of apoptosis is responsible for many disease states including autoimmune disorders, neurodegenerative diseases, ischemic damage and cancers (Mattson, 2000, Nagata, 2010, Hanahan and Weinberg, 2011).

The mechanisms driving the fate of apoptotic cells are mainly divided into two circuits: the extrinsic or death receptor pathway and the intrinsic or mitochondrial pathway (Ichim and Tait, 2016). There is an additional perforin/granzyme pathway involving T cell mediated cytotoxicity and activates apoptosis by either granzyme A or granzyme B in a perforin-granzyme-dependent manner (Chowdhury and Lieberman, 2008).

The intrinsic pathway, which is often deregulated in cancer, is initiated by a wide array of stress inside the cell, such as DNA damage, cytokine/nutrient deprivation, endoplasmic reticulum stress or virus infection (Ichim and Tait, 2016). B-cell lymphoma-2 (BCL-2) family proteins lie at the heart of regulating the intrinsic pathway. The BCL-2 family is formed of two groups: 1) pro-apoptotic proteins, such as Bax, Bak, together with Bcl-2-homology (BH)-3-only proteins Bid, Bad, and Bim, and 2) anti-apoptotic proteins Bcl-2, Bcl-x, Bcl-XL, Bcl-XS, Bcl-w, and BAG (Moldoveanu et al., 2013, Youle and Strasser, 2008). These proteins control the mitochondrial outer membrane permeabilisation (MOMP) and consequently the release of pro-apoptotic factors including cytochrome c, AIF and SMAC/DIABLO (Liu et al., 1996). Cytochrome c, considered as a most important regulator of apoptosis, is released into the cytosol, where it interacts with apoptosis protease-activating factor-1 (Apaf-1), deoxyadenosine triphosphate (dATP), and pro-caspase-9 to form a caspase-activating complex called the apoptosome (Acehan et al., 2002). The apoptosome activates caspase-9 which ultimately activates effector caspases (caspase-3, 6 and 7) (Taylor et al., 2008).

The extrinsic pathway is mediated by transmembrane receptor-mediated interactions involving the death receptors of the TNF superfamily including TNFR, Fas and tumour necrosis factor-related apoptosis-inducing ligand (TRAIL). Upon binding of extracellular ligands (such as FasL and TNFα) to death receptors, the cytoplasmic domains of the receptors, so called 'death domains' attract adaptor proteins such as Fas-associated death domain protein (FADD) (Ashkenazi and Dixit, 1998). This leads to the formation of the death-inducing signalling complex (DISC) resulting in the accumulation and activation of caspase-8, an initiator caspase which triggers the execution phase of apoptosis (Kischkel et al., 1995, Wajant, 2002, Creagh et al., 2003).

Perforin/granzyme pathways are mainly used by cytotoxic T cells and NK cells to kill target cells (Creagh et al., 2003, Brunner et al., 2003). Cytotoxic T cells exert their cytotoxic effects on target cells by secretion of perforin, a pore-forming protein, leading to the transmission of cytoplasmic granules containing granzyme A and granzyme B into the target cells (Trapani and Smyth, 2002). Granzyme A induces apoptosis by a caspase-independent mechanism by inducing DNA degradation (Fan et al., 2003, Lieberman and Fan, 2003). Granzyme B, can activate caspase-10, caspase-3, cleavage of ICAD (Inhibitor of Caspase Activated DNAse), and utilize the mitochondrial pathway, thereby triggering apoptosis (Sakahira et al., 1998, Sakahira et al., 2015, Barry and Bleackley, 2002, Russell and Ley, 2002).

The extrinsic pathway, intrinsic pathway and Perforin/granzyme B pathways converge on the execution phase. Initially synthesized as inactive pro-caspases, initiator caspases (caspase 8 and 9) gain catalytic activity in response to apoptosome stimuli, death receptors and granzyme B (Riedl and Shi, 2004). Initiator caspases activate executioner caspases (caspase 3, 6, and 7) (Riedl and Shi, 2004). Once activated, a single executioner caspase can cleave and activate other executioner caspases, leading to a cascade of catalytic activation (McIlwain et al., 2015). Effector caspases activate cleavage of various substrates that lead to the characteristic biochemical

changes causing the final destruction of cells (Hengartner, 2000, Elmore, 2007).

1.3.2 Apoptotic cell clearance

Apoptotic cells are normally cleared quickly and most of them are found within phagocytic cells *in vivo* (Kerr et al., 1972, Schrijvers et al., 2005). The clearance and phagocytosis of dying cells have been shown to achieved by neighbouring 'non-professional' phagocytes of various lineages including fibroblasts, epithelial cells, mesenchymal cells, as well as professional phagocytes, especially macrophages (Hall et al., 1994, Juncadella et al., 2013, Wood et al., 2000, Gregory and Pound, 2010). Many pathways have been descried in the process of clearance of apoptotic and three phases of 'recognition, response and removal' have been rationalized (Gregory and Pound, 2010).

Clearance of apoptotic cells is initiated by the 'recognition' of phagocytes through the release of 'find me' signals (Gregory and Pound, 2010). These 'find me' signals released from apoptotic cells provide a chemotactic gradient that attract the phagocytes to the apoptotic cell (Gregory and Pound, 2010). The chemotactic factors include lipids Sphingosine-1-phosphate (S1P) and lysophosphatidylcholine (LPC), nucleotides adenosine triphosphate (ATP) and uridine triphosphate (UTP), as well as classical protein chemokines CX3CL1 ((fractalkine) and monocyte chemotactic protein (MCP-1 or CCL2) (Gude et al., 2008, Lauber et al., 2003, Elliott et al., 2009, Chekeni et al., 2010, Truman et al., 2008, Kobara et al., 2008). ATP and UTP whose release is mediated by pannexin channels seem to serve as a short-range find me signal due to their readily degrading by extracellular nucleotidases (Hochreiter-Hufford and Ravichandran, 2013, Chekeni et al., 2010). Their sensing by macrophage may be through the P2Y2 receptor (Elliott et al., 2009). CX3CL1 is released from apoptotic B-lymphocytes and attracts macrophages via chemokine (CX3-C motif) receptor 1 (CX3CR1). CX3CL1 is contained within extracellular vesicles derived from apoptotic B cells and may

enhance the attraction effects (Truman et al., 2008). The release of LPC by apoptotic cells is dependent on caspase 3 and its recognition appears via the phagocyte receptor G2A (Peter et al., 2008). In addition to serving as 'find me' signals, some of the molecules exhibit other roles during the clearance of apoptotic cells. For example, ATP increases binding of apoptotic cells to macrophages (Marques-da-Silva et al., 2011). CX3CL1 has been shown to cause the expression of a bridging molecule of milk fat globule epidermal growth factor (MFG-E8) on macrophages, which lead to the enhanced apoptotic cell clearance (Miksa et al., 2007). LPC, S1P and nucleotides also shown to attract neutrophils (Chen et al., 2006b, Florey and Haskard, 2009). However, apoptotic cells show minimal, if any, neutrophil recruitment implying there are 'keep out' signals that coordinate with 'find me' signals to decide the types of recruited phagocytes (Savill et al., 2002, Gregory and Pound, 2010). The first molecule found as the 'keep out' signal was lactoferrin by its ability to inhibit the migration of granulocytes, but not macrophages, as shown both *in vitro* and *in vivo* (Bournazou et al., 2009).

When macrophages are recruited to the site of apoptosis, they need to distinguish their targeted dying cells from viable cells. This 'recognition' is achieved by 'eat me signals' on apoptotic cells and 'don't eat me' signals (CD47 and CD31) on viable cells (Truman et al., 2008, Gregory and Pound, 2010). Eat me signals include the translocation of intracellular structures to extracellular sites such as DNA, calreticulin and annexin I, glycosylation of surface proteins or changes in surface charge, expression of intercellular adhesion molecule 3 (ICAM-3) and low-density lipoprotein (LDL)-like moiety, binding of serum proteins to the apoptotic cell, including thrombospondin and complement C1q (Gregory and Pound, 2010, Schlegel et al., 1999). The most important signal may be the exposure of the phospholipid phosphatidylserine (PS) on the outer plasma membrane leaflet since its recognition by macrophages appears to be crucial in clearance of apoptotic cells (Tennant et al., 2013, Grimsley and Ravichandran, 2003). The co-localization of calreticulin and annexin I with PS on the surface of apoptotic

cells enhance the phagocytosis (Arur et al., 2003, Gardai et al., 2005). The recognition of apoptotic cells by phagocytes depends on the various receptors on the surface of phagocytic cells. For example, PS can be recognised directly by PS- recognition receptors including BAI-1 (brain-specific angiogenesis inhibitor 1), TIM-4 (T cell immunoglobulin mucin 4), and Stabilin-2, or indirectly through bridging molecules, for example, Tyro-3, Axl, and Mer, which bind PS via Gas6 and protein S, as well as αvβ3/5 integrins, which bind MFG-E8 (Miyanishi et al., 2007, Park et al., 2007, Park et al., 2008b, Hanayama et al., 2002). Other receptors on the surface of macrophage include CD14 that binds ICAM-3, the scavenger receptors, which binds LDL (Devitt et al., 1998, Gordon, 1999).

The engulfment and processing of apoptotic cells by macrophages involves the activation of guanosine triphosphatases (GTPases) and subsequent cytoskeletal organisation of the phagocyte membrane (Gumienny et al., 2001). The quick and effective clearance of apoptotic cells by macrophages is important since apoptotic cells, in contrast to necrotic cell death, do not release their cellular constitutes, which would prevent an immunogenic response. Furthermore, the phagocytosis of apoptotic cells by macrophages has been shown to suppress the production of pro-inflammatory cytokines such as IL-6, IL-8, IL-12, and TNFα, as well as activating downstream signalling pathways that cause the up-regulation and secretion of anti-inflammatory mediators such as IL-10, TGF-β (Voll et al., 1997, Fadok et al., 1998, McDonald et al., 1999, Ogden et al., 2005, Gregory et al., 2011).

Genes that control the removal of apoptotic cells may also function in the activation of cell death. Blocking the engulfment genes (*ced-6* and *ced-7*) in *C.elegans* enhances cell survival when cells are subjected to pro-angiogenic signals (Hoeppner et al., 2001). Mutations in engulf genes in *C.elegans* enhances the survival of cells with partial loss of function of killer genes and these mutations alone allow the survival and differentiation of some cells that were programmed to die by apoptosis (Reddien et al., 2001). In vertebrates,

the elimination or inhibition of macrophages interrupts apoptosis-related functions (Diez-Roux and Lang, 1997, Lang and Bishop, 1993, Little and Flores, 1993). The engulfment machinery may contribute to cell killing.

1.3.3 Apoptosis in the tumour microenvironment

Evasion of cell death is a well-established feature of tumour cells (Hanahan and Weinberg, 2011). Mechanisms contributing to evasion of apoptosis and carcinogenesis include defects or mutations of the p53 protein, also called tumour protein 53 (or TP 53). TP53 is one of the best known tumour suppressor proteins and defects in the *p53* tumour suppressor gene have been associated with more than 50% of human cancers (Shen et al., 2013). Promoting cell death by inducing apoptosis has been long represented as an important effector mechanism in cancer treatment. However, recent studies show that apoptosis can promote tumour growth (Ford et al., 2015). Indeed, high rates of apoptosis have been observed in many malignant tumours and high level of apoptosis have also been shown to correlate with poorer prognosis in some cancers indicating the potential of apoptosis to drive oncogenesis (de Jong et al., 2000, Alcaide et al., 2013, Ucker and Levine, 2018).

It seems likely that apoptotic tumour cells actively modulate the tumour microenvironment in favour of contributing to the development of tumours. The exact mechanism underlying the pro-oncogenic roles of apoptosis are still unclear. Possible mechanisms include apoptotic tumour cells lead to compensatory proliferation by releasing growth factors, promote angiogenesis by attraction and modulation of macrophages and provide antitumor immunity (Gregory et al., 2016, Gregory and Pound, 2010). .

The phenomenon of compensatory proliferation was first observed in *Drosophila* when irradiated discs recovered to form adult structures of normal size and shape (Bryant and Fraser, 1988, Haynie and Bryant, 1976). More recently, dying tumour cells were shown to stimulate the growth of surviving

tumour cells and caspase-3 was involved in the growth stimulation (Huang et al., 2011). The interactions of apoptotic cells and macrophages appears to lie at the centre of pro-oncogenic events as the fundamental roles of TAMs in angiogenesis and anti-inflammatory signalling (reviewed in 1.2.1). Detailed studies on the role of apoptosis in the pathogenesis of aggressive starry-sky B-cell non-Hodgkin's lymphoma, prototypically BL have been carried out in our group (Ford et al., 2015). Suppression of apoptosis by expression of the anti-apoptotic genes *bcl-2* or *bcl-xl* leads to impaired tumour growth, reduced TAM accumulation as well as decreased angiogenesis when lymphoma cells were implanted into SCID mice (Ford et al., 2015). In this same model, *in situ* gene expression profiling of TAMs revealed functional clusters closely associated with anti-inflammatory, proangiogenic, and extracellular matrix deposition and remodelling pathways (Ford et al., 2015).

1.4 Zebrafish models for cancer research

Zebrafish has emerged as an attractive vertebrate model organism for scientific research of human tumours since they provide various advantages over traditional vertebrate models, that include rapid generation time (only 3 to 4 month), large brood size (100 to 200 eggs weekly per adult female), the ease of keeping high stocking density in a relatively small space (Lieschke and Currie, 2007).

Moreover, zebrafish embryos are transparent during the early stages of life (through to 7 days post-fertilization (dpf)) and externally fertilized, which offers a unique opportunity for *in vivo* live imaging. The availability of transgenic zebrafish lines with specific fluorescent-tagged cell types of interest offers a direct readout of distinct cell populations by fluorescent or confocal microscopy.

Zebrafish has functional homologues for about 70% of human disease associated genes (Schartl, 2014). Most importantly, there are striking

histological similarities between carcinogen-induced neoplasms in zebrafish and certain human tumours (Grabher and Look, 2006, Stern and Zon, 2003). A high degree of conservation in gene expression between zebrafish and human tumours and oncogenes further validate zebrafish as a viable predictive organism for modelling human cancers (Yang et al., 2004, Patton et al., 2005, Lam et al., 2006, Amatruda et al., 2002).

1.4.1 Hematopoiesis in zebrafish

The hematopoiesis program is highly conserved during evolution and in the past two decades many studies have shown that both transcriptional regulation and cellular makeup of the hematopoietic system is largely conserved from zebrafish to humans.

Zebrafish also has two waves of hematopoiesis the primitive and the definitive hematopoiesis. Unlike mammals and birds, the primitive wave of zebrafish occurs in two intra-embryonic locations: the intermediate cell mass (ICM) in the trunk ventral to the notochord, and the rostral blood island (RBI) originating from the cephalic mesoderm (Detrich et al., 1995, Paik and Zon, 2010). The primitive wave generates myeloid cells. These primitive blood cells start to circulate in the embryo from 24 hours post-fertilization (hpf). Definitive hematopoietic stem cells (HSCs) arise from the ventral wall of the dorsal aorta and then migrate to the posterior region in the tail called the caudal hematopoietic tissue (CHT) (Murayama et al., 2006). This posterior wave mainly gives rise to erythrocytes and some myeloid cells. Lymphopoiesis originates in the thymus from 3dpf and by 4dpf, HSCs home to the kidney marrow which appears to be analogous to the bone marrow in mammals (Paik and Zon, 2010).

The first macrophages are detected in the lateral mesoderm of the head, just anterior to the cardiac field at the 3-somite stage and migrate to the yolk sac, where macrophages differentiate and either enter the blood circulation or invade the head mesenchyme (Lieschke et al., 2002, Herbomel et al., 1999).

These primitive macrophages are active from 26 hpf in the ducts of Cuvier where macrophages were observed to engulf apoptotic erythroblasts from the blood stream (Herbomel et al., 1999). Gradually multiple lineages of macrophages derived by definitive hematopoiesis replace primitive macrophages and between 24 and 48 hpf, some of the yolk sac macrophages, most of which were anchored to or spread on the basal lamina of the epidermis, start entering the thin monolayered epithelium (Herbomel et al., 2001). Following the second wave of hematopoiesis, macrophage precursors extravasate into tissues throughout the whole body and differentiate into tissue macrophages (Torraca et al., 2014). To date, there are two popular transgenic zebrafish with macrophages labelled using either the macrophage-expressed gene 1 (*mpeg1*) promoter or microfibrillar-associated protein 4 (*mfap4*) promoter. However, *mpeg1* transcription attenuates in the presence of intracellular pathogens at both endogenous and transgenic loci while transgenic lines using *mfap4* as promoter have macrophages that remain stable throughout several days of infection (Benard et al., 2015, Walton et al., 2015).

From 4dpf, the zebrafish kidney starts to develop and will progressively replace the embryonic hematopoietic system. Although understanding of B cell development in zebrafish is relatively limited, a B cell specific transgenic line (Tg(*IgM1::eGFP*) reveals that kidney would seem to be the main organ for B cell development and it is also one of the three sites where B cells initially appear around 20 days (Page et al., 2013). This model also suggests that B-cell ontogeny in zebrafish is similar to human as there are pro-B, pre-B, and immature/mature B cells in the adult kidney.

Many orthologues of the transcription factors that are involved in mammalian hematopoiesis are found in zebrafish, such as stem cell leukemia (SC*L*), a zinc finger transcription factor *gata2,* an ets domain containing gene *etsrp* (Paik and Zon, 2010). Gene expression analyses show that the temporal and spatial expression patterns of zebrafish hematopoietic development are comparable to their mammalian counterparts.

In summary, the zebrafish immune system shares similar genomic pathways and contains all counterparts of human immune cells including macrophages, neutrophils, T cells and B cells, thereby providing a relevant model system (Meeker and Trede, 2008, Traver et al., 2003).

1.4.2 Xeno-transplantation in the transparent zebrafish embryo

Xenograft models in zebrafish, especially embryos without a fully developed immune system are being exploited to study cancer-related phenomena such as invasion, metastasis, angiogenesis, and cancer stem cell renewal *in vivo* and in real time (Amatruda et al., 2002, Nicoli and Presta, 2007, Nicoli et al., 2009, Nicoli et al., 2007).

The zebrafish model provides unique advantages for visualization of tumor cell behaviour and interaction with host cells. For example, the Tg (*fli1::eGFP*) embryo in which the friend leukemia integration 1 transcription factor (*fli1*) promoter drives the expression of eGFP in all blood and lymphatic vessels throughout embryogenesis can be used for analyzing tumor-induced lymph/angiogenesis. The Tg(*flk1::mCherry*) and Tg(*flk1::eGFP*) are also available as transgenic lines labelling all blood vessels (Jin et al., 2005). The transgenic lines that specifically label macrophages Tg(*mpeg1::eGFP*) and Tg(*mfap4::Turquoius*) can be used to study inflammatory responses (Oehlers et al., 2015). In a zebrafish–Mycobacterium marinum infection model, with the help of blood vessel-labelled and macrophage-labelled zebrafish models, Stefan H. Oehlers and his colleagues found that mycobacterial growth is intimately associated with angiogenesis suggesting the potential utility of host-targeting by anti-angiogenic agents as adjunct therapies for mycobacterial disease (Oehlers et al., 2015).

Several human cell lines have been transplanted into zebrafish embryos and show different capacities for proliferation and migration in zebrafish. For example, Wietske van der Ent et.al compared several uveal melanoma cells

and indicated that cells derived from metastases showed more migration and proliferation than cells derived from the primary tumors in zebrafish (van der Ent et al., 2014).

Xenografts in zebrafish are also robust models for tumour metastasis studies. The zebrafish can also serve as a valuable mode to study cancer cell homing to the hematopoietic niche and to establish a screening platform for the identification of factors and mechanisms contributing to the early steps of bone metastasis (Sacco et al., 2016). Co-injection of TAMs and cancer cells into zebrafish showed that TAMs (human TAM isolated from primary breast, lung, colorectal, and endometrial cancers) and M2-like macrophages (induced by IL4, IL10, and TGF-β) rather than M1-like macrophages (IFNγ-lipopolysaccharide–induced) enhance metastases by binding tumour cells and mediating their intravasation (Wang et al., 2015).

Still, despite the high conservation of gene function between zebrafish and humans, the potential differences in zebrafish tissue niches and/or missing microenvironmental cues could limit the relevance and translational utility of data obtained from zebrafish human cancer cell xenograft models.

1.4.3 Transgenic zebrafish models of immune system malignancy

Following on from early studies of tumour induction with chemical carcinogens, within the past decade, advances in genetic techniques have led to the generation of new zebrafish cancer models including creation of numerous mutant and transgenic lines(Amatruda and Patton, 2008, Meeker and Trede, 2008). These models are able to induce tumours that phenotypically resemble their human counterparts.

The first transgenic immune system cancer model in zebrafish was T cell acute lymphoblastic leukemia (T-ALL) established by over-expression of mouse *cmyc* gene fused with eGFP under control of zebrafish *rag2* promoter (Langenau et al., 2003). Green leukemic cells were initially detected in the thymic region with subsequent local spread into surrounding tissues. Cells

later spread into muscle and abdominal organs including the kidney marrow. Molecular and cellular characterization of these green cells showed that they were clonal and arrested at an early stage of T cell development. Green T lymphoblasts also express the zebrafish orthologues of the human oncogenes, *tal1*/*scl* and *lmo2* (Langenau et al., 2005). The onset of T-ALL is early in this model and diseased zebrafish normally die before sexual maturity. To obtain a stable line of ALL, an inducible transgenic T-ALL model was established by inserting the *myc* gene into a floxed *dsred* construct. In this line, T cells only express MYC when the floxed segment is removed by heat-shock-induced expression of the Cre recombinase (Langenau et al., 2005).

The second T-ALL model was generated by putting the human T-ALL oncogene, *notch1* under control of the *rag2* promoter. This model develops T-ALL at a later stage (about 5 months of age) with similar pathology to that seen in the *myc* model. Unlike the *myc* model, they do not show increased expression of *tal1*/*scl* and *lmo2*, and *myc-a* and *myc-b* are not expressed above normal levels (Chen et al., 2007)

The only B cell malignancy model in zebrafish is a B cell leukemia model generated by expression of the fusion TEL-AML1 (ETV6-RUNX1) under the control of the ubiquitous promoter, Xenopus *elongation factor 1α* or *zebrafish β-actin* rather than zebrafish lymphoid-restricted promoter, *rag2* promoter (Sabaawy et al., 2006).

Modelling B cell malignancy in zebrafish has been challenging. The only B cell malignancy model in zebrafish established so far is a B cell leukemia model that was generated by expression of the fusion TEL-AML1 (ETV6-RUNX1) under control of the ubiquitous promoters, Xenopus *elongation factor 1α* or *zebrafish β-actin* rather than the zebrafish lymphoid-restricted *rag2* promoter (Detrich et al., 1995).

1.5 Outline & Aims of this project

The over-arching hypothesis of the project is that apoptotic tumour cells contribute to the pro-oncogenic microenvironment in aggressive B-cell lymphoma. This project aims to test the hypothesis that in aggressive B-cell lymphoma, apoptotic tumour cells produce early stimulatory signals for tumour lymph/angiogenesis and leukocyte infiltration and activation.

In order to address this hypothesis, the first part of the project aimed to generate a transgenic B cell lymphoma model in zebrafish. Since *myc* has been established to be the primary oncogene in BL, the overexpression of myc in B cells was used as the strategy to induce B cell lymphoma.

The second part of the project aimed to establish a xenograft zebrafish embryo model to study the pro-oncogenic mechanisms of apoptosis. Apo-EVs and TAMs were chosen as the candidates and their trophic effects in zebrafish were investigated.

Chapter 2 Materials and Methods

2.1 Tissue culture techniques

2.1.1 Cell culture

BL cells

The EBV-negative BL line, BL2 was chosen for initial xenotransplantation studies, together with an apoptosis-resistant bcl2 transfectant (BL2-bcl2). The BL2-bcl2 line used in the present study was a stable bcl-2 transfectant established by bcl2 expression vector pCΔJ bcl2 (Milner et al., 1992, Tsujimoto et al., 1987). Cells were cultured in RPMI 1640 medium containing 10% batch selected fetal bovine serum (FBS), L-glutamine (2 mM), 100 U/ml penicillin and 100μg/ml streptomycin. All cells were kept in a humidified condition of 37^{o}C or 34^{o}C and 5% CO_2, in 25 cm^2 or 75 cm^2 tissue culture flasks. In order to keep cells in logarithmic growth phase, all cell lines were maintained by replacing fresh culture medium every two or three days.

Melanoma cells

A375, a human malignant melanoma cell line, was used in this project as a comparison to BL2 cell in zebrafish transplantation experiments. This cell line was a gift from Dr Liz Patton (the University of Edinburgh). Cells were cultured in DMEM media containing 10% batch selected fetal bovine serum (FBS), L-glutamine (2mM), 100 U/ml penicillin, 100 μg/ml streptomycin, 10mm Sodium Pyruvate Solution and 1%MEM NEAA (100X). All cells were kept in a humidified condition of 37^{o}C or 34^{o}C and 5% CO_2, in 25 cm^2 or 75 cm^2 tissue culture flasks.

2.1.2 Adaptation of BL cells to grow at low temperatures

The optimum temperature for zebrafish growth and development is 28.5°C , but this will not support growth of mammalian cells. Therefore, to establish a xenograft model an intermediate temperature was sought which was capable

of sustaining BL2 cells at high viability and allowing them to proliferate while also allowing zebrafish to develop normally.

BL2 cells were cultured at 35^{o}C and maintained for 2 weeks and then transferred to 34^{o}C. Zebrafish were kept at 28.5°C until 2.5 days post fertilisation (dpf) and was moved to 34^{o}C after being injected with BL cells and kept at 34^{o}C.

2.1.3 Generation of BL cell lines & melanoma cell line that are fluorescently tagged

The modification of mammalian cells for the expression of genes encoding fluorescent protein was carried out using two strategies.

2.1.3.1 Transfection of cells with desired plasmid construct

The pcDNA3.1(+) (Invitrogen) with strong promoter CMV was chosen as the expression vector. pAmCyan (Clontech) was used as the fluorescent gene provider. Briefly speaking, the pAmCyan gene was inserted to the pcDNA3.1(+) backbone.

DNA digestion and purification

To get the backbone of pcDNA3.1(+) and insert of pAmCyan, both plasmids were double digested by Hind III and EcoR I. Single digestions by either Hind III or EcoR I were also performed (table 2.1, 2.2). After digestion at 37^{o}C overnight, digestion samples of pcDNA3.1(+) was run on 0.8% agarose gel for up to 4 hours at 120 V; digestion samples of pAmCyan was run was run on 0.8% agarose gel for 1 hour at 120 V. The target band was excised from the gel under UV light (254-366 nm) using a clean disposable scalpel. For purification of DNA from agarose gel, Qiangen Gel Extraction was employed following manufacture instructions. DNA was quantified by nanodrop and by visual comparison of band intensity with a standard.

Name	Hind III (µl)	EcoR I (µl)	Double (µl)
pcDNA3.1(+)	0.25	0.25	0.25
Hind III	0.125	0	0.125
EcoR I	0	0.125	0.125
10X NEB2	1	1	1
dH_2O	8.625	8.625	8.5
Total	10	10	10

Table 2.1 pcDNA3.1(+) digestion

Name	Hind III(µl)	EcoR I (µl)	Double (µl)
pAmCyan	0.25	0.25	0.25
Hind III	0.125	0	0.125
EcoR I	0	0.125	0.125
10X NEB2	1	1	1
dH_2O	8.625	8.625	8.5
Total	10	10	10

Table 2.2 pAmCyan digestion

DNA ligation

Ligation of pcDNA3.1(+) backbone and pAmCyan insert was achieved by using T4 ligase and was performed in T4 ligation buffer. 1µgof back bone and appropriate amount of insert (calculated by the formula below) at the molar ratio of 5:1 for insert to backbone were ligated overnight at 16-21°C. Two ligation reactions comprising one containing no ligase and the other containing no insert DNA were used as control.

$$\frac{\text{ng of backbone X kb of insert}}{\text{kb of vector}} \text{ X molar ratio of}\left(\frac{\text{insert}}{\text{backbone}}\right)$$

Transformation using electroporation

The pcDNA3.1(+)-pAmCyan was prepared as described above and plasmid was dissolved in TE which was provided in Qiangen Gel Extraction kit. Because Tris can kill cells after electroporation, buffer was replaced by water. Specifically, 1/10 volume 3M NaOAc (pH5.2) was add to 10 μg DNA. After mixing, 2X volume EtOH was added and mixed following lacing on dry ice for 10 minutes. DNA was spun at 14,000g for 10 minutes and supernatant was removed. Pellet was washed by 70% EtOH and dissolved in 10 μl of sterile water.

10^6 cells growing at logarithmic phase were suspend in100 μl nucleofector solution (prepared following manufacture guideline) and mixed with 2 μl plasmid (1 μg/μl). Mixed sample was transferred into amaxa cuvette and put on the nucleofector device. Electroporation was performed using program R-009. Immediately 500μl of pre-warmed culture medium was added into the cuvette and then cells were transferred into a 12-well plate.

2.1.3.2 Transfection of cells with lentivirus

Cells growing at logarithmic phase were diluted into culture medium to a final concentration of 10^5 cells/ml. 2 ml of cells were transferred into 15 ml FACON tubes and different volumes of virus were added to the cells such that the final multiplicity of infection (MOI) equals 0,0.1,0.5,1,5,10,25,50 per tube. Volume of virus was calculated by the formula shown as below. Final concentration of 1μg/ml polybrene was added to enhance transfect efficiency. Cells were spun at 800 xg for 90 minutes at 32^{o}C. Each cell pellet was resuspended in 2ml media and transferred to 6-well plates.

$$\mathrm{MOI} = \frac{\left[\mathrm{ViralTiter}\left(\frac{\mathrm{TU}}{\mathrm{ml}}\right)\mathrm{xVolumeof\,Virus(ml)}\right]}{\mathrm{NumberofCells}}$$

2.1.4 Selection of successful transformations

Antibiotic knock down

Cells were checked for target fluorescent protein expression 2 days after transformation. Cells were centrifuged at 200 xg for 5 minutes and suspended in culture medium with Blasticidin (Invitrogen). The amounts of Blasticidin for different cells were determined by kill curve. Cell medium was removed and replaced by fresh culture medium with Blasticidin every two days until antibiotic-resistant colonies could be identified (10-12 days after selection). Cells were then moved to incubator at 37°C, for 7-10 days.

2.1.4 Growth kinetics assay

Cells were resuspended at $2x10^5$ viable cells/ml in culture media and plated on 24-well plates (Nunc). Cells were incubated at 37˚C, 5% CO_2. The viability of cells was counted using trypan blue exclusion every 24 hours up to 5-8 days.

2.1.5 Induction of apoptosis of BL cells

2.1.5.1 Apoptosis induction by UV radiation

UV induced apoptosis of BL cell lines has been well characterised previously by the Gregory laboratory and reliable methods established. BL2 cells from confluent cultures were transferred into 15 ml Falcon tubes and centrifuged (300 xg/5min). After washing in PBS three times (300 xg/5 min) and taken off supernatant cells were resuspended at $1x10^6$ cells/ml serum-free RPMI 1640 medium supplemented with L-glutamine and penicillin/streptomycin and then exposed in 100 mJ/cm^2 UV-B. The intensity of the UV exposure was measured by a UV meter. The time of exposure was calculated using the formula: $\text{time required (seconds)} = \frac{100{,}000\ \mu\text{J}}{\text{meter reading}}$

When using CL-1000 Ultraviolet Crossslinker, 300 mJ/cm^2 UV-B was used. To induce high levels of apoptosis cells were returned to humidified incubator of 5% CO_2 at 37^{o}C for approximately 3 hours before use.

2.1.5. 2 Apoptosis induction by staurosporine

The broad spectrum protein kinase inhibitor, staurosporine was used as an alternative inducer of apoptosis which does not act via damage of DNA. BL2 cells from cultures were transferred into 15 ml Falcon tubes and centrifuged (300 xg/5 minutes). After washing in PBS three times (300 xg/5 min) and taken off supernatant cells were resuspended at $1x10^6$ cells/ml serum-free RPMI 1640 medium supplemented with L-glutamine and penicillin/streptomycin and staurosporine was added to a final concentration of 1 µM. To induce high levels of apoptosis cells were returned to humidified incubator of 5%CO_2 at 37^oC for approximately 3 hours before use.

2.1.6 Assessment of apoptosis of BL cells by flow cytometry

BL2 cell lines

Approximately $5x10^5$ cells were centrifuged (300 xg/5 min) and washed with 3 ml of cold AxV binding buffer (14 mM sodium chloride, 10 mM HEPES and 2.5 mM calcium chloride, pH 7.4) then resuspended in 100 µl AxV binding buffer. 1 µl of AxV-Alexa 488 was added and cells were incubated in a refrigerator for 15 minutes. After addition of 400 µl of cold AxV binding buffer, 10µl of PI was added and cells immediately analysed by flow cytometry.

BL2 fluorescent-tag lines

Approximately $5x10^5$ cells were centrifuged (300xg/5 minutes) and washed with 3 ml of cold AxV binding buffer (14 mM sodium chloride, 10 mM HEPES and 2.5 mM calcium chloride, pH 7.4) then resuspended in 100 µl AxV binding buffer. 1 µl of AxV-R-phycoerythrin conjugate was added and cells were incubated in a refrigerator for 15 minutes. After addition of 400 µl of cold AxV binding buffer, 5 µl of SYTOX BLUE was added and incubated for 5minutes before cells were analysed by flow cytometry.

2.1.7 Assessment of proliferation of BL cells by Immunohistochemistry (IHC)

2.1.7.1pHistone3 staining

10^5 cells were washed in DPBS once and resuspended in 100 µl of 10% BSA/DPBS. 10^5 Cells in 100 µl were added onto each slide in the cytospin chamber and cytocentrifugated for 3 minutes at 300g. After drying the slide for 2 hours at room temperature, slides were fixed in ice-cold acetone at 4°C for 10 minutes. Slides were washed twice in DPBS and loaded into Sequenza chambers. Cells were blocked by 125 µl of 1x casein protein for 10 minutes and then 125µl primary antibody (diluted in 1x casein protein block) (table 2.3) was added into each slide or no primary antibody for control slide without washing protein block off. After drying, the slides were washed twice by DPBS and 125 µl secondary antibody (diluted in 1x casein protein block) was added into each slide for 30 minutes. Slides were washed twice in DPBS following once in water. Slides were mounted using histomount and dried in fume hood over night before checked by microscope.

Antibodies	**Working concentration**	**Suppliers**
PHH3 (anti-rabbit)	1/1000	Abcam
Alexa Fluor® 546	1/250	invitrogen

Table 2.3 Antibodies used for IHC of cells in vitro

2.1.8 Preparation of extracellular vesicles from UV-treated cells

2.1.8.1 3-Step Differential Centrifugation Method

BL2 and/or BL2-Bcl-2 cells were washed once by RPMI 1640 and resuspend at 4 x 10^6 cells/ml in 0.1 µm-filtered RPMI 1640 medium containing 0.1% BSA, L-glutamine (2mM), 100 U/ml penicillin and 100µg/ml streptomycin. Cells were exposed to 100 mJ/cm^2 UVB then incubate at 37^0C for 2 hours.

Cells were then cleared by centrifuging twice at 400 xg for 5 minutes at 20°C followed by filtration of supernatant through a pre-wet 5 µm filter. EVs were then isolated from cleared supernatant by centrifugation at 2,000 xg for 30 minutes at 4°C. EVs form a pellet that could be resuspended in an appropriate 0.1 µm-filtered media/buffer.

2.1.8.2 Optimised gentle filtration method

BL2 and/or BL2-Bcl-2 cells were cultured at 20 x 10^6/ml in 50% X-vivo 20 and induced into apoptosis by UV treatment. The cells were usually split 1/2 the day before isolation. These culture conditions induce a fairly synchronous induction of apoptosis which is monitored by annexin V staining. Samples were taken at 1 hour, 3 hour and/or 5 hour and the EVs isolated by gentle centrifugation and two filtration steps – a 5 µm mesh filter and a 1.2 µm syringe filter. Specifically, cells were resuspended by swirling the flasks and decanted into 50ml Falcon tubes and spun at 300 xg for 5minutes, 20^{o}C and then supernatant discarded. Cells were re-suspended in a small volume of 0.1 µm filtered 50% x-vivo 20 and counted on the Attune by using events/µl on viable cell gate to calculate cell concentration with the aim of adjusting concentration to 20 x 10^6/ml with 0.1 µm filtered 50% x-vivo 20. Cells were UV treated for a total of 300mJ/cm2 as 6 x 50 mJ/cm2. Cells were monitored by AxV/Sytox blue on the Attune at hourly intervals swirling the flask to completely re-suspend the cells at each time point. At the appropriate time point, cells were spun at 25 xg for 1h at 4°C by adding 1.5 volume DPBS and then the supernatant were filtered through 5µm Pluristrainer mesh filter onto a 50 ml Falcon following a 1.2 µm syringe filter.

2.1.9 Preparation of Macrophages from human blood

Blood was prepared using the method kindly provided by Ian Dransfield and John Marwick of Lung Inflammation Group. Freshly drawn venous blood was collected in a 50 mL syringe. 40 mL blood was added into a 50 mL BD Falcon tube containing 4 mL of 3.8% sodium citrate solution. The tube was capped, inverted to mix and sealed with parafilm. Blood was centrifuged at

350 xg for 20 minutes at room temperature to separate cells from plasma. The top layer of platelet rich plasma (PRP) was transferred into 50 mL tubes without disturbing the pelleted cells and aliquoted as 10 ml per glass vials with addition of 220 µl 1M $CaCl_2$ to generate autologous recalcified plasma (serum) by gently mixing and incubating for 1 hour at 37°C. Leukocytes were enriched from the pelleted cells by differential sedimentation of erythrocytes by dextran. Specifically, the bottom layer was resuspended in 6 mL of dextran and topped up to 50 mL with 0.9% sodium chloride. The mixture was allowed to stand undisturbed for a maximum of 20 minutes or until sedimentation had taken place. The top layer was then moved into another 50 ml BD Falcon tube and topped up to 50 ml with 0.9% sodium chloride and spun at 350 xg for 6 minutes. After removing the supernatant the leukocytes were resuspended in percoll gradients of 81%, 70% and 55%. The gradient was spun at 720 xg for 20 minutes and mononuclear cells (MNCs - lymphocytes and monocytes) were collected from the 55%/70% interface and washed by topping up to 50 mL with 0.9% Sodium Chloride (Baxter) and spinning at 230 xg for 6 minutes. MNCs were counted before resuspending in the required volume of MACS buffer (PBS (pH 7.2) containing 0.5% BSA (or autologous serum) and 2 mM EDTA, sterile filtered through 0.22 µm filter). Monocytes were isolated from MNCs using Pan monocyte isolation kit, human (MACS Miltenyi #130-096-537) following manufacturer's instruction. The isolated monocytes were cultured in IMDM (Life Technologies) plus 1X Pen/Strep and 2 mM L-Glut (IMDM/PS/LG) for 40 – 60 minutes at 37°C to adhere onto tissue culture plastic and then the culture media was replaced by IMDM/PS/LG containing 2% Human AB serum. Monocytes were incubated for 5-7 days in total at 37°C, 5% CO_2 before use in downstream assays.

2.2 Zebafish methodology

2.2.1 Fish husbandry and housing

Zebrafish were kept and raised in the fish facility based in Queen's Medical Research Institute with a 14 hour-light and 10 hour-dark cycle at 28.5^{o}C

under the standard protocol of Westerfield(Westerfield, 1995b). The females have larger silver stripes and bigger white belly. Males are slimmer and have gold stripes between the blue stripes. Embryos were obtained by crossing sex mature fish in a pair-wise manner. Embryos were raised in conditioned aquarium water containing 0.00001% methylene blue or E3 media. Some embryos were kept with 0.003% 1-phenyl-2-thiourea (PTU) from 20 hours post fertilisation (hpf) to avoid pigmentation. All embryos were staged by hour post fertilization (hpf) or day post fertilization (dpf) using standard procedures (Kimmel et al., 1995).

In this study the reporter lines Tg(*fli1::eGFP*)(Lawson and Weinstein, 2002), Tg(*flk1::mCherry*), Tg(*mpeg1::mCherry*) (Ellett et al., 2011) and Tg(*mpeg1::mCherry/tnfα::eGFP*) (Nguyen-Chi et al., 2015) were used to monitor tumour cells and macrophage behaviour as well as tumour-induced angiogenesis.

2.2.2 Microinjection

Injection needles were pulled from glass capillary using P-97 Flaming/Brown micropipette Puller. All injections were performed under stereomicroscope microscope with the help of gas-pressure instrument PV 820 Pneumatic Picopump to provide consistent injections.

2.2.2.1 Transplantation of cells

Cells in the Log Phase were washed and resuspended in 1:1 of matrigel:DPBS or 0.5% Polyvinylpyrrolidone (PVP40) in DPBS at desired concentration. Cells were loaded into injection needle that was placed in the micromanipulator. Zebrafish embryos were kept at 28.5^{o}C until 2 dpf for injection. A final cell number of 200-500 cells/fish for injection was achieved by adjusting the size of cut end of the needle (not big enough to cause severe physically damage), injection pressure (20-30 psi) and injection time (200-300 msec). Injected volume was checked in mineral oil before transplantation. Cells were injected into the desired site (yolk sac, brain, circulation, pericardial cavity or perivitelline space) of anesthetized zebrafish

lying on the agarose coated plate. The transplanted fish were kept at 34^{o}C and selected for correct transplantation 2 hours later except the injection into circulation was checked immediately after injection.

2.2.2.2 Microinjection of tol2 transposon system

A total of 5-10 pg of plasmid DNA and 25-50 pg of synthesized mRNA was injected into one cell stage of zebrafish embryo (Kawakami, 2007).

2.2.3 Strategy of generating transgenic zebrafish

2.2.3.1 Generation of plasmid with a Tol2 constructs

Most plasmids generated in this project as shown in table 2.4 were using the gateway technology unless stated otherwise. p5E-IgM1 was generated from the plasmid of IgM1-eGFP (Page et al., 2013) which was a gift from Dr. Brad G. Magor (University of Alberta). Others were either obtained from members in our group or generated from existing plasmids by myself using gateway technology. Plasmids generated through PCR were sequenced by Eurofins genomics.

2.2.3.2 Generation of transgenic zebrafish lines

Synthetic Tol2 transposase mRNA was co-injected with transgenic constructs containing Tol2 elements into one-cell stage embryo. Surviving embryos with selection marker were kept until sexual maturity. The founder fish were mated with wild type to get F1 generation. The F1 progeny with successful integration of transgene into genome were checked by fluorescent microscope for presence of selection marker (green heart or blue eye).

2.2.4 FACS sorting, single-cell suspensions of adult/larvae zebrafish kidney

2.2.4.1 Prepare of single cell suspension

Kidney was collected by opening the abdomen of zebrafish as shown in figure 2.1 (a) and removal of all internal organs to expose the kidney as in figure 2.1 (b) using forceps and a dissection microscope. Whole kidney

comprising the head, trunk and tail (figure 2.1 (c) (d)) was carefully removed away from the body wall by forceps and put into ice-cold staining medium (0.9X Dulbecco's PBS + 5% FCS). Kidney was aspirated vigorously by 1 ml pipetteman before filtered through 40 μm Cell Strainer (Falcon) and washed by staining media. The flow through was centrifuged and filtered again through 40 μm Cell Strainer. 1:1000 Sytox Blue (excited by the 405 nm laser) was added for dead cell discrimination.

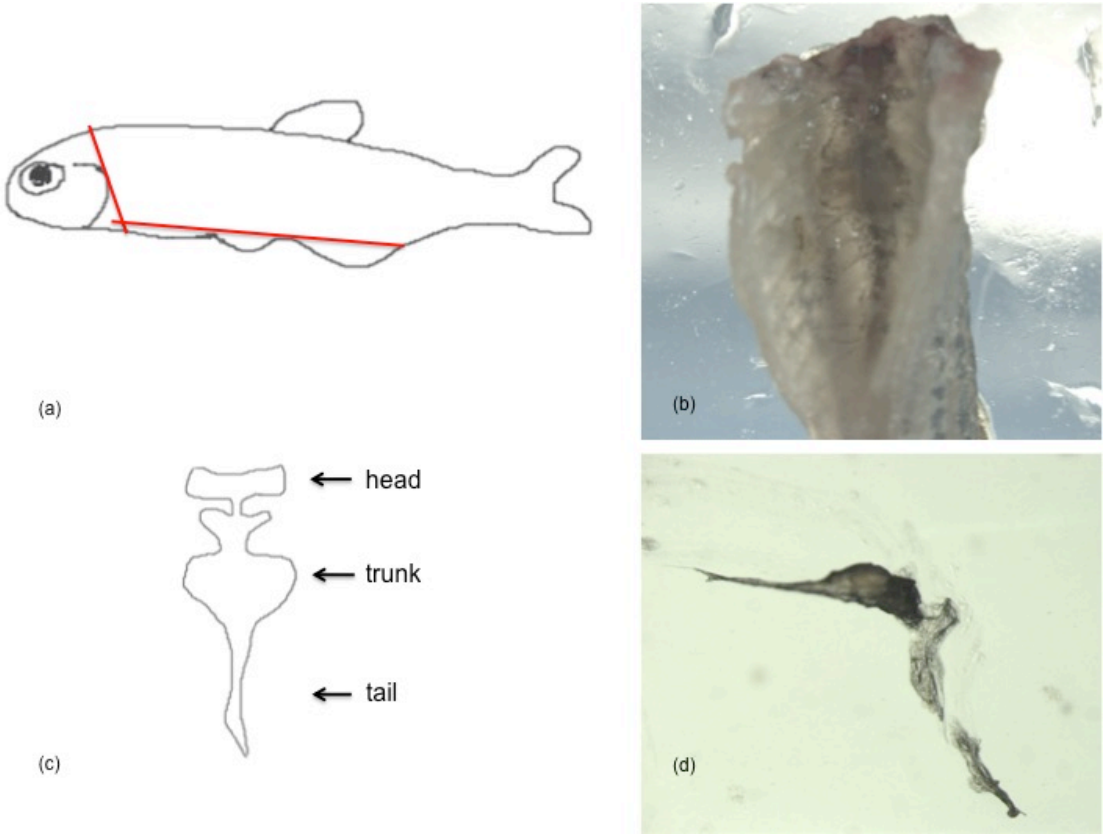

Figure 2.1 Kidney collection of zebrafish juvenile and adult

(a) Red lines show the dissection for the exposure of abdomen of zebrafish (b) Kidney are exposed after removal of organs in the abdomen (c) Cartoon shows the structure of whole kidney (d) Whole kidney are detached from the body wall.

2.2.5 IHC on whole-mount embryos

Zebrafish embryos were fixed in 4% Paraformaldehyde (PFA)/PBS with 0.4% Triton X-100 for 2 hours at room temperature (RT) or overnight at 4^{o}C. Embryos were washed in DPBT (0.1% Triton X-100 in DPBS) for 5 minutes 4 times before blocking for 2 hours at RT in 5% goat serum/DPBT. Embryos were incubated in 5% goat serum/DPBT containing the primary antibody (table 2.4) with gentle shaking at 4 ^{o}C over night. Embryos were rinsed with DPBT twice and washed in DPBT (0.1% Triton X-100 in DPBS) for 30 minutes 10 times. Embryos were incubated in 2% goat serum/DPBT containing the secondary antibodies conjugated with fluorescent label (table 2.4) at 4˚C over night and kept in dark as much as possible from this stage. Embryos were stained with counting reagent if needed for 30 minutes at RT then rinsed twice following washes in DPBT for 20 minutes 10 times. Embryos could be stored in 70% CITIFLUOR (citifluor limited) if not observed immediately.

Antibodies	**Working concentration**	**Suppliers**
PHH3 (rabbit)	1/500	Abcam
Alexa Fluor® 546	1/250	invitrogen

Table 2.4 Antibodies used for IHC on whole amount zebrafish embryo

2.3 General molecular biology techniques

2.3.1 Polymerase chain reaction (PCR)

PCR reactions were carried out using Q5® High-Fidelity DNA Polymerase (New England Biolabs) or CloneAmp™ HiFi PCR Premix (Clontech). Appropriate annealing temperatures were selected depending on the length of the products and the Tm of the primers (table 2.5).

Primer name	Sequence
p5E-IgM1 F	Ggggacaactttgtatagaaaagttgcagccctttctagagctcgtgcctcg
p5E-IgM1 R	Ggggactgctttttttgtacaaacttgcgcgaccggtcagccaaaaacagtc
p3E-cmyc-eGFP F	Ggggacagctttcttgtacaaagtggtagccaccatgcccctcaacgtgaac
p3E-cmyc-eGFP R	Ggggacaactttgtataataaagttgcaagctgggtttacttgtacagctc

Table 2.5 Primers used for generating plasmids

2.3.2 Restriction enzyme digestion

Appropriate NEB enzymes and buffers were used for restriction digestions following the manufacturer's instructions. The products of the digestion were analysed by agarose gel electrophoresis.

2.3.3 Gel electrophoresis and extraction

DNA fragments were analysed in 1% Agarose gel with the help of GelRed Nucleic Acid Gel Stain (1/10,000) to visualise the DNA under ultraviolet (UV) light. Gel extraction was performed using QIAquick Gel Extraction Kit (QIAGEN) following the manufacturer's instructions.

2.3.4 Electroporation of Electrocompetent E.coli and DNA plasmid preparation

1 µl to 5 µl of DNA were transformed into 50 µl One Shot® TOP10 cells using electroporator under the setting of 1.7 Kv, 200 Ohms and 25 µF. Immediately after electroporation, cells were resuspended in prewarmed (37^{o}C) LB media and recovered for 1 hour at 37^{o}C/250RPM. 50 µl of different dilutions of cell culture including neat, 1/10 and 1/100 dilutions were plated onto 9 cm Agar plates containing TYE Agar with 1% Glucose and appropriate antibiotics. After 24 hours incubation at 37^{o}C, several colonies for each plasmid were picked and grew in 5 ml volume of LB media containing 1% Glucose

appropriate antibiotics overnight at 37^{o}C/250RPM. Qiagen Miniprep Kit (Qiagen) was used for isolated plasmid DNA as manufacturer's instructions. To get more DNA, cells were transferred to 50ml media containing 1% Glucose appropriate antibiotics to grow overnight at 37^{o}C/250RPM. For collecting DNA cloning in competent cells, plasmids were prepared using Qiagen Midi Prep kit (Qiagen) as per manufactures instructions. Concentration (ng/µl) and purity of purified DNA samples were analysed by NanoDrop 1000 Spectrophotometer.

2.4 Image acquisition and Image procession

All 3.5x and 11x fluorescence images were collected using Leica Stereo AF 6000 combined with digital camera DFC or Leica M205 FA with Leica DFC345 FX and Leica M165 FC with HAMAMATSU digital camera. Higher magnification images were taken by Leica TCS SP5 confocal microscope (Leica). Confocal stacks were processed for maximum intensity projections by Leica software. Images were adjusted for brightness and contrast with Adobe Photoshop CS6 if necessary. Overlays of images were generated with Adobe Photoshop CS6. Imaris 8.0.2 (Bitplane, Zurich, Switzerland) was used to analyse the morphology of macrophages.

2.5 Statistical analysis

Values from groups shown as means±SEM using GraphPad Prism software (version 6; GraphPad Software Inc., San Diego, CA, USA). Mann whitney test was used to detect significant difference between means of two groups, and one way Analysis of Variance (ANOVA) was used for analysing significant difference among three groups. All significant values are given with p values indicated.

2. 6 List of Regent

10x DPBS without CaCl2 and MgCl2	Invitrogen
4-(2-hydroxyethyl)-1-piperazineethanesulfonic acid (HEPES)	Sigma
Ampicillin	Sigma
ApopTag® Red In Situ Apoptosis Detection Kit	Millipore
AxV-Fluos	Roche
Biomax 300KDa Ultrafiltration Discs	Millipore
Bovine Serum Albumin (BSA)	Sigma
Bradford's assay solution	Bio-Rad
casein protein block	Vector labs
Cell TrackerTM (CM-Dil, Molecular Probes®),Dio7778	Invitrogen Life Technologies
Click-iT EdU Alexa Fluor 647 Imaging Kit	Life Technologies
Dulbecco's Modified Eagle Medium (DMEM)	Gibco
ECL Western Blotting Detection Reagents	GE Healthcare
Ethylenediaminetetraacetic Acid (EDTA)	Sigma
Fetal bovine serum (FBS)	BioWhittaker
GelRed Nucleic Acid Gel Stain, 10,000X in water	Biotium
Hechest 33342	Sigma
Hign Fidelity PCR Eco Dry Premix	Clontech
Hybond-P (nitrocellulose) membrane	GE Healthcare
Hybridoma-selected fetal calf serum (HYB-FCS)	PAA

Hydrogen peroxide	Sigma
Hyperfilm ECL	GE Healthcare
Kanamycin	Sigma
L-glutamine	PAA
Matrigel (Cultrex® Basement Membrane Extract,Reduced Growth Factor)	Trevigen
Methanol	Fisher Scientific
Minimum Essential Medium Non-Essential Amino Acids Solution (MEM NEAA)(100X)	Gibco
Non-fat milk powder	Tesco
Nuclease-Free Water	Invitrogen Life Technologies
NuPAGE LDS sample buffer	Invitrogen
NuPAGE MES SDS Running buffer 20x	Invitrogen
NuPAGE Novex 4-12% Bis- Tris pre-cast gels	Invitrogen
NuPAGE reducing agent	Invitrogen
NuPAGE Transfer buffer	Invitrogen
Paraformaldehyde	Sigma
Penicillin	Invitrogen
Propidium Iodide (PI)	Bender MedSystems
Protease inhibitor cocktail P8340	Sigma
PTU (1-phenyl-2-thiourea)	Sigma
Q5® High-Fidelity DNA Polymerase	New England Biolabs
QIAquick Gel Extraction Kit	QIAGEN
RPMI 1640 growth medium	Gibco

SeeBlue Plus2 Pre-Stained Standard	Invitrogen
SIGMAFAST BCIP/NBT	Sigma
Sodium chloride	Fisher Scientific
Sodium Pyrurate Solution	Sigma
SP-DiOC18(3)	Invitrogen
Staurosporine	Calbiochem
Streptomycin	Invitrogen Life Technologies
SYTOX® Blue Dead Cell Stain	Thermo Fisher
Triton X-1000	Sigma
Trypan Blue	Sigma
Tween20	Sigma

2.7 List of Equipment

Equipment	Suppliers
96-well Nunc-Immuno plate	Thermo
Class II microbiological safety cabinets	BIOMAT
Coulter EPICS XL-MCL flow cytometer	Beckman Coulter
D-78532 Tuttingen	Sartorius
Filter system 0.22µm, 500ml	Corning
Incubators	LEEC
Microplate autoreader Anthos HTII	Anthos Labtech Instruments
Sigma 1-15K	Sigma
Tissue culture flasks	Iwaki
Tissue culture plates	Costar
CL-1000 Ultraviolet Crossslinker	Ultra-Violet Products
Zeiss Axiovert 25	Zeiss
Nucleofector	Lonza
PV 820 Pneumatic Picopump	World Precision Instruments
Digital camera C1144O	HAMAMATSU
Leica M165 FC	Leica
Leica M205 FA	Leica
Leica DFC345 FX	Leica

2.8 List of zebrafish line

Name	Description
AB	wildtype line
WIK	wildtype line
fli1::eGFP	promoter of *fli1a* gene drives expression of enhanced GFP in the blood vasculature, the dorsal aorta, the posterior cardinal vein and the thoracic duct and lymphatic vessles (Lawson and Weinstein, 2002)
flk1::eGFP	promoter of *flk1/vegfr2* gene drives expression of enhanced GFP in all endothelial cells (Jin et al., 2005)
flk1:: mCherry	promoter of *flk1/vegfr2* gene drives expression of mCherry in all endothelial cells (Wang et al., 2010)
mpeg1::mCherry	mpeg1-driven transgenes express in macrophage-lineage cells (Ellett et al., 2011)
mpeg1::mCherry/ tnfα::eGFP	mCherry labelled macrophages and cells will turn green when TNFα signals are activated (Nguyen-Chi et al., 2015)
IgM1::Cre-ER^{T2}	details in result chapter 3
IgM1::LoxP-H2B-mCherry-LoxP-cmyc-eGFP	details in result chapter 3
IgM1::cMyc-eGFP	details in result chapter 3

Chapter 3 B cell lymphoma transgenic models generation and characterization in zebrafish

3.1 Introduction

The common characteristic of virtually all BL is chromosomal translocation of the *myc* proto-oncogene to an immunoglobulin (Ig) locus leading to deregulation and constitutive expression of c-myc with an overall effect of uncontrolled proliferation as well as a reduced threshold for induction of apoptosis (God and Haque, 2010, Gregory and Hann, 2000).

Myc is estimated to play a role in 20% of all cancers and to target 15% of all known genes (God and Haque, 2010). *Myc* contributes to the metabolic reprogramming that essential for cancer cells to adapt to the tumour microenvironment, and highly dependent on cell-intrinsic signals thereof (Stefan and Bister, 2017, Crunkhorn, 2017, Camarda et al., 2017). By placing the *myc* gene under the enhancer region of immunoglobulin (Ig) H chain or kappa (Ig kappa) or lambda (Ig lambda) L chain genes in mouse, different types of B cell lymphoma including those mimicking BL were developed and the phenotypes of lymphoma seemed to be linked to the onset time of tumour development (Kovalchuk et al., 2000, Adams et al., 1985). Despite the opportunities of studying pathogenesis provided by these transgenic murine models, it is still difficult to explore early events and observe the direct interactions of tumour cells and stromal cells *in vivo* during tumour development and these are possibly achieved by establishing a transgenic zebrafish B cell lymphoma model.

The zebrafish immune system contains most if not all counterparts of human immune cells including macrophages, neutrophils, T cells and B cells, thereby providing a relevant model system. There are several transgenic zebrafish lines of immune system malignancies showing morphological and genetic similarity to human cancers. T cell acute lymphoblastic leukemia (T-ALL) models were established by either introducing the mouse *cmyc* or the

human T-ALL oncogene, *notch1*, into zebrafish under control of the *rag2* promoter (Langenau et al., 2004, Le et al., 2007, Langenau et al., 2003, Langenau et al., 2005). The only B cell malignancy thus far reported in zebrafish is a leukaemia model induced by over expression of TEL-AML1 (ETV6-RUNX1) under control of ubiquitous promoters, Xenopus elongation factor 1α or zebrafish β-actin (Sabaawy et al., 2006). However, no zebrafish B cell lymphoma model has so far been established.

3.1.1 Aims

Hypothesis:

Zebrafish will develop different types of B cell malignancies including leukaemia and lymphoma that mimic human cancers by over-expressing *cmyc* in B cells at different stages of B cell development.

My specific aims:

1. Generation and analysis of constitutive B cell-specific expression of cmyc-eGFP in driving B lymphocyte tumorigenesis in zebrafish.
2. Generation and analysis of inducible Cre/loxP recombination to conditionally control cmyc-driven B lymphocyte tumorigenesis in zebrafish.

3.2 Results

3.21 Generation of constitutive and inducible B cell-specific expression of oncogenic *cmyc* in driving B lymphocyte tumorigenesis in transgenic zebrafish.

In order to generate a B cell lymphoma model in transgenic zebrafish, it was essential to express a relevant oncogene under the control of an appropriate B cell promoter. I generated a plasmid construct harbouring mouse *cmyc* fused with enhanced green fluorescent protein (eGFP) under control of the B cell specific promoter, the major immunoglobulin M (*IgM1*) (Page et al., 2013) (figure 3.1 a).

This construct of IgM1:cmyc-eGFP, also contained *Tol2* transposon sequences and was co-injected with Tol2 transposase mRNA into one-cell stage embryos (Suster et al., 2009). The earliest IgM1 B cells appear between the dorsal aorta and posterior cardinal vein and also in the kidney around 20 days postfertilization (Page et al., 2013) and therefore green heart was used as the selection marker to screen embryos. Zebrafish embryos with fluorescent green lenses, resulting from crossing individual genetically mosaic F0 transgenics to wild-type (WT) fish and indicating the successful germline transmission of the transgene to the subsequent F1 generation (figure 3.1 b).

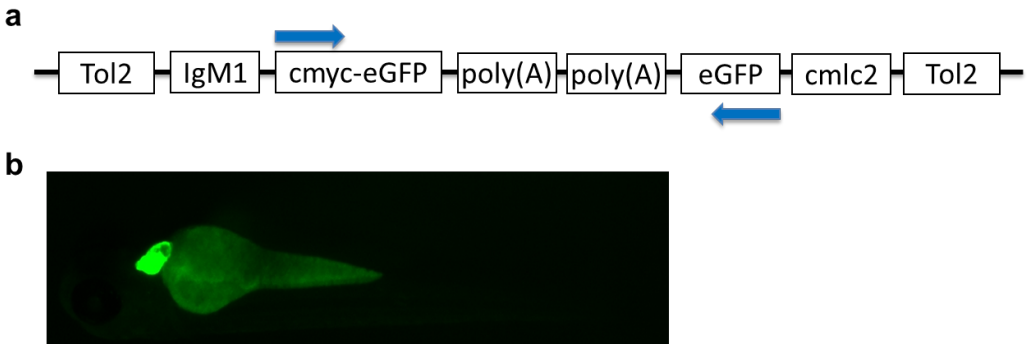

Figure 3.1 Schematic illustration of the strategy of generating spontaneous transgenic B cell lymphoma models in zebrafish

(a) Schematic depiction of the transgene utilized in the spontaneous model. (b) Representative image of generated F1 Tg(*IgM1::cmyc-eGFP*) transgenic fish with green heart as selection marker.

In order to image the early events by controlling cell transformation in a temporal manner, I generated an inducible Cre/loxP system to control B cell specific cmyc expression in transgenic zebrafish.

This transgenic system is comprised of two separate lines as depicted in Figure 3.2. The B cell driver line, Tg(*IgM1::Cre-ER*^{T2}), expressing the Cre-ER^{T2} in B cells under the IgM1 promoter. This line contained green heart as selection marker. The second effector line, Tg(*IgM1::LoxP-H2B-mCherry-LoxP-cmyc-eGFP*), contained a selection marker of blue lens. This transgene was also used as a B cell reporter in this project. Crossing the B cell-driver and cmyc-effector lines resulted in double transgenic offspring (figure 3.2).

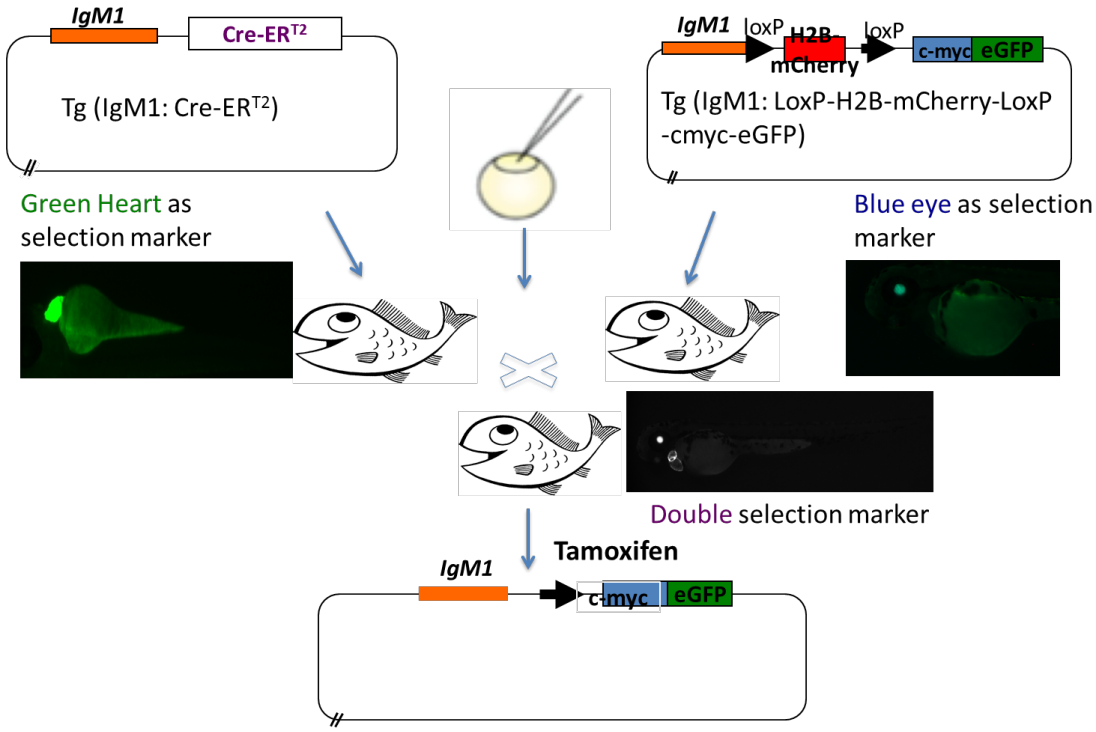

Figure 3.2 Schematic illustration of the strategy of generating inducible transgenic B-cell lymphoma models in zebrafish

Schematic depiction of the system design of Cre-LoxP regulated conditional model with representative images of generated transgenic fish.

3.2.2 Analysis of constitutive and inducible B cell-specific expression of oncogenic *cmyc* in driving B lymphocyte tumorigenesis in transgenic zebrafish

Tg(*IgM1::LoxP-H2B-mCherry-LoxP-cmyc-eGFP*) was not only the effector line of inducible model but also could be used as the B cell reporter line in this project. Tg(*IgM1::LoxP-H2B-mCherry-LoxP-cmyc-eGFP)* had B cells expressing mCherry signal.

Zebrafish head kidney, which is equivalent to the haematopoietic bone marrow of mammals and was chosen as the organ to observe B cells (Page et al., 2013, Ivanovski et al., 2009). But the position and structure of zebrafish kidney as a single, flattened organ that is adherent to the dorsal body wall via connective tissues made it difficult to directly observe mCherry

signal from intact adult zebrafish by fluorescent microscopy (Gerlach et al., 2011). Therefore, kidney was isolated from adult Tg(*IgM1::LoxP-H2B-mCherry-LoxP-cmyc-eGFP*) and cell suspensions from isolated kidney were analysed by FACS. The data showed the mCherry+ cells were found in the gating for lymphocytes and the percentage of lymphoid cells was similar to that of WT zebrafish (figure 3.3).

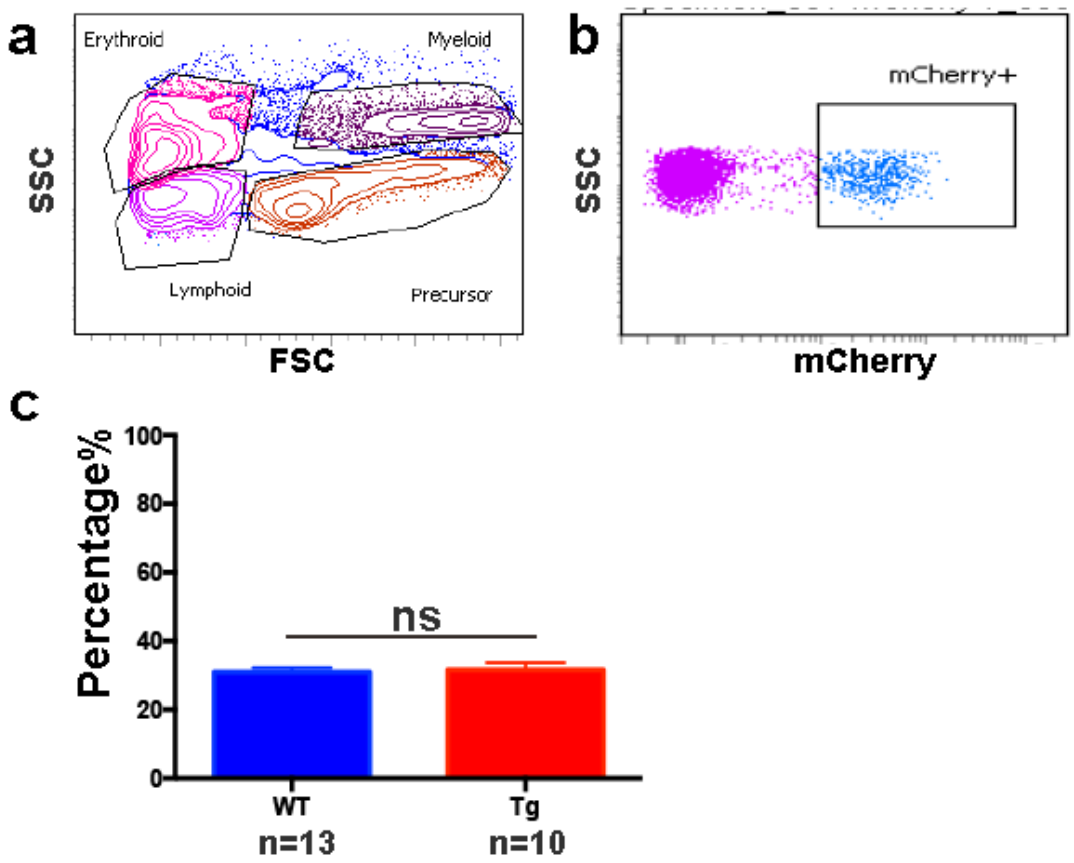

Figure 3.3 FACS analysis of Tg(*IgM1::LoxP-H2B-mCherry-LoxP-cmyc-eGFP*)

(a) The forward scatter (FSC) versus side scatter (SSC) profile of zebrafish Tg(*IgM1::LoxP-H2B-mCherry-LoxP-cmyc-eGFP*) whole kidney shows four cell populations: erythroid, lymphoid, myeloid, and precursor cells. (b) Scatter for mCherry expression of cells within the lymphoid gate. (c) Population of lymphoid cells gate among all cells isolated from zebrafish kidney of WT and Tg(*IgM1::LoxP-H2B-mCherry-LoxP-cmyc-eGFP*). (Error bar is means + SEM, Mann Whitney test, ns, p=0.7727).

No obvious abnormality was observed in larvae and adult zebrafish of Tg (*IgM1::cmyc-eGFP*) from F1 to F2. The possible reasons were 1) the expression level of cmyc in B cells in this model leads to B cells undergoing apoptosis, 2) the expression levels of cmyc driven by IgM1 were not high enough for tumorigenesis of B cells. Thus, cells from kidney of F2 Tg (*IgM1::cmyc-eGFP*) were analysed by FACS. The data showed that there were barely any GFP+ cells and the percentage of lymphoid cells was lower than that of WT zebrafish (figure 3.4).

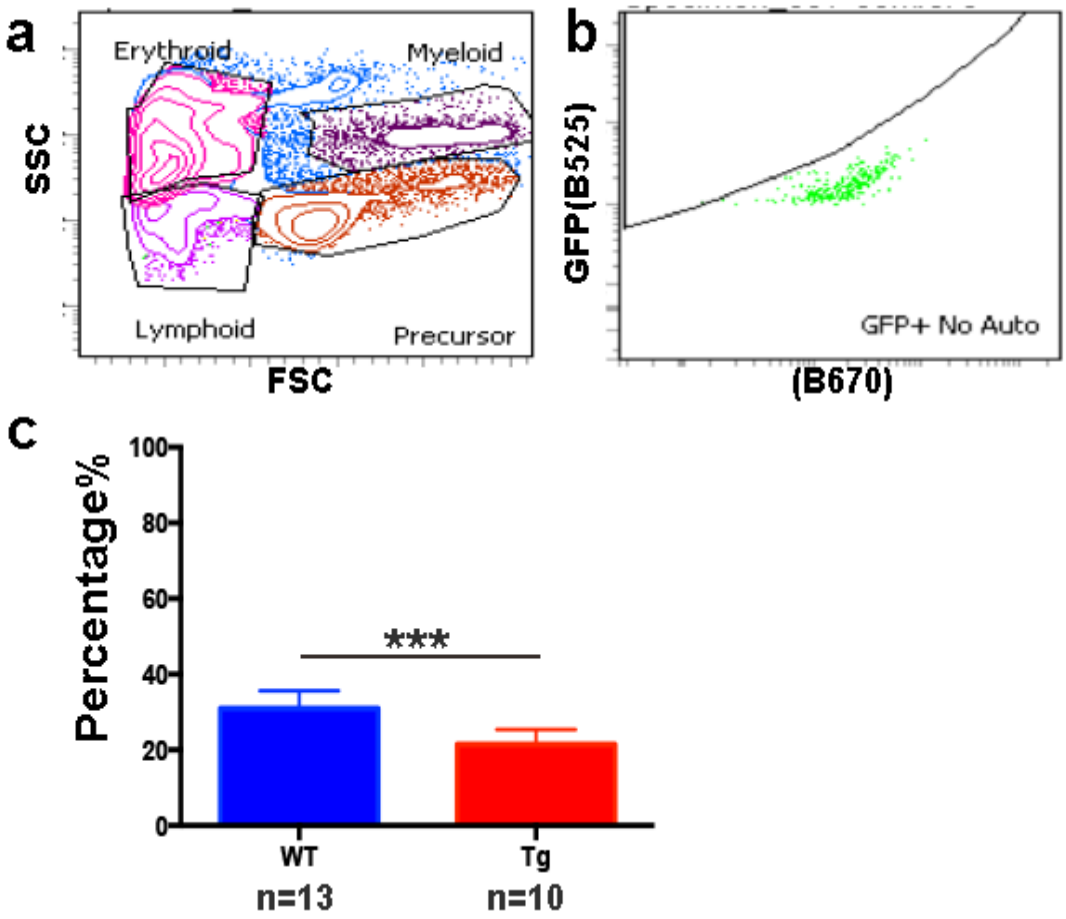

Figure 3.4 FACS analysis of Tg(*IgM1::cmyc-eGFP*)

(a) The forward scatter (FSC) versus side scatter (SSC) profile of zebrafish Tg(*IgM1:cmyc-eGFP*) whole kidney shows four cell populations: erythroid, lymphoid, myeloid, and precursor cells. (b) Scatter for GFP expression of cells within the lymphoid gate. The adjacent laser was used to exclude the auto-fluorescence. (c) Population of lymphoid cells gated among all cells isolated from zebrafish kidney of WT and Tg(*IgM1::cmyc-eGFP*). (Error bar is means + SEM, Mann Whitney test, ***p=0.0001).

3.3 Discussion

This chapter attempted to generate different types of B cell malignancies including leukaemia and lymphoma that mimic human cancers by over-expressing cmyc in B cells at different stages of B cell development.

Despite the evolutionary distance between fish and mammals, dating back 300 million years, the largely conserved genetic programmes between fish and mammals provides a possibility of using zebrafish to establish cancer models by transgene manipulation (Zhao et al., 2015, Etchin et al., 2011, Mione and Trede, 2010).

As the potent oncogenic roles of *cmyc* in BL is well established, and many successful transgenic cancer models in zebrafish rely on zebrafish promoters driving expression of human or mouse oncogenes (Langenau et al., 2003, Park et al., 2008a, Patton et al., 2005), zebrafish B cell specific promoter *IgM1* driven mouse cmyc expression was used to generate B cell lymphoma in this project.

Tg(*IgM1::cmyc-eGFP*) was generated to constitutively express oncogenic cmyc in B cells. Meanwhile, Cre/LoxP system was used to generate inducible B cell lymphoma models by controlling cell transformation in a temporal manner. This inducible system included two transgenes: the driver line, Tg(*IgM1::Cre-ER^{T2})* and the effector line, Tg(*IgM1::LoxP-H2B-mCherry-LoxP-cmyc-eGFP*). The latter transgene could be used as a B cell reporter in this project as they have mCherry labelled B cells.

Zebrafish kidney is a flattened organ and very fragile making it difficult to conserve structure during procedures including isolation, fixation. Moreover, the strong auto-fluorescence of the kidney increased the difficulty of

analysing B cells by fluorescence microscopy. Therefore, FACS was chosen as the method to analyse B cells in these transgenic models.

However, transgenic zebrafish Tg(I*gM1::cmyc-eGFP*) did not develop B cell malignancies. The FACS analysis showed lymphocyte depletion in head kidney of Tg(*IgM1::cmyc-eGFP*). There were very few green-labelled cells in the kidney suspension of Tg(*IgM1::cmyc-eGFP*) while Tg(*IgM1::LoxP-H2B-mCherry-LoxP-cmyc-eGFP*) had much more mCherry-labelled cells in the lymphocyte gated population. The percentages of different cell populations in kidney of Tg(*IgM1::LoxP-H2B-mCherry-LoxP-cmyc-eGFP*) are consistent with the literature (Traver, 2004, Chi et al., 2018). These data indicated a lack of a detectable B cell malignancy in Tg(*IgM1::cmyc-eGFP*) Instead cmyc over-expression in mature B cells might leads to cell death.

P53 is a well characterised tumour suppressor gene with mutations observed in many human cancers (Sherr, 2004, Olivier et al., 2002). Moreover, *p53* has been shown to regulate cell-cycle checkpoints and cell apoptosis (Berghmans et al., 2005, Levine, 1997) When *p53* is mutated, cells will lack apoptosis and cell-cycle arrest in response to DNA damage, leading to accumulation of mutations to cause oncogenesis. Therefore, a *p53-/-* mutant zebrafish (Berghmans et al., 2005) may provide the opportunity for *cmyc* transformed B cells to survive to initiate B cell lymphoma.

The efforts to generate B cell lymphoma models in zebrafish were not pursued further as the observations so far clearly indicate the difficulty in live imaging early events in B cell transformation in zebrafish kidney due to the late appearance of B cells (20dpf) and the anatomy of zebrafish kidney. Without the advantages of live imaging, it is not very appealing to generate B cell lymphomas for my research purposes given the established and relatively well-characterised murine models of B cell lymphoma (Mattarollo et al., 2012, Han et al., 2005, Liu et al., 2010, Donnou et al., 2012, Kovalchuk et al., 2000).

Chapter 4 Generation of zebrafish xenograft models of Burkitt's lymphoma

4.1 Introduction

Zebrafish xenograft models have contributed to our understanding of various cancer-related phenomena such as invasion, metastasis, angiogenesis, and cancer stem cell renewal due to their amenability for imaging and large-scale chemical genetic screening (Amatruda et al., 2002, Nicoli and Presta, 2007, Yen et al., 2014).

The zebrafish embryo is translucent allowing direct in vivo imaging of transplanted tumour cells, less challenging than other xenograft models. Therefore, zebrafish embryos are widely used to study tumour cell proliferation and metastasis. With the availability of transgenic zebrafish lines bearing fluorescently-labelled blood vessels, tumour angiogenesis is also being explored in zebrafish xenografts and have shown great potential. Significantly, zebrafish and human share common features in their immune systems ,in terms of development and cellular diversity, cell types, thereby providing a relevant model system to study interplay between malignant cells and the tumour microenvironment (Traver et al., 2003).

Many tumours, especially leukaemia, rhabdomyosarcoma, and melanoma have been intensively studied using zebrafish models (Langenau et al., 2005, Langenau et al., 2003, Langenau et al., 2007, van der Ent et al., 2014). However, there are no published studies of B cell lymphoma models in zebrafish.

Burkitt's lymphoma, with the characteristics of high rate of proliferation and extensive apoptosis, as an example of aggressive B cell lymphomas has been chosen to study the role of apoptosis in tumour progression in this project. Apoptotic cells have been shown to promote and coordinate tumour growth, angiogenesis and modulation of tumour-associated TAMs in

aggressive B cell lymphomas (Ford et al., 2015). The complex mechanisms underlying apoptosis-mediated tumour progression are still unclear, especially the early cellular events that are difficult to investigate in traditional mammalian models.

4.1.1 Aims

This chapter focuses on the generation of zebrafish xenograft models to observe the early events in Burkitt's lymphoma development with the aim of revealing possible roles for apoptotic tumour cells in promoting an oncogenic tumour microenvironment as suggested by mouse xenograft models.

My specific aims:

1. To establish a temperature that would allow both normal development of zebrafish embryos and uninhibited growth, viability and apoptosis rate in a human Burkitt's lymphoma cell line, BL2.
2. To observe the BL2 cells' behaviour in the zebrafish host, specifically the induction of lymph/angiogenesis.
3. To determine whether the extent of apoptosis in the transplanted inoculum influences BL2 cell growth in zebrafish.
4. To investigate whether macrophages facilitate the survival of BL in zebrafish.

4.2 Results

4.2.1 Identification of a temperature that meets the requirement for normal development of zebrafish embryos without significantly affecting BL cell proliferation and apoptosis

4.2.1.1 Assessment of temperature effects on zebrafish development

Zebrafish embryos were generated by natural mating of adult zebrafish according to a standard protocol (Westerfield, 1995a).

Zebrafish were housed at their optimum temperature of 28.5^{o}C for 2.5 days then for a further 5 days at various temperatures between 32^{o}C and 35^{o}C and the gross morphology of the embryos was compared. Those kept at 34^{o}C continued to develop normally (figure 4.1) but when maintained at 35^{o}C, some showed major deformations of the trunk (not shown). The size of the zebrafish larvae did not show large differences while some fish had darker skin, implying that pigment development may be enhanced by high temperature (not shown).

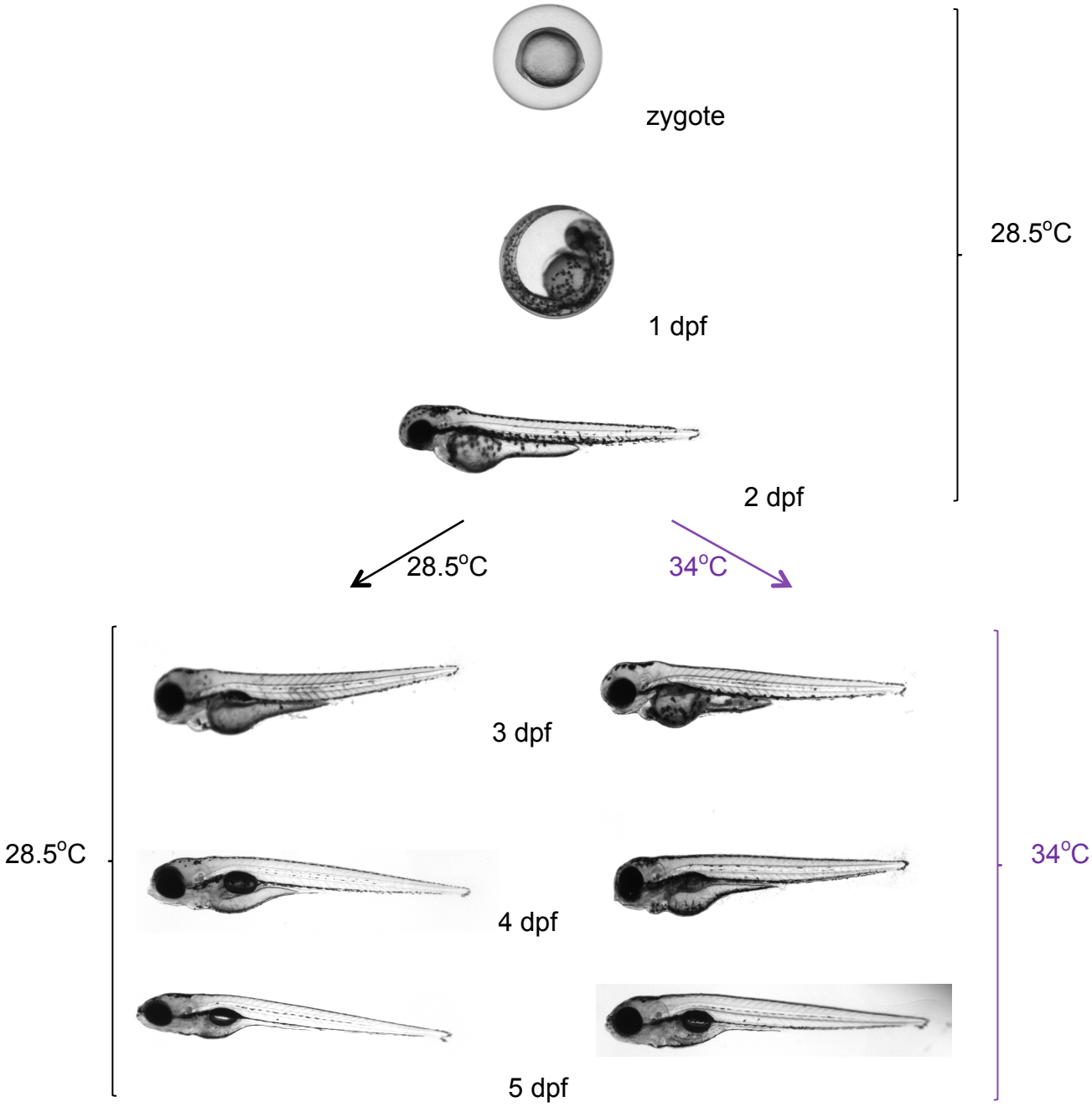

Figure 4.1 Normal development of zebrafish at 34°C from 2.5dpf to 5dpf

Zebrafish embryos were housed at 28.5°C until 2.5 dpf then some were transferred to 34°C for a further 2.5 days. Embryos housed at the higher temperature showed no obvious differences in gross morphology (over 50 embryos have observed).

4.2.1.2 Effect of reduced in vitro culture temperature on rates of growth and apoptosis of BL cells

BL2 cells were transferred from 37^{o}C to 32^{o}C incrementally by reducing the temperature by 1 or 2 degree per week. At each temperature (35^{o}C, 34^{o}C, 33^{o}C, and 32^{o}C), cell' growth conditions were monitored by trypan blue exclusion.

Cells cultured at 32^{o}C died after a week while those at 33^{o}C survived but grew slower than at 37^{o}C (figure 4.2).

At 34^{o}C and 35^{o}C the growth rates were slightly lower than those observed at 37^{o}C (figure 4.2). 33^{o}C, the lowest temperature which allowed BL2 cells to divide was chosen to further investigate the impact of reduced temperature on cells. The apoptosis-inhibited counterpart of BL2 cells, BL2-bcl2 cells showed similar responses to temperature change as they were able to proliferate at a lower rate (figure 4.3).

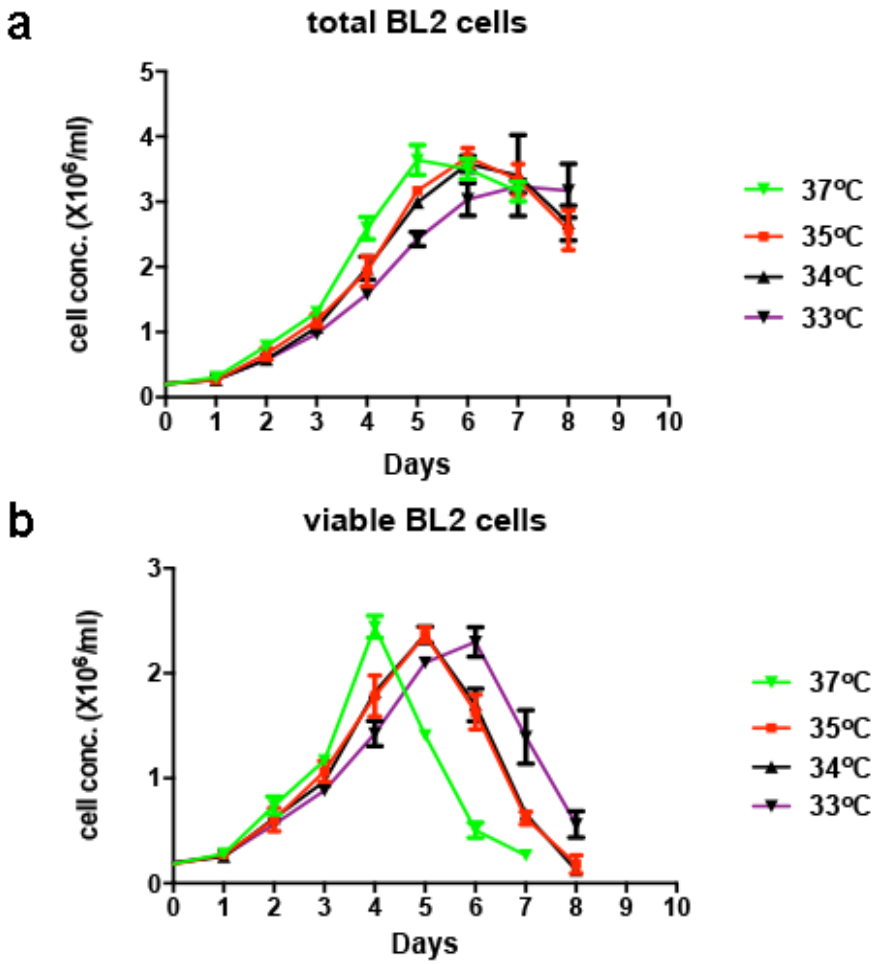

Figure 4.2 Proliferation of parental BL2 cells at various temperatures

Cells were adapted to in vitro culture at 33^{o}C by gradually lowering the temperature for 4 weeks and their total number counted daily by haemocytometer. Seeding densities were 0.2 x10^{6} cells /ml. (Data presented are means ± SEM for three independent experiments).

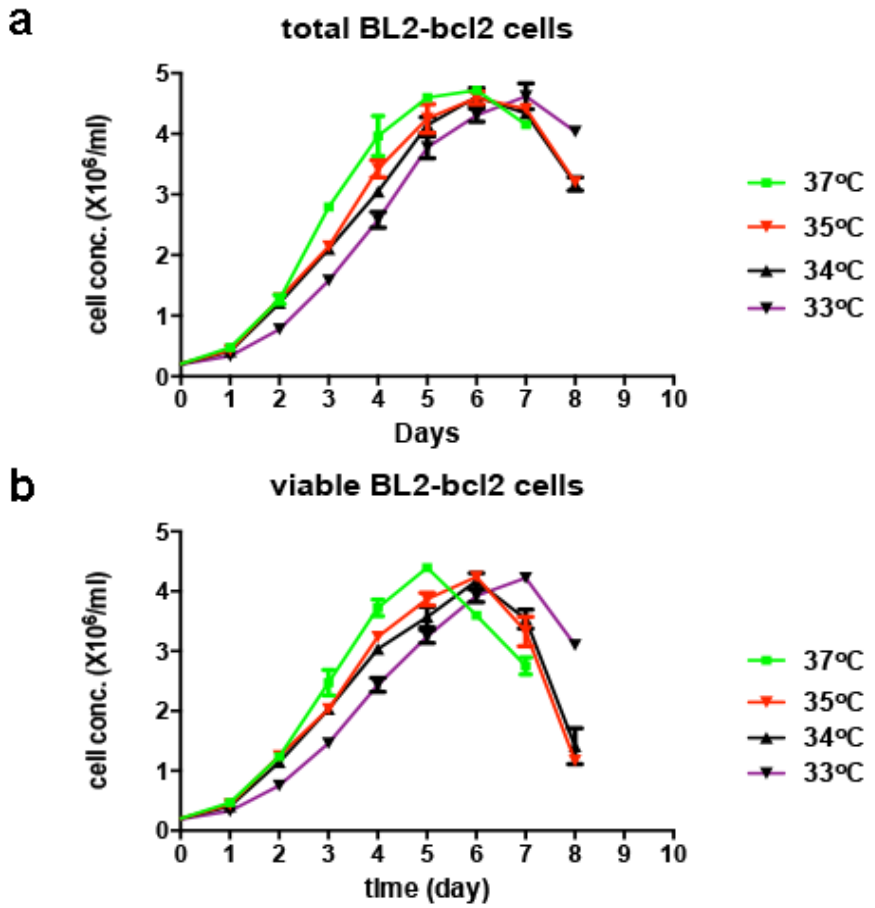

Figure 4.3 Proliferation of BL2-Bcl2 transfectants at various temperatures.

Cells were adapted to in vitro culture at 33^{o}C by gradually lowering the temperature for 4 weeks and their total numbers counted daily in a haemocytomete. Seeding densities were 0.2 x10^{6} cells /ml. (Data presented are means ± SEM for three independent experiments).

BL cells have a characteristically high rate of spontaneous apoptosis which has been suggested to contribute to development of tumours (Ford et al., 2015). Flow cytometric analysis of the binding of annexin V (AxV) and propidium iodide (PI) by the cells was used to assess apoptosis and membrane integrity (respectively) before and after exposure to UV radiation or the protein kinase inhibitor, staurosporine (Stau).

The viability of BL2 cells cultured at 33°C was slightly greater than those cultured at 37°C as indicated by the higher proportion of AxV+/PI- cells (fig 4.4). There were correspondingly fewer cells in early apoptosis as indicated by the lower proportion staining for AxV+ but PI-. However >90% of cells from both culture conditions were induced into apoptosis by UV irradiation or Stau as indicated by AxV binding. Flow cytometry results showed that the majority of BL2 cells growing at 33°C underwent apoptosis after UV or Stau treatment which is consistent with that of cells at 37°C (figure 4.4). These data showed that when the temperature was reduced to 33°C, cells maintained their sensitivity to apoptotic stimuli, as at 37°C.

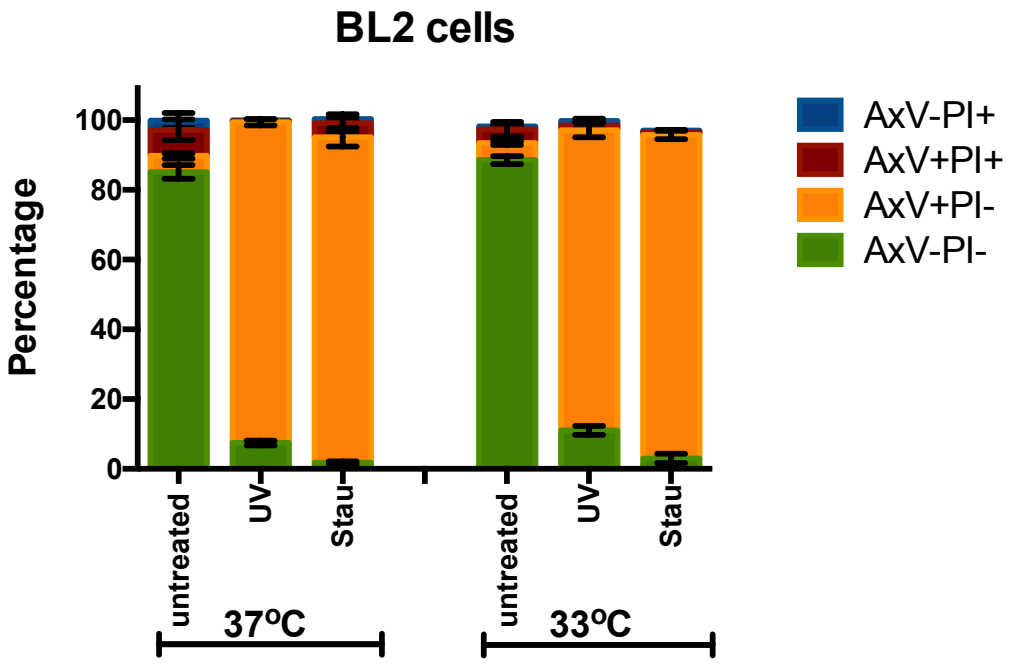

Figure 4.4 Induction of apoptosis of BL2 cells at 33°C

BL2 cells were induced by UV treatment and incubated in serum-free medium for 3 hours or were incubated in serum-free medium with 1μM staurosporine (Stau) for 3 hours before assessment by AxV/PI. Summary graph shows the percentage of viable (AxV-PI-), early apoptotic (AxV+PI-) late apoptotic (AxV+PI+) and necrotic cells (AxV-PI+) at 37°C and 33°C. (Data presented are means ± SEM of three independent experiments).

Binding of AxV and PI was also assessed for BL2 cells which over-expressed BCL2, a suppressor of apoptosis after UV-irradiation and stimulation with staurosporine. These *bcl2* transfectants served as control cells in transplantation experiments (see later). Less than 20% of these cells could be induced to undergo apoptosis when cultured at 37°C but a larger proportion was induced at the lower temperature (figure 4.5).

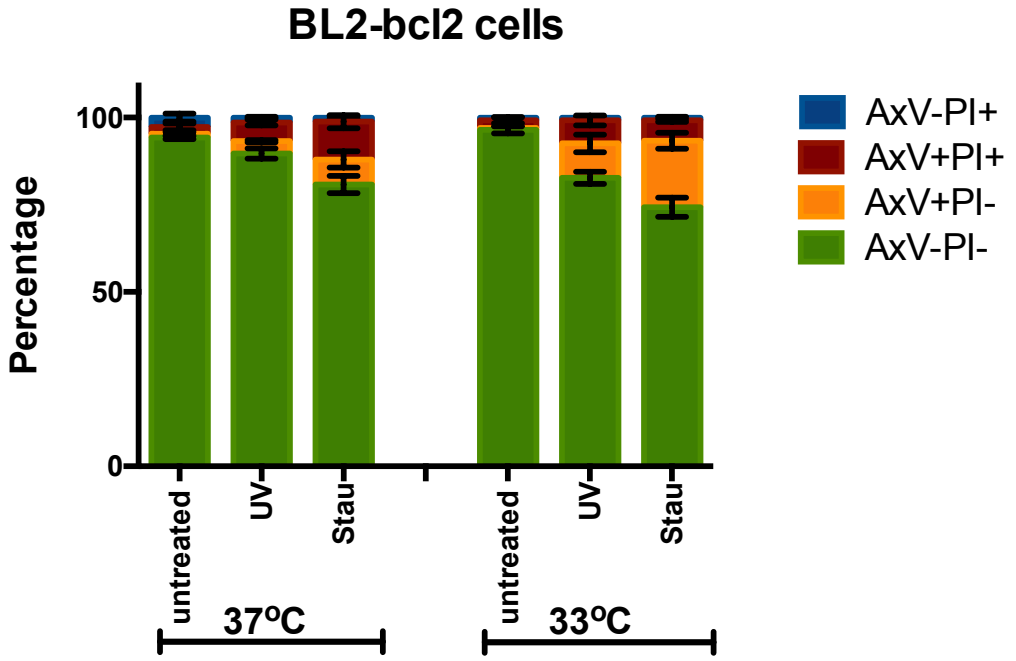

Figure 4.5 Commitment to apoptosis by UV or Stau induction can be inhibited by bcl-2 overexpression at 37°C and 33°C.

BL2-bcl2 cells were induced by UV treatment and incubated in serum-free medium for 3 hours or cells were incubated in serum-free medium with 1μM Stau for 3 hours before assessment by AxV/PI. Summary graph shows the percentage of viable (AxV-PI-), early apoptotic (AxV+PI-), late apoptotic (AxV+PI+) and necrotic cells (AxV-PI+) at 37°C and 33°C. (Data presented are means± SEM of of three independent experiments).

These results indicated that zebrafish develop normally at increased temperatures up to 34°C while BL2 cells retained their viability together with most of their proliferative capacity and potential for apoptosis as far as 33°C.

This provided a rational basis for the choice of a satisfactory compromise experimental temperature at which transplantation studies of BL2 cells into zebrafish could be performed. A temperature of 34^{o}C was chosen, allowing BL2 cells to proliferate and undergo apoptosis at rates near to those observed at their normal physiological temperature while maintaining healthy zebrafish larvae with unimpaired development. This balance is critically important when studying the interplay between tumour cells and their host environment so as to determine tumorigenic parameters, such as tumour cell invasion, metastasis and angiogenesis.

4.2.2 Construction of BL xenograft zebrafish models

In order to directly observe tumour cell behaviour in zebrafish embryos, BL2 cells were fluorescently labelled (figure 4.6). Fluorescent BL2 cells retain the properties of parental cells already described, at 34^{o}C.

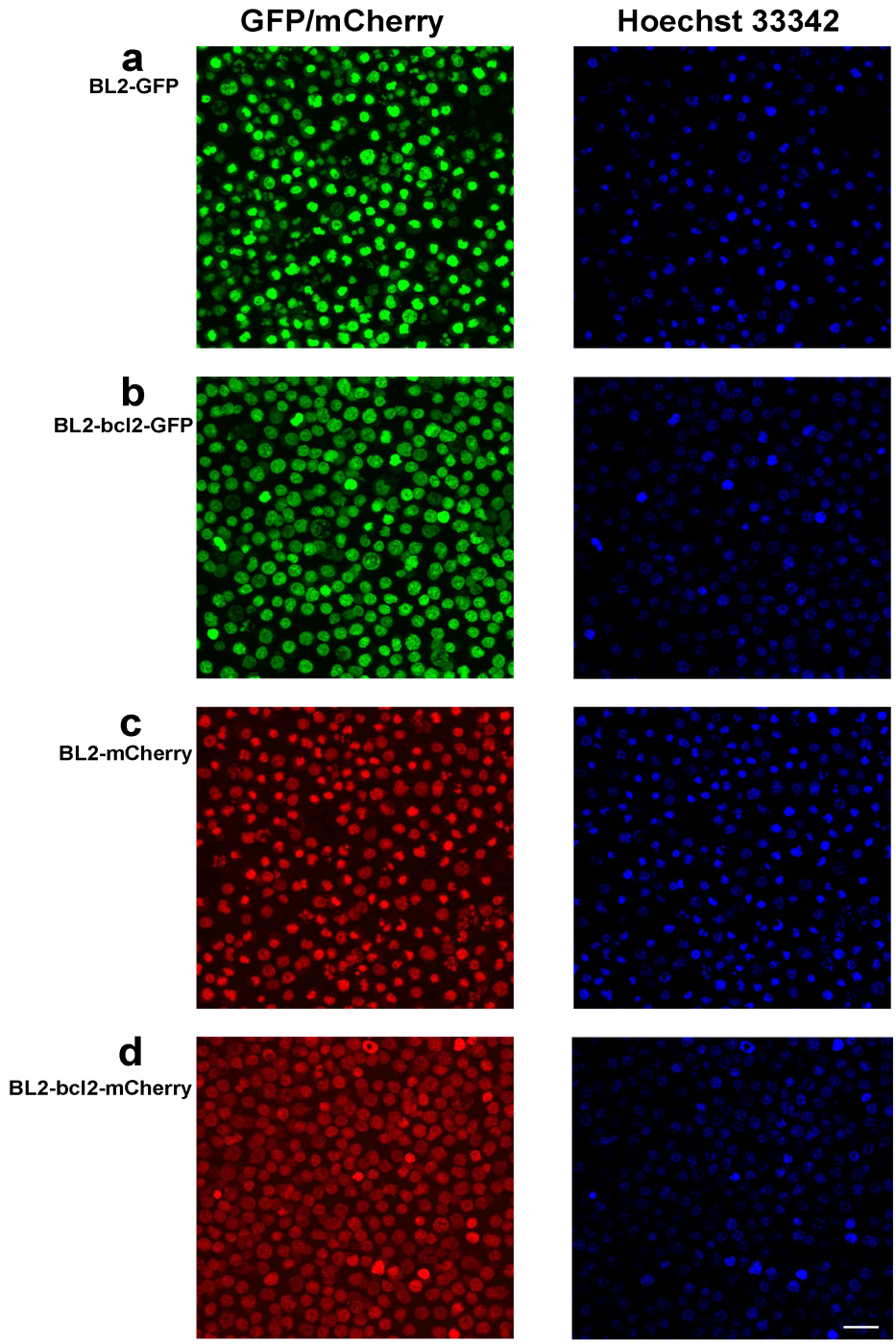

Figure 4.6 Generation of fluorescent-tagged BL cell lines

(a) BL2 cells were transfected with Lentivirus-cppt-emGFP-opre. (b) BL2-bcl2 cells were transfected with Lentivirus-cppt-emGFP-opre. (c) BL2 cells were transfected with Lentivirus-cppt-IRES-mcherry-opre. (d) BL2-bcl2 cells were transfected with Lentivirus-cppt-IRES-mcherry-opre. (Scale bar = 20 μm).

As shown in figure 4.7, prior to injecting BL2 cells at 2dpf zebrafish embryos were incubated at 28.5^{o}C. Fluorescence labelled BL2 cells were loaded into a pulled glass micropipette and the tip of the needle was inserted into the yolk sac of zebrafish embryo. The size of the tip was crucial and a sharp needle cut in the yolk reclosed immediately without any loss of contents. The yolk sac was chosen as the injection site as it has obvious advantages including relatively large transplantable cell burden. Moreover, for the angiogenesis study, the clear pattern of normal sub-intestinal vessels (SIV) in the yolk sac facilitates semi-quantitative detection of tumour induced angiogenesis (figure 4.8).

Zebrafish were observed by fluorescence microscopy at 1hpi to detect the labelled cells in the yolk sac and to select 'clean' injection embryos (figure 4.7). 'Clean' injected embryos were maintained in at 34^{o}C up to 5dpf when tumour formation, invasion and their association with angiogenesis or co-option of surrounding vasculature in the host were assessed by fluorescence microscopy. In order to address lymph/angiogenesis, transgenic zebrafish Tg(*flk1::mCherry*) (Jin et al., 2005) and Tg(*fli1::eGFP*) (Lawson and Weinstein, 2002) were employed. The former labels all blood vessels and the latter labels all vessels including blood and lymphatic vessels.

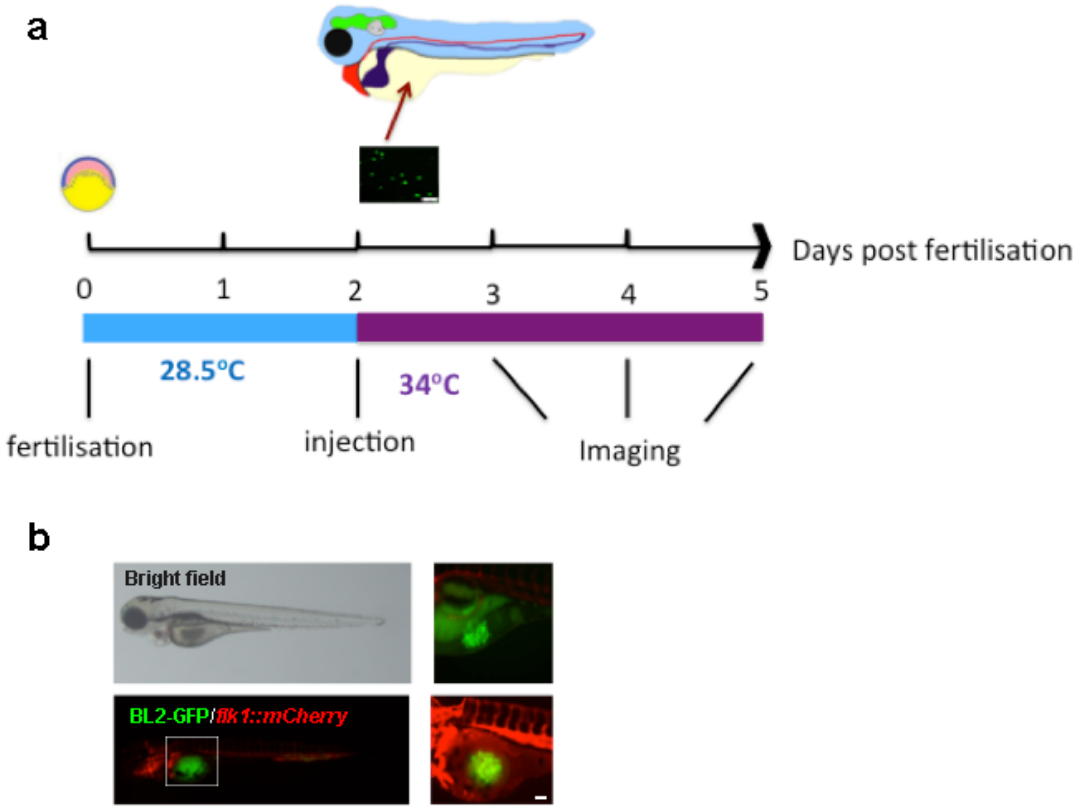

Figure 4.7 Schematic illustration of zebrafish xenotransplant lymphoma model

(a) Prior to injecting BL2 cells on 2 dpf, zebrafish were incubated at 28.5°C. Fluorescently labelled BL2 cells were injected into the yolk sac. Zebrafish were incubated at 28.5°C for an hour for recovery and then observed for the detection of a fluorescent cell mass localized at the injection site and to confirm a 'clean' injection. Selected xenografts were maintained at 34°C up to 5 dpf when images were recorded by fluorescence microscopy and confocal microscopy to study lymph/angiogenesis as well as interactions between cancer cells and stromal cells. (b) Representative photos of zebrafish xenografts bearing BL2-eGFP cells in the yolk sac of Tg(*flk1::mCherry*). (Scale bar = 100 μm)

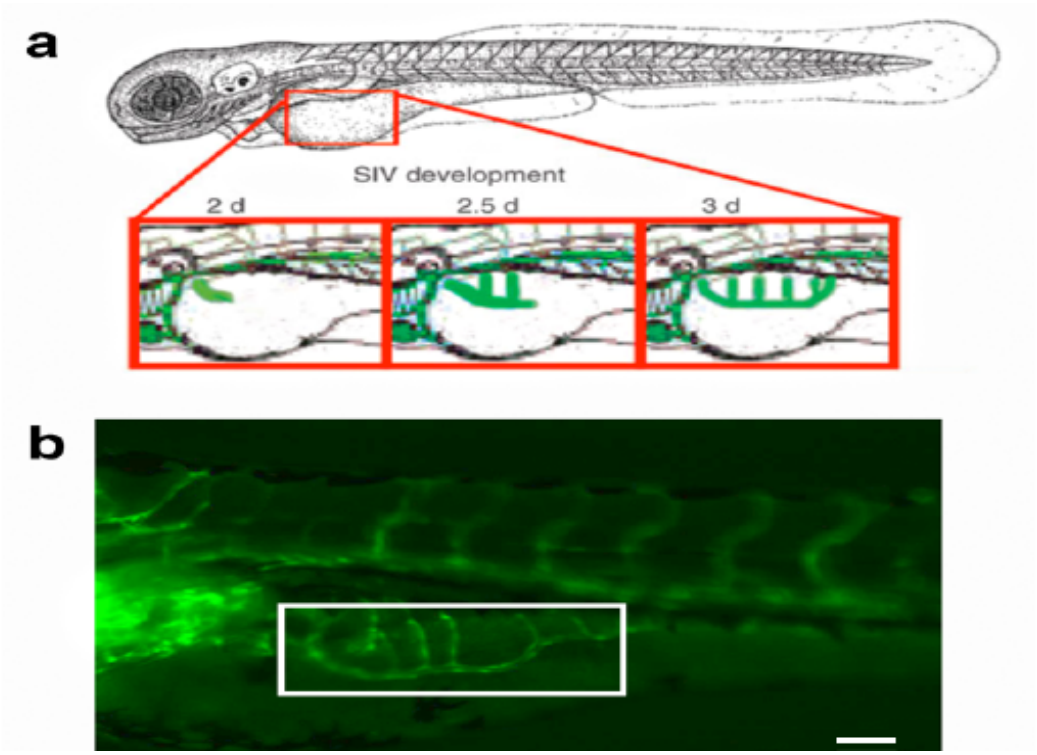

Figure 4.8 Normal SIV development in zebrafish embryo

(a) Schematic cartoon representation of SIVs in zebrafish from 2dpf to 3dpf (adapted from Stefania Nicoli & Marco Presta, 2007 (Nicoli and Presta, 2007)) (b) Lateral view of the normally developed SIV plexus of 3dpf Tg(*fli1::eGFP*). Square box indicates the SIVs where the induced angiogenesis is observed. (Scale bar = 100 μm)

4.2.3 Loss of proliferative capacity of BL2 cells in zebrafish: no detectable angiogenesis or metastasis

Since 2005 with the first transplantation of human tumour cells into zebrafish, the first and possibly most reported cancer cell lines in zebrafish xenograft models are highly tumorigenic melanoma cells (Lee et al., 2005). Therefore a human malignant melanoma cell line (A375) was used to assess the sensitivity of the putative zebrafish lymphoma model described here. A375 cells were labelled with Cyan or eGFP and referred to as M-eGFP or M-cyan here. The melanoma cells proliferated at the injection site and metastasized in the zebrafish after 3dpi and induced angiogenesis after 1dpi (fig 4.9). This is consistent with the literature and indicates the potential for engraftment of

human tumours into zebrafish (Lee et al., 2005, Nicoli et al., 2007, Haldi et al., 2006). This also confirmed that this optimised putative zebrafish lymphoma model was suitable to investigate the tumour cell proliferation, angiogenesis, and metastasis *in vivo*.

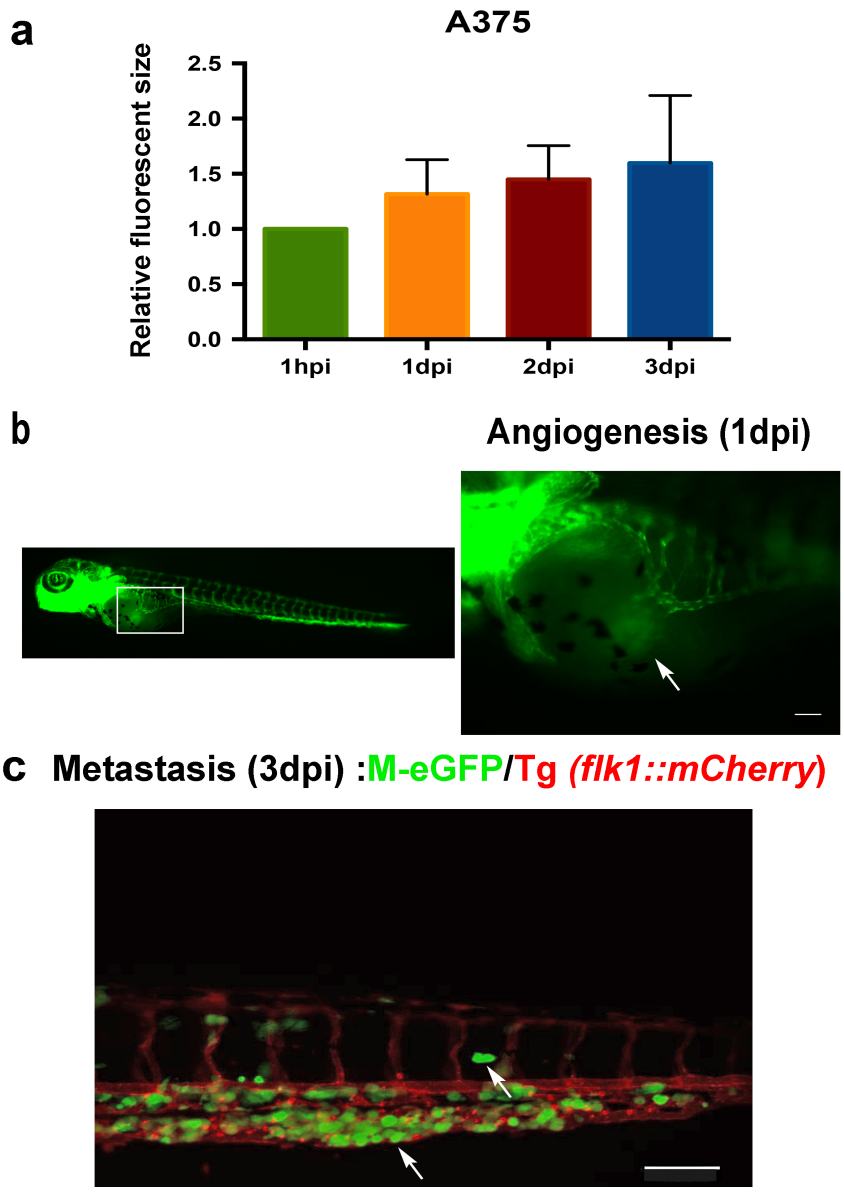

Figure 4.9 Transplanted human melanoma cells can form tumours in zebrafish

(a) Melanoma cells proliferated in zebrafish up to 3 dpi. (b) Melanoma cells induce angiogenesis (branches from SIV) within 1dpi in zebrafish Tg(*fli1::eGFP*). Arrow indicates the injected melanoma cells. (c) Melanoma cells metastasise and form tumour clogs in the tail of the Tg(*flk1::mCherry*) zebrafish favouring the circulatory loop at the end of the tail at 3dpi. Arrows indicate the melanoma cells. (zebrafish head to left of image, Scale bar = 100 μm)

BL2 cells however, did not proliferate in zebrafish and did not survive longer than 4 days. When 50 cells were injected, none could be detected at 2dpi while for injections of 200 to 500 cells, most of the xenografts have no detectable BL2 cells at 3dpi. When the injected cells were increased to 1000 cells per fish, 90% of xenografts still bore BL2 cells at 3dpf but lacked BL2 cells at 4dpf.Thus, the length of time in which they could be detected was associated with the implanted cell number. Different injected cell numbers were chosen for different aims in this project. For the angiogenesis assay, considering the increasing complexity of vessels in the trunk of embryos, it was desirable to induce angiogenesis in a relatively shorter time by increasing the injected cell number. Meanwhile, it was crucial to limit the size of injected cells and not to disturb the development of SIVs by physical stress. Therefore, 200 to 500 cells per fish the injected cells were chosen for the following angiogenesis assays. Zebrafish embryos bearing 200 or 500 BL cells in the yolk sac were observed daily until 3dpi and neither angiogenesis nor lymphoangiogenesis were detected (figure 4.10). Most of xenografts bearing 500 cells (left column in figure 4.10) had detectable tumour cells until 3dpi while most of xenograft bearing 200 cells (right column in figure 4.10) had detectable tumour cells until 2dpf. As shown in the figure, the size of transplanted cells did not decrease in the first 24 hours and started to decrease slowly until the final 24 hours before the cell mass disappeared. These observations suggested that the transplanted BL cells survived in the zebrafish until lack of certain factor(s) impacted on their viability, since most of the cells started to die in a synchronous manner.

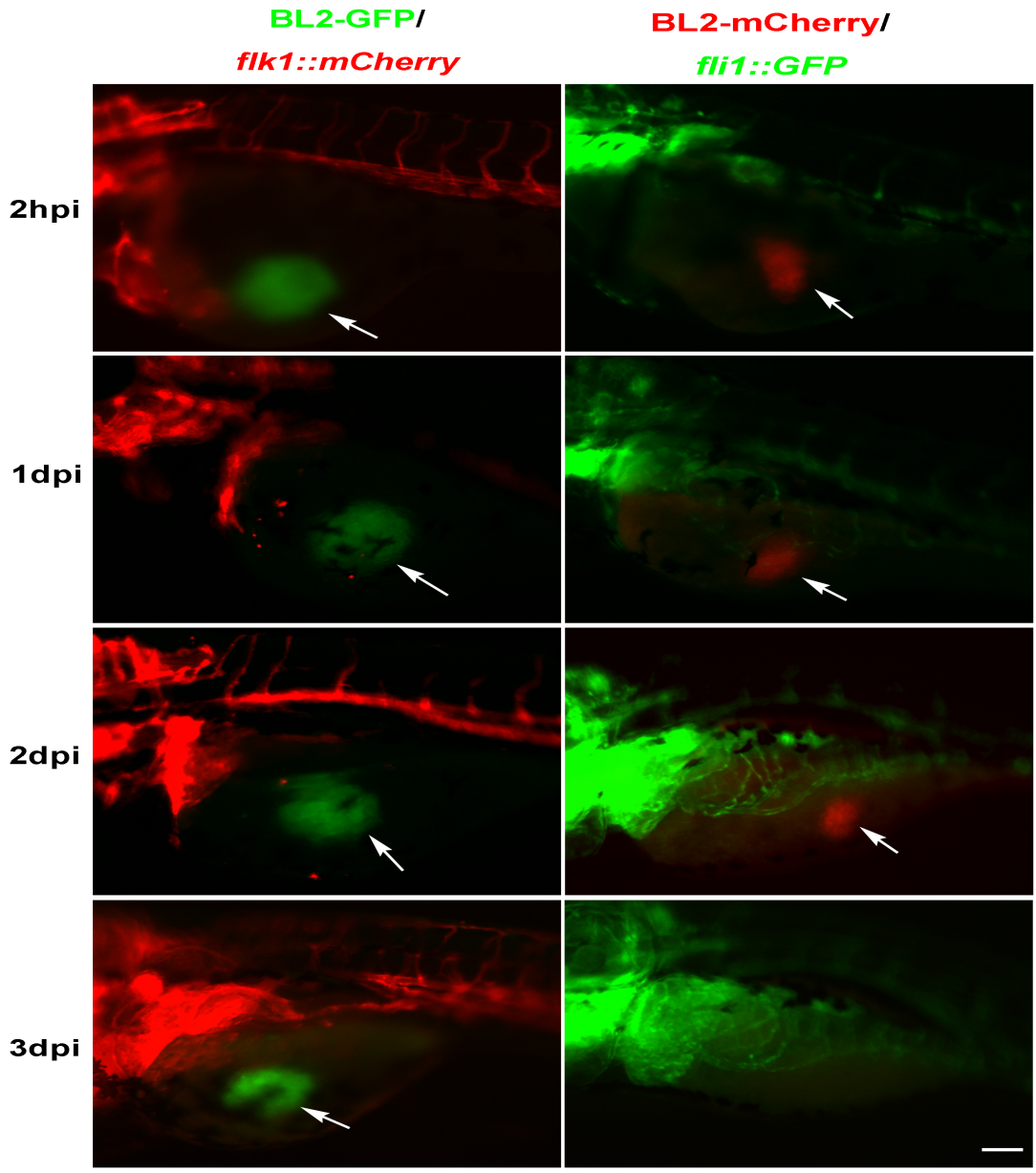

Figure 4.10 Transplanted BL2 cells did not induce lymph/angiogenesis

Representative fluorescence images represent zebrafish at 2 hpi, 1 dpi, 2 dpi and 3 dpi of injection of about 500 BL2-GFP cells into Tg(*flk1::mCherry*) (left lane, BL2-GFP/*flk1::mCherry*) or 200 BL2-mCherry cells into Tg(*fli1::eGFP*) (right lane, BL2-mCherry/*fli1::eGFP*). Arrows indicate the injected cells. No detectable lymph/angiogenesis in Tg(*flk1::mCherry*) and Tg(*fli1::eGFP*). (Total over 50 samples each group from 3 independent experiments were observed. Scale bar = 100 μm)

To further investigate cell behaviour, day-to-day observations were employed to study the activity of BL cells in zebrafish. BL2 cells were dying in zebrafish and did not survive over 4dpi irrespective of cell number transplanted. This survival assay used 1000 cells as transplanted cell number. Fluorescence photos of injected cells were taken from 1hpi daily until no detectable signal using the same magnification and the size of cells was calculated using Image J for two-dimensional area quantification (figure 4.11a). The proliferation of cells was assessed by phosphor-histone-3 (Histone-3) and all cells lost their proliferative capacity at 3dpi (figure 4.11b).

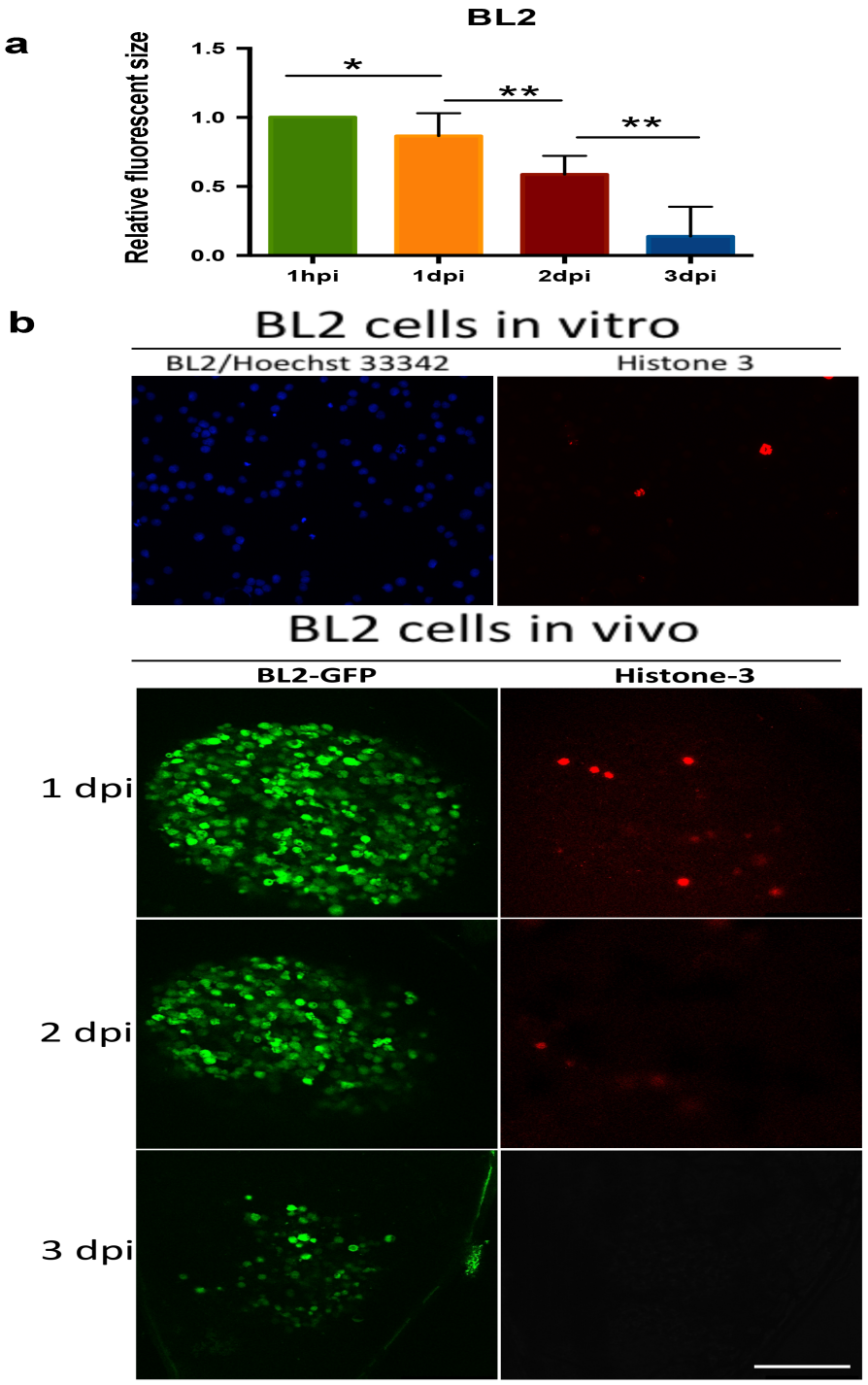

Figure 4.11 Transplanted BL2 cells lost proliferative ability

(a) BL2 cells were dying in zebrafish (Data presented are means± SEM of of three independent experiments. Mann Whitney test, *p<0.05, **p<0.01). (b) Histone-3 staining shows no proliferating BL2 cells from 3dpi in zebrafish. (Scale bar = 100 μm).

Despite transplanted cell viability loss by 3dpi and disappearance no later than 4 dpi, there was variability between xenografts. Therefore, time-lapse of cells in zebrafish were recorded and the results demonstrated that neighbouring BL cells died synchronously within 40 minutes (figure 4.12) and the whole cell mass disappeared. These data showed that the transplanted cells tended to die in a synchronous manner, which indicated that the failure of BL2 engrafted in zebrafish might be due to the lack of certain survival factor(s) or necessary tissue structure rather than the nutrient deficiency.

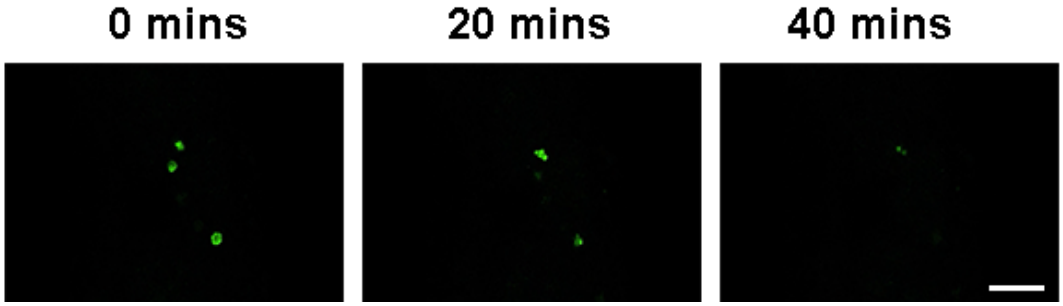

Figure 4.12 Neighbouring BL cells die synchronously

In a BL2 cells xenograft embryo, time-lapses of focused three neighbouring shows all three viable cells start to die synchronously and loose their fluorescent signals in 40 minutes. (Scale bar = 50 μm).

Since data so far had indicated the importance of environmental factors in supporting BL cell viability in zebrafish, other niches might promote BL cell survival in zebrafish. Therefore, most of the reported injection sites in literature were tested to determine whether there was a suitable niche for BL cell survival and proliferation in zebrafish (figure 4.13) and in all the xenograft sites tested, BL2 cells did survive over 4dpi. Injections sites included the yolk sac, the pericardial cavity, the brain, in the otic space, the perivitelline space (figure 4.13, a to e). Cells were also injected into circulation through duct of cuvier to see whether cells managed to locate at a favourable place to survive and injected cells reached posterior blood island within 15 minutes (figure 4.13, f). Some cells remained within caudal hematopoietic tissue while others left via blood and all of the cells died within 2dpi.

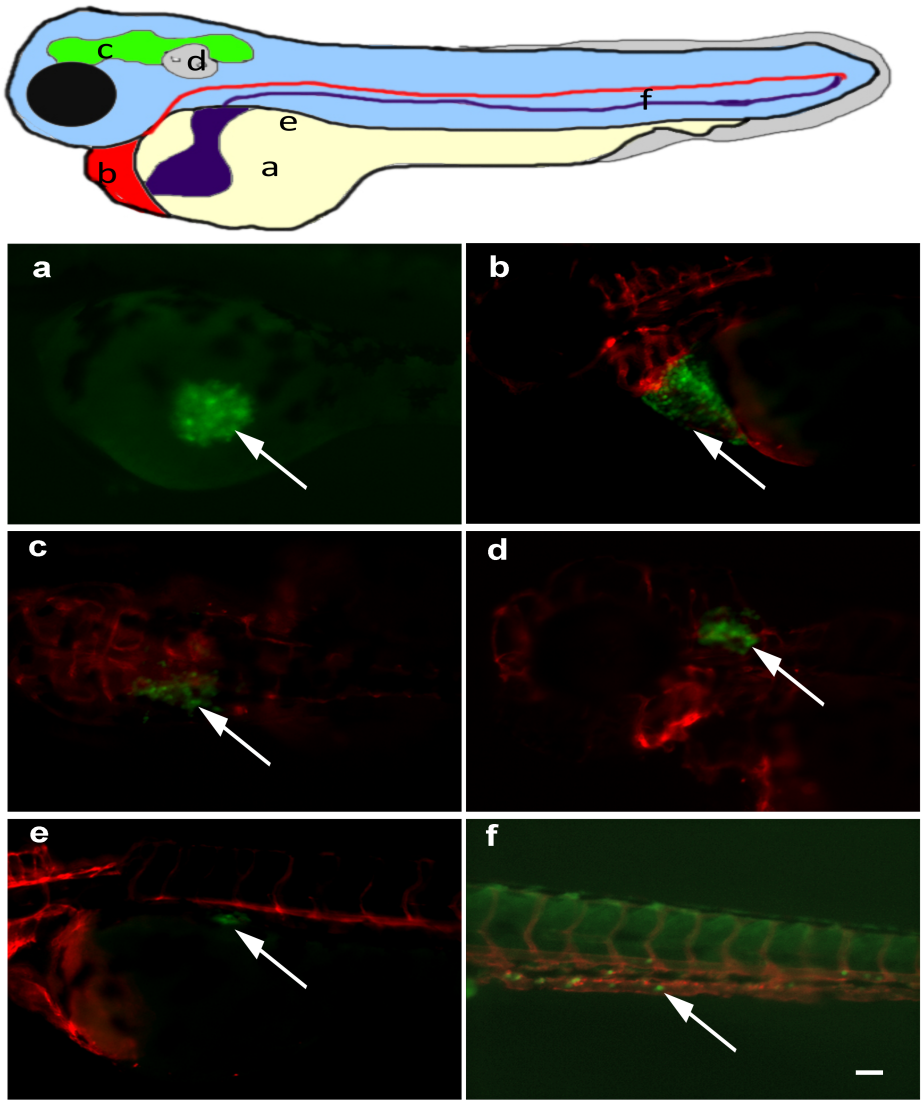

Figure 4.13 Representative photos of transplantation of cells into zebrafish

Cartoon provides the schematic depiction of injected sites of transplantation of BL2-eGFP cells in Tg(*flk1::mCherry* a. Cells transplanted in the yolk sac, b. Cells transplanted in the pericardial cavity, c. Cells transplanted in the brain, d. Cells transplanted in the otic space, e. Cells transplanted in the perivitelline space. f. Cells transplanted in the circulation. Arrows indicate the injected cells. (zebrafish head to left of images in a,b,d,e,f , dorsal view of zebrafish head in image c. Scale bar = 100 μm)

4.2.4 BL cells resistant to apoptosis demonstrated reduced capacity to survival in zebrafish

The transplanted BL2 cells cannot survive longer than 4dpi in zebrafish despite various injection sites including yolk sac, brain, perivitelline space, pericardial cavity and circulation. Even so, the yolk sac maintained cells longer than other sites, possibly due to the higher cell burden capacity.

The mouse xenograft models of BL established by our group demonstrated that apoptosis-suppressed BL cells showed an equivalent or slightly slower growth trend as compared to their ‘‘pro- apoptotic’’ parental counterparts (Ford et al., 2015). To determine whether apoptosis in lymphoma cells affects tumour growth in zebrafish, parental BL2 cells and their apoptosis-inhibited counterpart BL2-bcl2 cells were transplanted into the yolk sac of zebrafish. 1000 cells were chosen to transplant for these experiments aiming to achieve long survival without compromising zebrafish viability. For each experiment, approximately 20 embryos for each group were analysed including 1) embryos injected with medium only, 2) BL2 cells transplanted and 3) BL2-bcl2 cells transplanted were examined. All embryos survived and grew healthily during the experimental period. 90% BL2 transplanted zebrafish had visible tumour mass while only 55% BL2-bcl2 transplanted larvae displayed tumour mass 3dpi (figure 4.14).

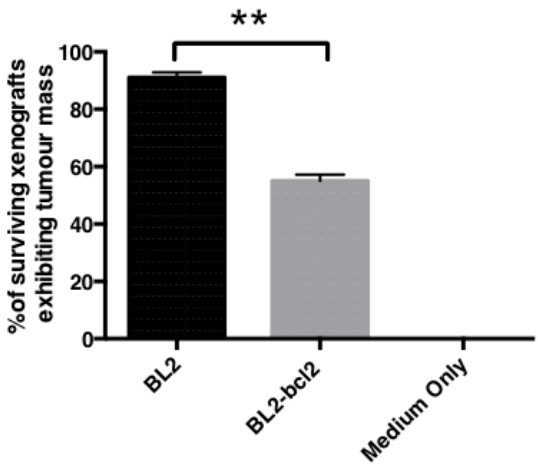

Figure 4.14 B lymphoma cells resistant to apoptosis demonstrated reduced capacity to survive in zebrafish

Growth of BL2 cells and BL2-bcl2 transfectant in fish at 34^{o}C 3dpf. (Data presented are means± SEM of three independent experiments, Mann Whitney test, p**=0.0079)

4.2.5 Macrophages are modulated by apoptotic BL cells

Within the BL umour microenvironment, macrophages contribute to a significant proportion of the tumour mass and unbiased "in situ transcriptomics" analysis-gene expression profiling have demonstrated apoptotic tumour cells modulate macrophages to promote a tumour growth phenotype in mouse models (Ford et al., 2015).

To investigate whether apoptotic tumour cells could polarise macrophages to a pro-tumour growth phenotype, peripheral monocyte derived macrophages (PMDM) were stimulated by apoptotic BL2 cells (referred as M2) and then co-injected with BL2 cells into zebrafish embryos. PMDM were treated with 50ng/ml LPS + 20ng/ml IFN and this treatment (referred as M1) was generally considered to activate macrophages to M1 subtype. Another group of PMDM underwent similar culture procedures without additional stimuli (referred as M0).

Macrophages with different polarisation were co-injected with 200 of BL2 cells into the YS of zebrafish. The ratio of macrophage and BL cells was 1 : 1, while 200 BL2 cells alone were injected as a control.

To see whether and how endogenous macrophages actively interact with injected tumour cells, I used transgenic line Tg(*mpeg1::mCherry/tnfα::eGFP*) in which macrophages express red fluorescent protein and when pro-inflammatory activated can also express fluorescent protein green (Nguyen-Chi et al., 2015) as TNFα (tumour necrosis factor alpha) is considered as a marker of M1 macrophages (Eisenman et al., 2015, Fiers, 1991).

The xenografts were examined at 2hpi, 1dpi and daily until either injected cells disappeared or fish died. Xenografts showed no significant difference in their interaction with endogenous macrophages and no TNFα activation in macrophages was seen in all groups (figure 4.15 a). The xenografts of all groups had no mortality in the first 48 hours (figure 4.15 a, b) and the

xenografts bearing the mixture BL2 and M2 macrophages showed high mortality at 3dpi while larvae in other group showed no significant viability change (figure 4.15b). As shown in figure 4.16 a, BL2 cells co-injected the M2 macrophage tended to spread along the outline of YS while the other group of BL2 cells maintained as a single colony at the injection site at 2dpi. This altered behaviour of BL2 cells may account for the high mortality of xenografts at 3dpi (figure 4.15 b).

At 3dpi, in the group of BL2 + M1 macrophage co-injection, only about 5% of the xenografts had live BL2 cells while the 72% of the BL2 + M0 macrophage co-injected fish had viable BL2 cells (figure 4.15 c).

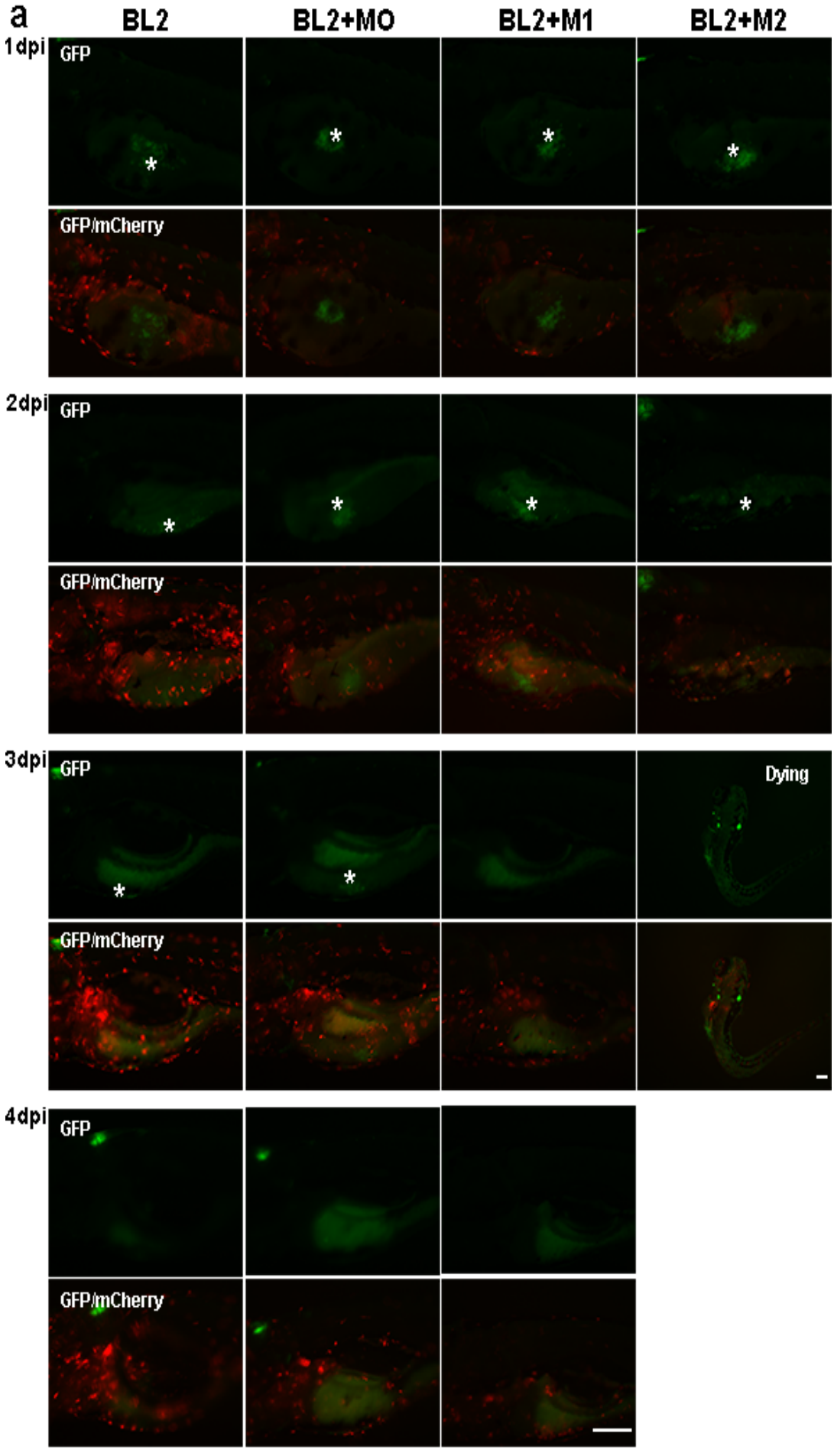
a
BL2
BL2+MO
BL2+M1
BL2+M2
1dpi
GFP
GFP/mCherry
2dpi
GFP
GFP/mCherry
3dpi
GFP
Dying
GFP/mCherry
4dpi
GFP
GFP/mCherry

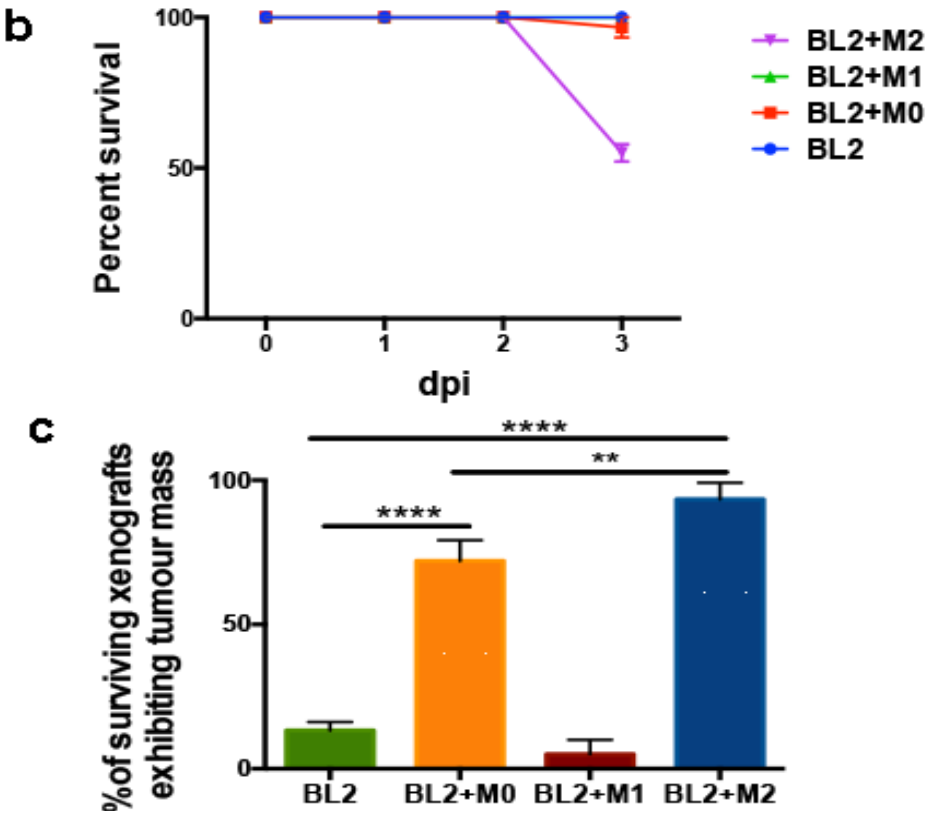

Figure 4.15 Apoptotic BL cells polarised macrophages facilitate xenograft BL2 cells survival in zebrafish larvae

a. Representative confocal images of Tg(*mpeg1::mCherry/TNFα::eGFP*) larvae bearing BL2 cells, BL2 cells with M0 macophages, BL2 cells with M1 macrophages from 1dpi to 4dpi and BL2 cells with M2 macrophages from 1dpi to 3dpi. At each dpi, upper panel shows the GFP channel and lower panel shows the overlay of GFP channel and mCherry channel. Stars indicate the injected cells. All the images except 'BL2 cells with M2 at 3dpi' are focused at yolk sac of zebrafish and 'BL2 cells with M2' show the whole fish body (Scale bar = 200 μm). b. Survival of xenografts from the day of injection to 3dpi. c. The percentages of living xenografts still have transplanted tumour cell at 3dpi (Data presented are means± SEM of three independent experiments, **p<0.01, ****p<0.0001, one-way ANOVA).

4.3 Discussion

The translucency of embryos and availability of many transgenic reporter zebrafish provides a clear advantage in studying early events in tumour angiogenesis and metastasis by allowing the visualization of fluorescently labelled human tumour cells and interaction with stromal cells (Lee et al., 2005, Haldi et al., 2006, Nicoli et al., 2007a, Marques et al., 2009, Tobia et al., 2011). This chapter focused on establishing a robust and reliable zebrafish model to study tumour cell behaviour and key events in tumour growth including angiogenesis and metastasis of B cell lymphoma with the aim of identifying mechanisms underlying apoptosis promotion of tumour growth.

In order to assess proliferation and migration of injected tumour cells in zebrafish, we generated fluorescent-tagged BL cell lines. And with the availability of other reporter lines allowing intravital imaging of cancer growth events, such as the fluorescent vascular system allowing the observation of lymph/angiogenesis induced by engrafted tumour cells; or macrophage reporter lines allowing the study of the interaction of macrophages and tumour cells.

The first part of this chapter was to optimise xenograft models for BL cells including the incubation temperature, the injection day, the injection site and the injection cell number dependent on the research purpose.

Zebrafish are normally maintained at 28.5^{o}C while human BL cells are cultured at 37^{o}C.The incubation temperature of xenograft zebrafish in the literature varied from 31^{o}C to 37^{o}C (Lee et al., 2005, Haldi et al., 2006, Nicoli and Presta, 2007). It was desirable to assess the highest temperature tolerance of zebrafish embryos and biological properties of BL2 cells at lower temperatures in order to establish a suitable compromised temperature.

An obvious problem in establishing xenograft human cancer models in zebrafish is that zebrafish are usually maintained at 28^{o}C and 9 degrees lower than that of mammalian cells. Studies on temperature effects on zebrafish embryo development are sparse. In the existing zebrafish xenograft models, the optimal incubation temperatures usually vary from 31^{o}C to 37^{o}C depending on the purpose of experiments and type of tumour cells used (Jung et al., 2012, He et al., 2012, Berman et al., 2012, Zhao et al., 2011, Tobia et al., 2011, Pruvot et al., 2011, Corkery et al., 2011, Moshal et al., 2010, Marques et al., 2009, Nicoli et al., 2007, Nicoli and Presta, 2007, Haldi et al., 2006, Lee et al., 2005). In this work, with the aim of mimicking the BL microenvironment, the temperature should be suitable for BL cells to proliferate and to maintain the parental phenotype of BL tumour cells. Growth kinetics and apoptosis assays were carried out at 35^{o}C, 34^{o}C, 33^{o}C, 32^{o}C and cells grew normally at 35^{o}C, 34^{o}C, 33^{o}C with reasonable decreased growth rates while cells incubated at 32^{o}C failed to proliferate. We also incubated zebrafish at different temperatures and observed their viability and morphology. Zebrafish seemed to grow healthily at 34^{o}C when some showed abnormal sharps maintained at 35^{o}C. Therefore, 34^{o}C represented a rational compromise: it allowed cancer cells to proliferate while maintaining zebrafish larval health and development, which is important when studying the interplay of tumour cells and tumorigenic parameters, such as tumour formation, invasion, metastasis, especially angiogenesis and with the advantage of highly regulated pattern of blood vessels in zebrafish (Isogai et al., 2001).

Various tumour cells and different transplantation sites of tumour cells into zebrafish embryo to study different aspects of tumour progression have been described in the literatures (Konantz et al., 2012, Wertman et al., 2016, Nicoli and Presta, 2007). For angiogenesis studies, the yolk sac and perivitelline space are the most popular sites. The primary embryonic vascular plexus of dorsal aorta (DA) and axial vein (AV) are formed by vasculogenesis by approximately 24hpf and by 3dpf, angiogenic vessels including the SIV have

formed. The organised pattern of SIVs make it a suitable model to study induced sprouting.

Optimal conditions for cell transplantation were established and these generated a reproducible xenotransplant zebrafish model using human BL cells. Parameters including the site and stage for transplantation, number of injected cancer cells, incubation temperature were optimised. Specifically, yolk sac can bear more cells than other injection sites. At 2dpf, the body plan of zebrafish is completely formed reducing the probability of passive transport during gastrulation. Up to 1000 cells within 10nl causes little surgical damage to zebrafish embryos. To avoid spatio interference of the SIVs development, 200 to 500 cells were used for angiogenesis assays and for proliferation studies up to 1000 cells were employed in this project.

BL cells were transplanted into the zebrafish yolk sac at 2dpf and checked daily until 5dpf. There was no detectable lymph/angiogenesis and no obvious metastasis in xenograft models. One possible explanation for no detectable lymph/angiogenesis is that BL cells are not aggressive enough to induce lymph/angiogenesis in this zebrafish model. Although there was some variability among fish, the cells were no longer detectable in xenografts at 4dpi. Engrafted BL cell death was measured by the fluorescent signals daily followed by immunohistochemistry experiments using phospho-histone H3. BL cells lost their ability to proliferate and just survived until they died in a synchronous manner. The lower injected cell number with decreased survival time indicate the failure of proliferation of BL cells in zebrafish might be caused by missing key growth-supporting factor(s) rather than nutrient deficiency. It is well known that zebrafish has no adaptive immune response at least till 10 dpf and the disappearance of BL cells happened in a relative short time. The most reasonable explanation is that BL cells started to undergo extensive apoptosis during this period due to the lack of certain factor(s) and were cleared by professional phagocytes such as neutrophils,

macrophages which develop at an early stage in zebrafish (Meeker and Trede, 2008, Renshaw and Ingham, 2010, Traver et al., 2003).

In other xenograft zebrafish models to study angiogenesis, more malignant tumour cells, mainly melanoma (Zhao et al., 2011, Haldi et al., 2006), or tumour cell lines that express the angiogenic FGF 2 and/or VEGF were used. I also used a human melanoma cell line (A375) as "positive control" to exclude the possibility of technical issues. Melanoma cells proliferate and induce angiogenesis in zebrafish. From observations of cell morphology and behaviour of BL2 cells and melanoma (A375) cells, it is easy to notice significant differences in that BL cells stick together and remain at the injection site while melanoma cells are much mobile and able to survive and even proliferate as single cells. Different tumour cells have their own growth patterns in human and this also is true for zebrafish.

The survival of BL cells in zebrafish was closely correlated with the injected tumour cell numbers and they seemed to prefer to stick with each other implying the supportive roles of tumour cells for each other. Moreover, the implanted tumour cells died in a synchronous manner and this may be caused by the lack of certain growth factor(s) or environmental cue(s) rather than the deprivation of nutrients in the YS.

In comparing the survival of BL2 and BL2-bcl2 cells, BL cells resistant to apoptosis demonstrated reduced capacity for survival in zebrafish indicating the pro-oncogenic role of apoptotic tumour cells.

Therefore, the next step was to provide a possible supportive player which might reveal a possible mechanism for supporting tumour growth. The supportive mechanisms of apoptosis might include direct interaction, secreted molecules, released vesicles and regulation of stromal cells in the tumour microenvironment. One possible candidate is the most abundant non-malignant cell population observed in Burkitt's lymphoma tumours (Wright,

1963). TAMs, which are attracted into the tumour niche and activate multiple pro-tumour pathways in mouse xenografts in unbiased ‘‘in situ transcriptomics’’ analysis (Ford et al., 2015). Despite the well-accepted notion of supportive tumour growth of TAMs, the details of how macrophages are polarised and how certain subtype influence the tumour cells behaviour are not fully understood.

PMDM were polarised by 1) apoptotic tumours, 2) traditional pro-inflammatory macrophage stimulation of cytokines (LPS and IFN) (Dale et al., 2008) 3) no external stimulation. Macrophages after different treatments were mixed with BL2 cells and transplanted to 2dpf embryos. To take advantage of the zebrafish model, I used transgenic fish Tg (*mpeg1::mCherry/tnfα::eGFP*) with macrophage fluorescent-tagged with cells turning green if expressing TNFα. When observed by fluorescent microscopy, there were no significant differences in macrophage numbers or morphologic features surrounding the injected cells. The reasons for this may lie in 1) at the selected time points there were no differences in the numbers and morphology of macrophages surrounding injected tumour cells, 2) the sensitivity of the fluorescent microscopy used cannot capture the differences between macrophages. However, the subtypes of macrophages modulated the tumour cell survival and behaviour differently. Macrophages polarised by apoptotic tumours gave the BL2 cells’ ability to survive as individuals even though this time length was quite short and cells died shortly after. The decreased survival of BL2 when co-injected with M1 was consistent with the known function of pro-inflammatory macrophages drive tumour cell death (Mosser and Edwards, 2008, Edwards et al., 2006, Li et al., 2018).

In conclusion, engrafted BL cells cannot proliferate in zebrafish and have no ability to induce lymph/angiogenesis. Reduced survival of apoptosis-inhibited human BL cells in zebrafish indicate the possible oncogenic properties of apoptotic BL cells. This model provides opportunities to dissect the mechanisms underlying oncogenic roles of apoptosis as well as the

signalling pathways that may be involved by co-injection of possible candidates with BL cells. One of the most promising candidates, macrophages, which are potent in a BL tumour microenvironment, was further investigated in this established model. Results indicated that macrophages could be polarised by apoptotic tumour cells and affect tumour cell behaviour and viability of xenografts.

Chapter 5 Pro-tumour growth role of apoptosis induced EVs (Apo-EVs) in B cell lymphoma

5.1 Introduction

The zebrafish embryo offers distinct advantages for studying aspects of tumorigenesis *in vivo*, in particular, angiogenesis and metastasis. This is mainly due to transparency of the embryo and the availably of fluorescent-labelled blood vessel reporter transgenic lines.

Various tumour cell types, such as melanoma cells (A375, WM-266-4, B16-BL16), ovarian carcinoma cells (MDA-MB-435, OVCAR8), colorectal cancer cells (ATCC), and glioma cells (U87) have shown the potential to proliferate, metastasise or induce angiogenesis in zebrafish (Konantz et al., 2012, Veinotte et al., 2014). However, BL cells do not form tumors in zebrafish possibly due to lack of essential growth and survival factor(s) as demonstrated by the results in chapter 4. The present chapter presents the results of experiments designed to identify possible candidate micro-environmental mechanisms in BL.

Constitutive high rates of apoptosis in BL foster the accumulation of TAMs (tumour associated macrophages), giving rise to the hallmark ‘starry-sky’ histological picture. Apoptosis-suppressed Bcl2-expressing BL populations demonstrated constrained proliferation in a mouse xenograft model, which suggests apoptotic cells could promote BL cell growth through recruitment of tumour-promoting TAMs (Ford et al., 2015). In situ transcriptomics analysis of TAM from BL indicates that TAMs are activated in a variety of ways to promote tumor growth (Ford et al., 2015). Furthermore, the reduced capacity of apoptosis-inhibited BL2-bcl2 cells to survive in zebrafish compared to their apoptosis-competent parental counterparts supports the notion that apoptosis of tumor cells might promote BL cell survival in the zebrafish model.

EVs appear to be released continuously from cancer cells and their release is increased by various stimuli. Several studies have shown that the molecular signature of EVs is characteristic of their cell of origin and is modulated by the type of stimulus suggesting that the activation regulates the non-uniform distribution of various contents compared to their originating cells and is closely associated with functions.

In the Gregory group, previous work has shown that EVs from apoptotic BL cells, called Apo-EVs contain higher level of B cell surface markers (CD19 and CD20), apoptosis associated proteins, DNA and RNA than EVs from viable tumour cells (Patience, 2016) (unpublished data). Furthermore, the presence of matrix metalloproteinases, MMP2 and MMP12 in Apo-EVs suggests the possibility that they may play regulatory roles in angiogenesis that is further confirmed by preliminary in vitro human umbilical vein endothelial cell (HUVEC) angiogenesis assays (Patience, 2016). It is possible that EVs from apoptotic BL2 cells can modulate the activation of TAM and drive angiogenesis which in turn promotes BL2 cell survival in a zebrafish larval model.

5.1.1 Aims

The hypothesis underlying this chapter is that the EVs released from apoptotic BL cells (Apo-EVs) modulate host macrophages and promote angiogenesis which in turn promotes BL2 growth *in vivo.*

My specific aims:

1. To determine the profile of apoptosis-mediated EV release
2. To compare the pro-angiogenic effects of Apo-EVs with EVs obtained from non-apoptotic BL cells stimulated *in vivo*
3. To compare the pro-angiogenic effects of secretome from apoptotic BL cells and Apo-EVs with secretome obtained from non-apoptotic BL cells stimulated and non-Apo-EVs *in vivo*
4. To assess whether Apo-EVs selectively recruit and/or activate macrophages

5.2 Results

5.2.1 Characterisation of EVs released from B cell lymphoma cells

In Chapter 4, results showed that both staurosporine and UV treatments were capable of inducing apoptosis in BL2 cells while BL2-bcl2 cells did not undergo apoptosis due to their expression of BCL2. To generate apoptosis related EVs (Apo-EVs), BL2 cells were induced to undergo apoptosis by UV treatment. EVs from UV-treated BL2-bcl2 cells were used as the control since their production is not through apoptosis. Here I use non-Apo-EVs to describe the EVs from BL2-bcl2 cells after UV treatment.

Firstly, the time course of apoptosis after UV treatment was studied. Cell death was assessed by the exposure of PS on the outer membrane by AxV and membrane integrity was assessed by PI. Apoptotic cells were measured by AxV+PI- staining and the percentage of apoptotic cells (AxV+PI-) reached a peak at 4 hours post UV treatment (figure 5.1a). At 4 hours post UV treatment, the apoptotic population was normally between 60% and 80%. When the culture time was increased to 6 hours, the percentage of apoptotic cells (AxV+PI-) showed a decreasing trend and the population of late apoptosis (AxV+PI+) increased by over 20%. Therefore, BL2 cells at 4 hours after UV treatment were chosen as the provider of Apo-EVs. Meanwhile, BL2-bcl2 cells were treated and assessed by the same procedure. The results showed that 4 hours after UV treatment, only a very small percentage of BL2-bcl2 cells underwent apoptosis (less than 5%) (figure 5.1b) and therefore was a suitable control for apoptotic cells.

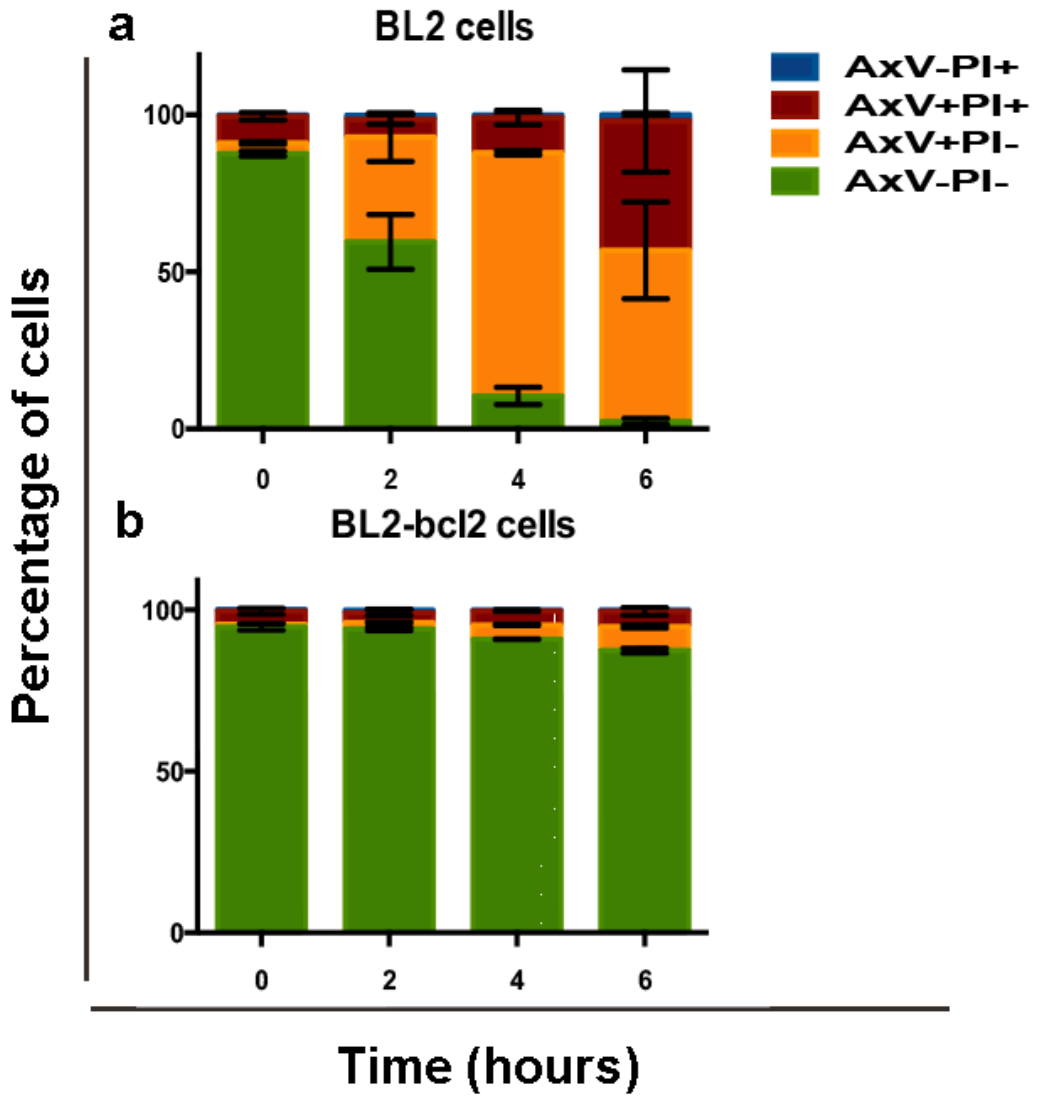

Figure 5.1 UV treatment timecourse of BL cells

(a) Flow cytometry for annexin V (AxV) and propidium iodide (PI) showing UV-irradiation induces apoptosis in BL2 parental cells and the apoptotic population increases until reaching its peak at 4 hours post treatment. (b) Flow cytometry for annexin V (AxV) and propidium iodide (PI) showing UV-irradiation barely induces apoptosis in Bcl-2-expressing BL2 cells. (Mean ± SEM of three independent experiments).

For all the Apo-EVs preparations in the presented data, the percentage of apoptotic BL2 cells (AxV+PI-) was monitored to make sure the percentage of apoptotic cells was above 60 % while the late apoptotic population (AxV+PI+) did not exceed 20 % and the percentage of necrosis (AxV-PI+) did not exceeded 5 %.

EVs released from BL2-Bcl2 cells that had been treated by UV and gone through similar isolation procedures were used as the control representing EVs produced from non-apoptotic cells (non-Apo-EVs). Isolated Apo-EVs and non-Apo-EVs were measured by nanoparticle tracking analysis (NTA). NTA has been shown as a method to accurately determine EV size and concentration in our group. Although UV treated BL2-Bcl2 cells also released non-ApoEVs, the NTA results demonstrated that significantly more EVs produced by UV treated BL2 cells which correlated with increased apoptosis of BL2 cells (figure 5.2a). Furthermore, NTA also demonstrated a different size profiles between Apo-EVs and non-Apo-EVs (figure 5.2b).

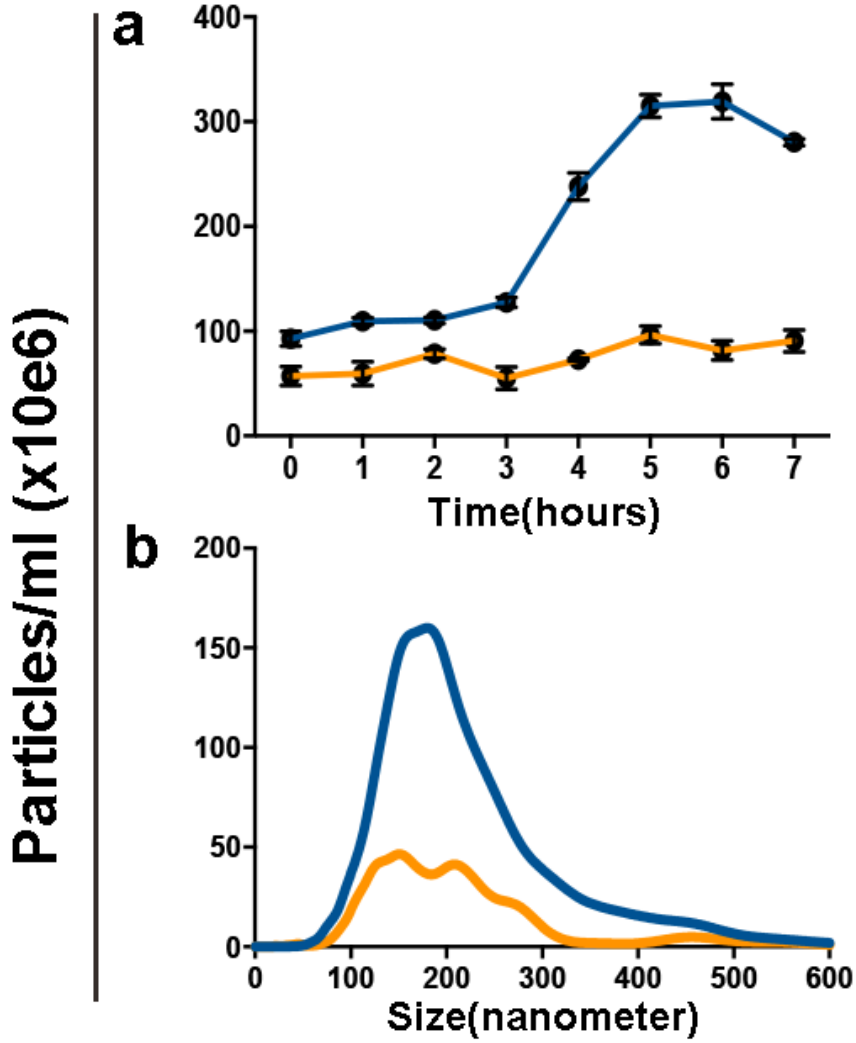

Figure 5.2 Production of EVs by BL cells is apoptosis associated

(a) Nanoparticle tracking analysis (NTA) showing increased release of EVs from BL2 cells in line with increased apoptosis (Mean ± SEM of three independent experiments). (This work was performed by Margaret Paterson in our group). (b) NTA size profiles demonstrate different size profiles between Apo-EVs (blue line) (EVs from BL2 cells 4 hours post UV treatment) and those from bcl2-transfected BL2 cells 4 hours post UV treatment (orange line) representing non-Apo-EVs. Typical profiles from three independent experiments.

5.2.2 Apo-EVs induce angiogenesis in zebrafish

Zebrafish embryos provide a convenient model to study angiogenesis. At 2.5 dpf, the zebrafish body plan has fully developed and SIVs grow in a tightly organised fashion. Based on the findings of chapter 4, the yolk sac of 2.5 dpf Tg(*fli1::eGFP*) zebrafish was chosen as the injection site of EVs. Induced branches from SIVs was observed at 24 hpi with stereo-fluorescent microscope (figure 5.3).

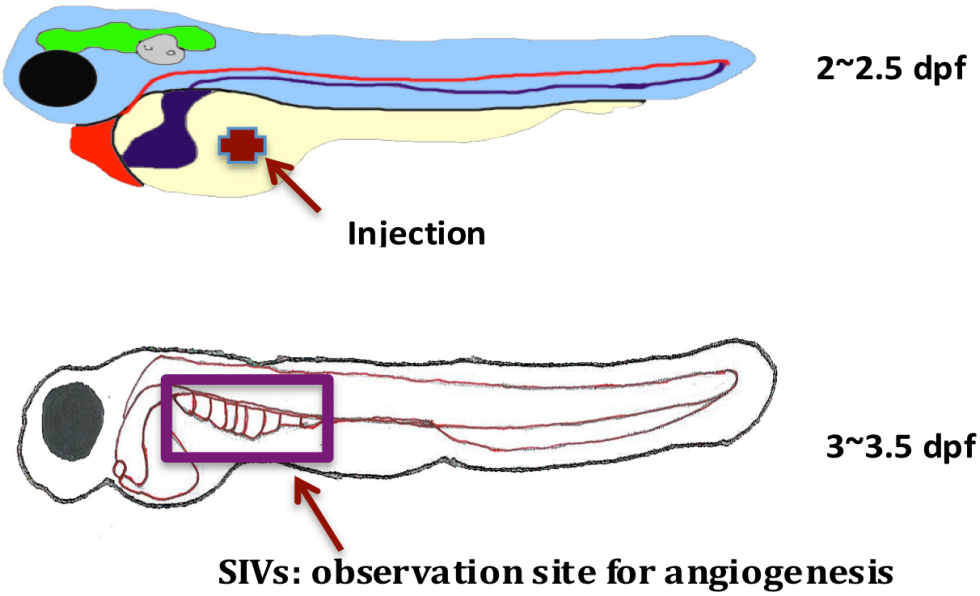

Figure 5.3 Schematic illustration of zebrafish model for EVs-induced angiogenesis assay

EVs were injected into the yolk sac at 2.5dpf and blood vessel pattern were observed 24hpi. Zebrafish were kept at 28.5°C.

Initially, a 3-Step Differential Centrifugation Method (details in chapter 2) was used to obtain Apo-EVs and cell number was used as the reference for quantifying Apo-EVs. Approximately 20nl of EVs from $80x10^6$ UV treated BL2 cells in 100µl DPBS were injected to assess the pro-angiogenic functions of Apo-EVs. EVs from UV treated BL2 cells were injected into the yolk sac of GFP-labelled vessel zebrafish Tg(*fli1::eGFP*). At 24 hpi, 30% of EV xenografts showed induced branches and 5% of xenografts exhibited malformation with significant difference from mock controls (figure 5.4).

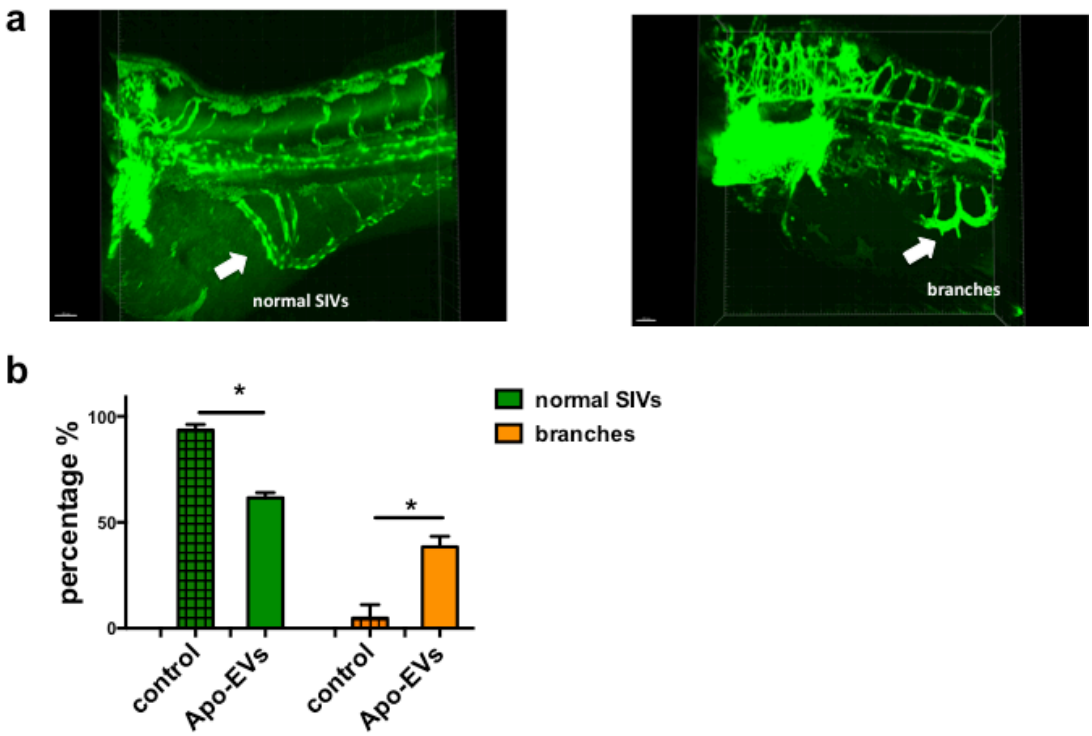

Figure 5.4 Apo-EVs modulate angiogenesis in zebrafish

(a) Representative images of SIVs following different treatment. Arrows indicate observation sites. (b) Statistical anaysis shows promotion of angiogenesis by Apo-EVs. Xenografts of Apo-EVs show about 35% branches with a significant difference from mock controls (Mean ± SEM of three independent experiments, Mann Whitney test, *$p<0.05$).

These preliminary observations showed the EVs from apoptotic BL2 can induce angiogenesis *in vivo*. To further confirm that this pro-angiogenic function was Apo-EV specific, effect of non-Apo-EVs were evaluated in subsequent experiments. The isolation method for EVs was continually optimised in our group and the gentle filtration method (details in chapter 2) was shown to produce EVs with high consistency and integrity. Therefore, all the subsequent EVs experiments used filtration method. Furthermore, as shown in figure 5.2, the number of EVs was related to the number of apoptotic cells and apparently the same number of BL2-bcl2 cells produced much less EVs by the same treatment. Therefore, for the comparison of EVs from BL2 and BL2-Bcl2, I used the number of EVs rather than parental cell number as the standard for injection purposes. To exclude possible angiogenic effects of soluble molecules released by apoptotic BL cells, EVs were purified by 300kDa ultrafiltration before the angiogenesis assay. I tried different amounts of EVs and found that 10^7 particles/fish was a suitable amount. The sprouting from zebrafish SIVs was detected and quantified approximately 24hpi (figure 5.5).

Control zebrafish were injected with media under the same treatment and barely induced branches from SIV (figure 5.5 a i). Apo-EVs induced on average over 1.5 branches per fish while non-Apo-EVs induced slightly over 0.5 branch per fish (figure 5.5 b). The pooled data presented here clearly indicated that EVs released from apoptotic BL cells have a significantly higher ability to induce angiogenesis (figure 5.5).

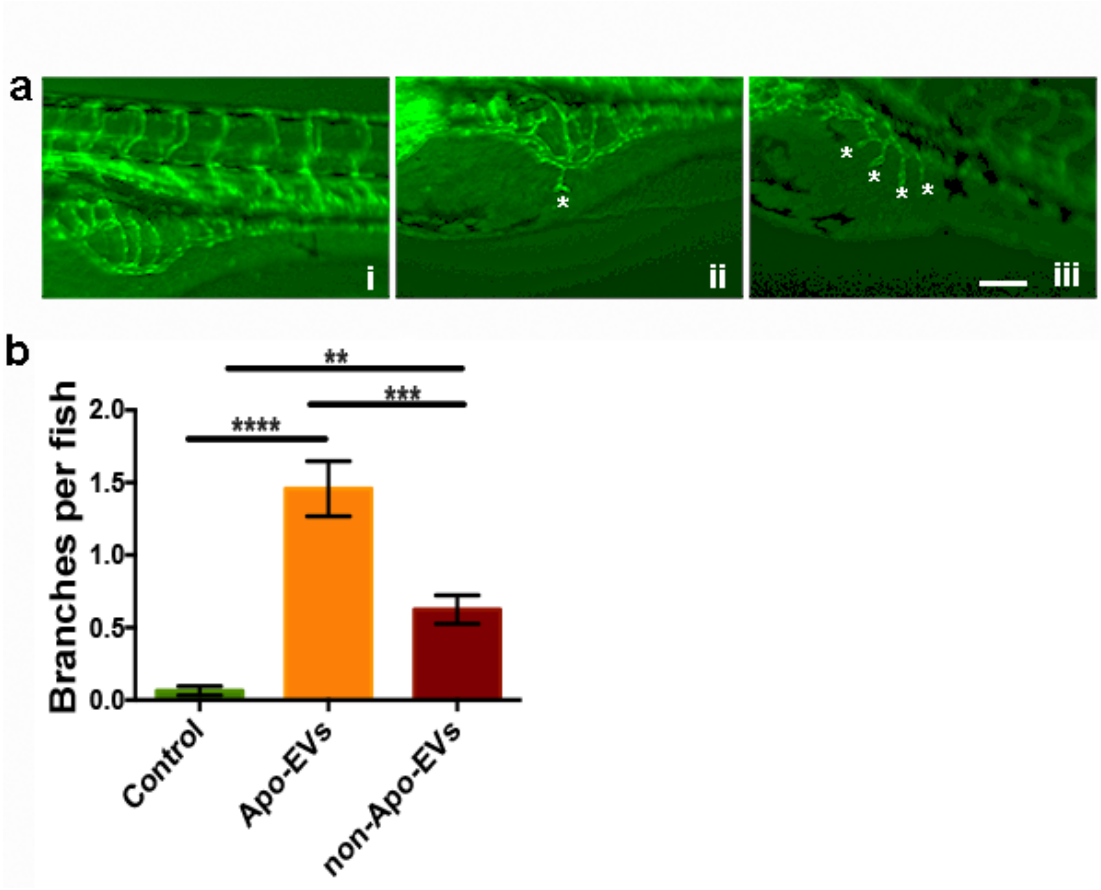

Figure 5.5 BL2 Apo-EVs have significantly higher ability to induce angiogenesis in zebrafish Yolk Sac xenografts than non-Aop-EVs

(a) Representative images of SIVs with or without induced branches in zebrafish yolk sac. i represents no branches. ii represents single branches. iii represents multiple branches. (b) Branches from SIV of each EVs-injected zebrafish were calculated. Statistical analysis shows promotion of angiogenesis by EVs with a significant higher ability by Apo-EVs. The control represented zebrafish injected with DPBS. Data here are pooled from three independent experiments with each group including at least 30 samples. (Mean ± SEM. Mann Whitney test, **p=0.001, ***p=0.0005, ****p<0.000, Scale bar =100 μm.)

As mentioned previously, soluble molecules are released by apoptotic BL cells as well as EVs and both may have angiogenic effects. To test this theory, secretome from BL2 cells and their EVs, BL2-bcl2 cells and their EVs were collected and injected into zebrafish. Products from culture media

collected by the same procedure were used as control. Secretome from different groups were adjusted to 0.25 mg/ml and volumes were adjusted to 2nl per embryo, equivelant to 500 pg of secretome was injected into each zebrafish. Secretome secreted from BL2 cells and their EVs after UV treatment, named Apo-S, showed an ability to induce branches from SIVs. Secretome from BL2-bcl2 cells and their EVs after UV treatment, named non-Apo-S, showed reduced angiogenesis compared to their apoptosis counterparts (figure 5.6 a). To text whether the protein products are, at least partially responsible for the pro-angiogenic effect, proteins of secretome from BL2 cells and their EVs was inactivated by stardard heat treatment. The ability of Apo-S to induce branches from SIVs in zebrafish was reduced after standard heat treatment (Apo-S HT) (figure 5.6b).

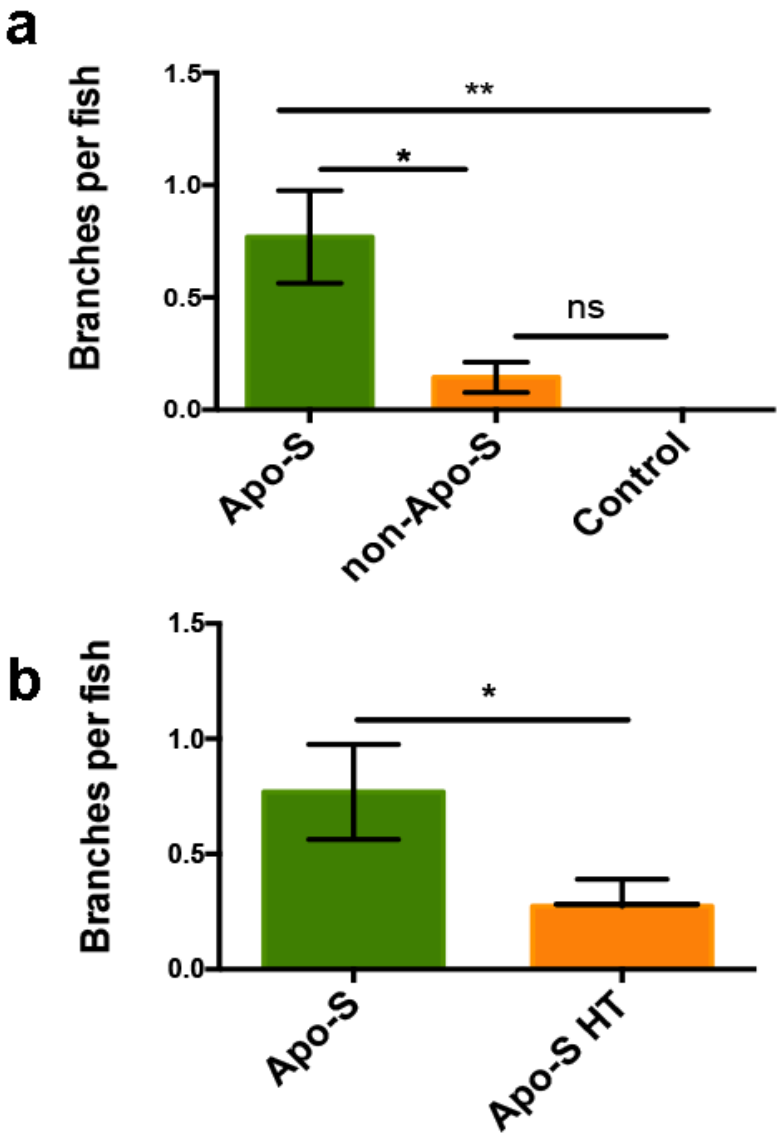

Figure 5.6 Secretome from BL2 cells promote tumour angiogenesis

(a) Secretome secreted from BL2 cells and their EVs (Apo-S) showed an ability to induce branches from SIVs in zebrafish. Reduced angiogenesis was observed in apoptosis-suppressed xenografts of secretome from BL2-bcl2 cells and their EVs (non-Apo-S). Products from culture media collected by the same procedure were used as control. Each sample in three groups contains 500 pg of secretome. (b) The pro-angiogenic ability of Apo-S was reduced after standard heat treatment (Apo-S HT). (Data here are pooled from three independent experiments with each group including at least 30 samples. Mean ± SEM, Mann Whitney test, * $p<0.05$, **$p=0.0011$)

5.2.3 Macrophages are activated and polarised by Apo-EVs in zebrafish

Macrophages have been closely associated with tumour angiogenesis (De Palma et al., 2017, Sica and Mantovani, 2012). However, due to their high plasticity and versatility, the exact subsets for certain functions and the mechanisms underling their activation and polarisation still remain unclear. To determine whether Apo-EVs promote angiogenesis through modulation of macrophages, I used transgenic line Tg(*mpeg1::mCherry/tnfα::eGFP*).

In Tg(*mpeg1::mCherry/tnfα::eGFP)* larvae, TNFα are not activated in macrophages as there are no GFP signals in mCherry+ cells (figure 5.7 a). EVs and control solution (media underwent the same treatment) were injected into YS as described before. Macrophages in the YS (as indicated by white box in figure 5.7 a) were observed 1 day after the EVs injection. As shown previously, at 1 dpi of EVs, Apo-EVs showed significantly higher ability at inducing angiogenesis (figure 5.5). At the same time point, Apo-EVs impacted on macrophage morphology and TNFα activation differently from non-Apo-EVs and control (mock control is media underwent the same treatment) (figure 5.7 b). Quantification of macrophages in the YS showed that the numbers of macrophages in the injection sites were not increased in EVs injected zebrafish while the phenotype of macrophages showed significant differences (figure 5.7). Some cells are activated to express TNFα in Apo-EVs, non-Apo-EVs, media injected groups but not HBSS injected group and intact zebrafish (figure 5.7.c). Interestingly, non-Apo-EVs and media activated TNFα expression mostly in macrophages while Apo-EVs activated much less TNFα expression in macrophages (figure 5.7.d). Nearly 50% of macrophages in the injection site of non-Apo-EVs injected group expressed TNFα while only about 4% of macrophages in the injection site of Apo-EVs injected group were expressing TNFα (figure 5.7.e). These results showed Apo-EVs impacted on the macrophages not by recruiting them but by induce phenotypic polarisation of macrophages *in vivo*.

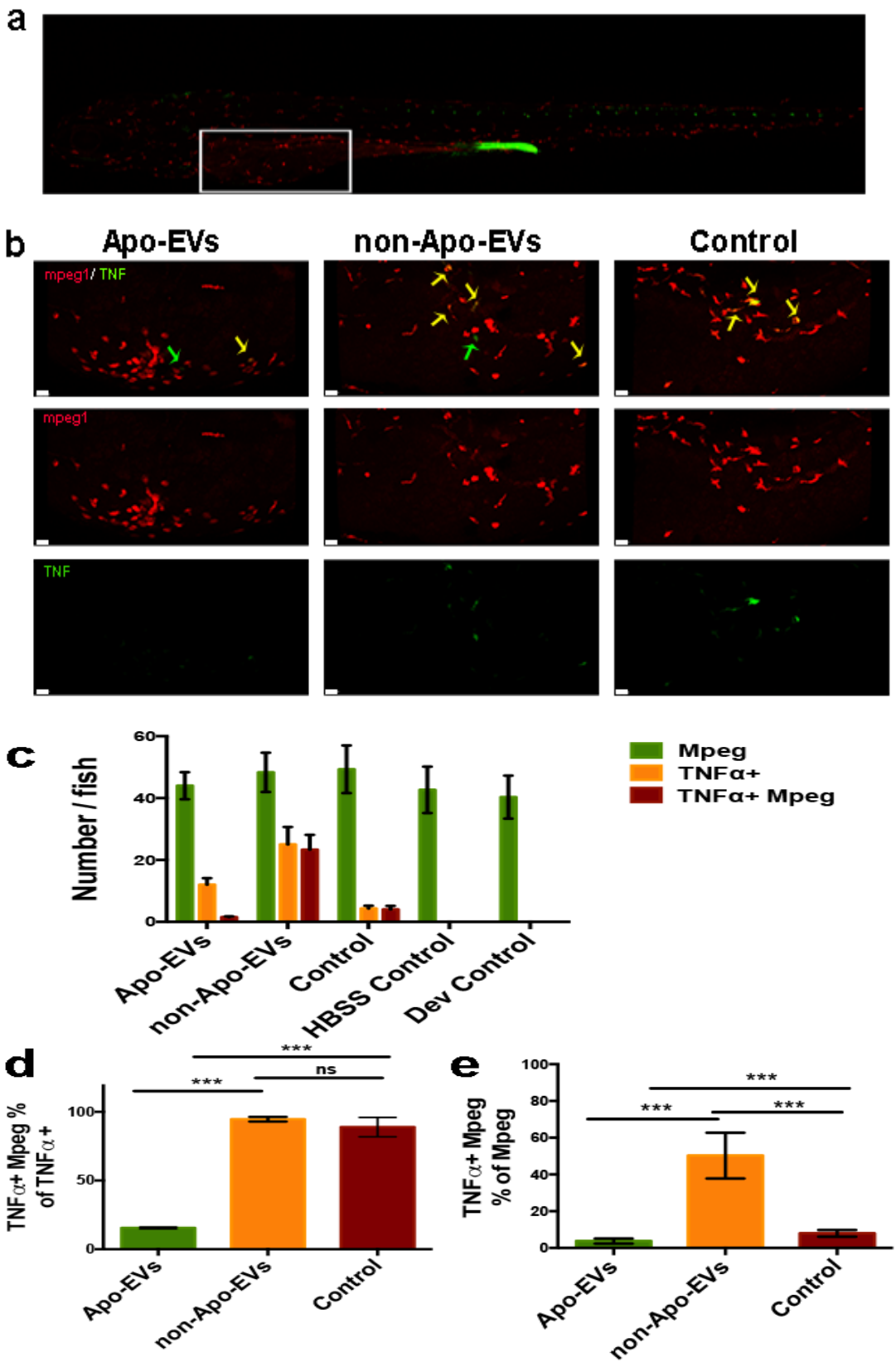

Figure 5.7 Macrophages respond differently upon Apo-EVs and non-Apo-EVs

(a) Tg(*mpeg1::mCherry/tnfα::eGFP*) larva exhibits mCherry+ macrophages. The green fluorescent signals in the back head and auns a s well as auto-fluorescent pigments can be used as selection marker for TNFα:eGFP which is not activated in intact zebrafish. (b) Representative maximum projections show the different morphology and activation of TNFα::eGFP at 1dpi YS of zebrafish with different treatment: injected with Apo-EVs, non-Apo-EVs and media underwent the same treatment. Green arrows show TNFα+ cells that are not macrophage, yellow arrows show macrophages that express TNFα. (c) Quantification of the numbers of macrophages, TNFα+ cells and TNFα+ macrophages in the YS of zebrafish injected with Apo-EVs, non-Apo-EVs, media underwent treatment (Control group) and HBSS as well as intact zebrafish. Dev (Developmental) control represents intact zebrafish. (d) The percentage of TNFα activated macrophage in non-Apo-EVs injected xenografts is significantly higher than TNFα activated macrophages in Apo-EVs injected zebrafish. (e) 48.3% of macrophages in the injection site of non-Apo-EVs injected group were expressing TNFα while 3.8% of macrophages in the injection site of Apo-EVs injected group were expressing TNFα. Control group has 6% TNFα expressing macrophages of total macrophages in the YS. (Mean ± SEM, Mann Whitney test, **p<0.01, ***p<0.001. Scale bar = 20 μm).

EVs especially Apo-EVs induced macrophages to display amoeboid phenotype as shown in figure 5.7. This change in morphology causes a change in the ratio of the macrophage cell surface to cell volume, which can be used as a read out for their activation. Therefore, the morphology of macrophages was further analysed. Based on the morphological criteria, macrophages in YS in Apo-EVs injected zebrafish were analysed and compared to non-Apo-EVs injected xenografts and control group (figure 5.8). This analysis showed a significantly higher percentage of amoeboid (activated) macrophages in the YS of Apo-EVs injected zebrafish compared to non-Apo-EVs injected xenografts and control xenografts.

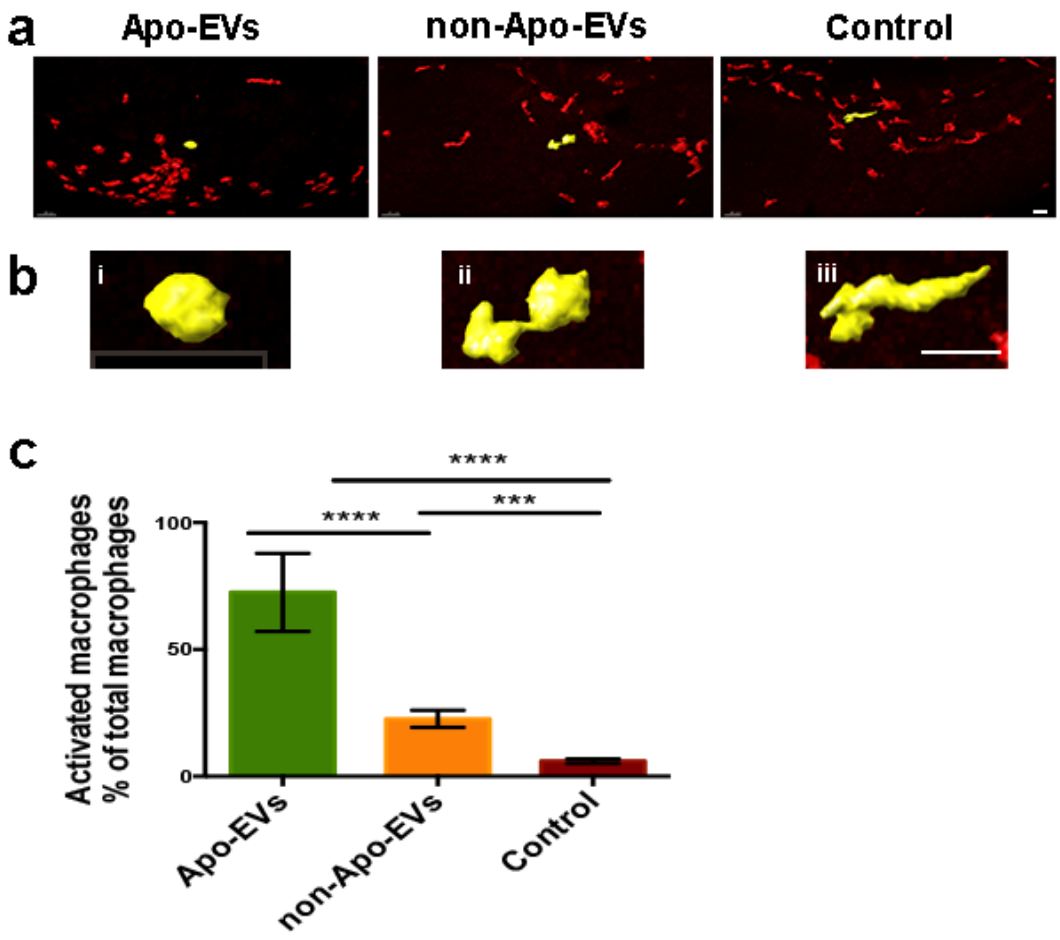

Figure 5.8 Apo-EVs activate macrophages

(a) Representative images showing morphological details of macrophages using the surface tool in Imaris. (b) Photo shows segmented images using the surface tool in Imaris. i shows a fully activated (amoeboid) cell (surface/volume ratio < 0.6), ii represents an activated cell (surface/volume ratio 0.6~0.8), iii shows a ramified cellac (surface/volume ratio 0.8~1). (c) Quantification of the percentage activation within macrophage population within YS in Apo-EVs injected zebrafish (n=8), non-Apo-EVs injected zebrafish (n=6) and control zebrafish (n=9). (Mean ± SEM, Mann Whitney test, ***p<0.001, ****p<0.0001, Scale bar = 20 μm.)

5.3 Discussion

This chapter has focused on establishing possible mechanisms underlying apoptosis promotion of BL growth. I established a quick and reliable zebrafish model to investigate tumour-induced angiogenesis mediated by EVs from apoptotic BL cells. This provided the first *in vivo* evidence of the pro-angiogenic function of Apo-EVs and suggests a mechanism by which tumor apoptosis may promote tumor growth. Furthermore, the phenotypic observation of activated macrophages in the angiogenesis area, suggest that the pro-angiogenic action of EVs possibly may be due to 1) direct interaction with endothelial cells 2) modulation of macrophage behaviour.

EVs contain various cargoes, such as DNA, mRNA, microRNA, growth factors, adhesion proteins, lipids, tissue factors and protease inhibitors, based upon their cellular origin and biogenesis pathway (Inal et al., 2012, Rak, 2013, Vader et al., 2014). In tumours, EVs have been implicated in the extracellular matrix remodelling, fibroblasts function modification, angiogenesis, tolerogenic immune response, drug resistance and modulation of the metastatic niche (Minciacchi et al., 2015, Taylor and Gercel-Taylor, 2011, Muralidharan-Chari et al., 2009, Castellana et al., 2009, Zhuang et al., 2012, Peinado et al., 2012, Lesnik et al., 2016). One obstacle to study EVs has been the technical challenges of isolating EVs due to their small size and sensitivity to stressful handling. Currently there is still no consensus isolation procedure and also the lack of widely accepted specific markers to identify functionally distinct subpopulations of EVs, including apoptosis-induced EVs.

The conventional 3-step differential centrifugation protocol was used widely in the literature and a method which involved centrifugation (details see chapter 2) was developed by a previous student in our group and used for some experiments (data for figure 5.4). The fragility of apoptotic cells and their susceptibility to damage from harsh isolation methods make the preparation and characterisation of Apo-EVs difficult. Furthermore, in the need to study its function, it is desirable to avoid introducing additional

molecules or beads during separation of EVs. An optimal “gentle” and ‘clean’ method to produce and isolate EVs from UV treated BL cells were developed in our group during this project (shown in chapter 2). This method minimises extraneous stress without introducing beads or molecules during the production of EVs used for all the studies in this chapter except figure 5.4.

The Nanoparticle Tracking Analysis (NTA) has been established as a more accurate way to quantify EVs than flow cytometry and was employed in this project to calculate EVs. NTA also provided a size profile to ensure the consistency of EVs amongst different EVs isolates. NTA results showed a clear correlation between the proportion of apoptotic cells and the number of EVs produced, which indicated the EVs produced from BL2 cell after UV treatment were apoptosis associated.

In BL, where apoptosis is constitutively prominent, EVs are enriched in certain molecules, lipids, RNAs and extra-chromosomal DNA implying their possible role in a BL microenvironment. Therefore, after choosing the most suitable and reliable methods to isolate and characterize the EVs, I established a zebrafish model for study EVs-induced angiogenesis based on my findings in the previous chapter. I assume that EVs are not as sensitive as viable cells to temperature and are biologically active at 28.5^{o}C. EVs xenografts were kept at 28.5^{o}C to optimise zebrafish development.

The established zebrafish models allowed a quick assay of the pro-angiogenesis ability of EVs. EVs from UV treated BL2 cells whose production was apoptosis-dependent were considered as Apo-EVs in this project. EVs from bcl2 transfected BL2 cells underwent the same treatment and were used as controls for non-Apo-EVs in this project. Results showed that Apo-EVs have a significantly higher ability to induce angiogenesis in zebrafish than non-Aop-EVs. Studies in cancer derived EVs demonstrate that EVs can directly interact with endothelial cells to induce tumour angiogenesis. EVs from cancer cells harbour interleukin-6 (IL-6) and VEGF, the neutral

sphingomyelinase 2, potent pro-angiogenic factors, as well as other molecules able to interact with endothelial cells leading to enhanced endothelial cell invasion (Skog et al., 2008, Thompson et al., 2013, Kosaka et al., 2013).

Secretome as another source from tumour cells often display altered profile of macromolecules compared to the normal tissue from which they are derived (Paltridge et al., 2013, Taylor and Gercel-Taylor, 2011). Studies show that the altered composition secreted from tumour cells contributes to the acquisition and maintenance of the recognised hallmarks of cancer and malignant disease progression (Paltridge et al., 2013, Neilsen et al., 2011). . It is possible that apoptotic tumour cells may secret soluble products to promote tumour growth. Therefore, secretome from apoptotic cells and their EVs were collected and compared. Secretome from apoptotic BL cells and their EVs showed a higher ability at inducing angiogenesis than from UV treated BL2-bcl2 cells and their EVs. This result suggested that apoptosis regulated the composition of secreted factors to promote tumour angiogenesis. Now, it is accepted that secretome are composed of proteins, lipids, micro-RNAs (miRNA) and messenger RNA (mRNA) (Agrawal et al., 2010, Iorio and Croce, 2012, Makridakis and Vlahou, 2010). Inactivation of proteins in the secretome by standard heat treatment showed decreased ability of inducing angiogenesis indicating that proteins in the secretome were important players for angiogenesis. It is possible that apoptosis not only produces soluble proteins but also modulates the molecular expression of EVs to further enhance tumour angiogenesis. These data indicated that apoptotic tumour cells may release EVs and soluble factors to promote angiogenesis by direct interaction with endothelial cells and/or fibroblasts.

Increased local vasculature in tumours is closely associated with cancer progression towards malignancy and is critically influenced by the presence of macrophage and their phenotypic state (Gurevich et al., 2018, Lin et al., 2006, Williams et al., 2016). Therefore, another obvious candidate

mechanism for apoptosis induced angiogenesis is modulation of macrophage phenotype. Macrophages are critical regulators in a tumour microenvironment and are closely associated with tumour angiogenesis (Nathan, 2008, Sica and Mantovani, 2012). Macrophages acquire different morphology, biochemistry, and functions based on environmental cues. Through their diversity, macrophages are regulated to meet different needs. For example, macrophages are polarised to an M1 phenotype and produce inflammatory cytokines by inflammatory stimuli from invading pathogens. In contrast, macrophages are polarised toward an M2 phenotype in a wound healing environment to help tissue repair (McWhorter et al., 2013). M2 phenotype in a wound healing environment to help tissue repair [27]. Despite the well-acknowledged consensus that macrophages are highly plastic and comprised of distinct subpopulations, the mechanism regulating the polarisation of macrophages still remains poorly defined (McWhorter et al., 2013). Most studies of macrophage population diversity are carried out in vitro, for example, using monocyte-derived macrophages treated with specific stimuli. Macrophage subtypes are still poorly characterized in live animals.

In a tumour environment, especially solid tumours with high rates of apoptosis, for example in BL, macrophages have been shown to accumulate in tumours and promote tumour growth (Ford et al., 2015). To establish whether macrophages are modulated by Apo-EVs to a pro-tumour growth phenotype, I used Tg(*mpeg1::mCherry/tnfα::eGFP*) to observe the polarisation of macrophages *in vivo*. Results showed that Apo-EVs impacted on the morphology of macrophages towards an amoeboid phenotype and most of the macrophages were not expressing TNFα. In contrast, non-Apo-EVs stimulated most of the macrophages to express TNFα. TNFα is a secreted pro-inflammatory cytokine that signals several cellular processes, including apoptosis, cell survival, and proliferation (Tartaglia et al., 1993, Cheng et al., 1994, Chan and Lenardo, 2000, Gupta, 2001). TNFα expressing macrophages are generally considered as M1 polarised in

mammals (Parameswaran and Patial, 2010). In wound healing and bacterial infection models, zebrafish Tg (*mpeg1::mCherry/tnfα::eGFP*) show that unpolarised macrophages move to the sites of inflammation where they become polarised to M1 phenotype initially and later change to M2-like phenotype (Nguyen-Chi et al., 2015). In this xenograft model, Apo-EVs leads to macrophage activation but not TNFα expression suggest that Apo-EVs induce a M2 phenotype. Combined with the finding that Apo-EVs enhanced tumour angiogenesis indicated TNFα+ macrophages were not involved in the induction of angiogenesis in this model. However, during wound induced angiogenesis $TNF\alpha^{-}$ M2 macrophage is involved in vessel remodelling after the initial sprouting (Gurevich et al., 2018).

The morphology of macrophages has been used to indicate their activation status. For example, *in vitro* maturation of macrophages by stimulation of bone marrow-derived macrophages (BMDMs) with cytokines to M1 or M2 polarization exhibited different cell morphologies: M1 cells displayed a round, pancake-like shape while M2 cells displayed cellular elongation (McWhorter et al., 2013). In zebrafish, an amoeboid morphology of macrophage stimulated by pathological insults in brain are considered to reflect their activation (Karperien et al., 2013, Chia et al., 2018). By analysing the morphology of macrophages in EVs xenograft models, Apo-EVs displayed higher ability to active macrophages indicating their activation may promote tumour angiogenesis.

Chapter 6 General discussion

6.1 Thesis objectives and summary of findings

In my thesis I aimed to reveal how apoptotic tumour cells manipulate the tumour microenvironment to promote cancer, focusing on the mechanisms underlying their pro-angiogenesis roles. B cell lymphoma, prototypically BL was used as the model due to the extensive apoptosis and high infiltration of macrophages.

Zebrafish was chosen as a model due to the ease of gene manipulation and translucency during the larval stages offering the opportunity of direct live-imaging (Zhao et al., 2015, Trede et al., 2004). Efforts were made to generate transgenic B lymphoma models and xenograft models in zebrafish.

Initially I tried to induce B cell lymphoma in zebrafish by over-expressing the *cmyc* oncogene under the control of a specific B cell promoter constitutively, Tg(*IgM1::cmyc-eGFP*) or in an inducible manner, Tg(*IgM1::CreERT2/IgM::lox-H2BmCherry-lox-cmyc-eGFP*). Unfortunately, no detectable tumours were developed in transgenic zebrafish. Flow cytometry analysis showed normal distribution of cell populations in zebrafish kidney which is considered as the site of B cell development in Tg(*IgM1::lox-H2BmCherry-lox-cmyc-eGFP*) and mCherry labelled cells were found in the lymphocyte population. The percentages of different cell populations in kidney are consistent with the literature (Traver, 2004, Chi et al., 2018). Further analysis of zebrafish kidney showed that there was a loss of lymphocyte populations in Tg(*IgM1::cmyc-eGFP*) and no detectable eGFP positive B-cells. These data suggest that the *cmyc* over-expression in IgM+ B cells might lead to cell death in zebrafish. However, further analysis on isolated lymphocytes from Tg(*IgM1::cmyc-eGFP*) fish is required to confirm this possibility. However, this has not been pursued because of time constraints.

Xenograft models using zebrafish larvae were also generated to visualise the direct interactions of tumour cells and host cells within the tumour microenvironment. Consistent with previous observations in mice, the suppression of apoptosis by over-expression of *bcl2* in BL2 cells decreased their viability in zebrafish larvae (Ford et al., 2015). The mouse models of BL indicate that TAMs are attracted by apoptotic BL cells and accumulate within the BL microenvironment (Ford et al., 2015). To evaluate whether macrophage functions are modulated by apoptotic cells and might regulate BL cell survival in the zebrafish model, human monocyte derived macrophages that had been differentially polarized were co-transplanted with BL cells. Three treatment groups that potentially represented different phenotypes were compared: 1) 'M0' macrophages matured from monocytes without additional activation, 2) 'M1' macrophages matured from monocytes and activated by IFN-γ / lipopolysaccharide (LPS) and 3) M2-like macrophages matured from monocytes and activated by co-culture with apoptotic BL2 cells. Unexpectedly, the co-injection of BL2 and M2 macrophages lead to mortality of the host, although M0 macrophage facilitate the survival of BL2 cells in zebrafish. These data suggest that apoptotic BL2 cells can polarize host macrophages to a tumour promoting phenotype. M1 macrophages on the other hand decreased the viability of BL2 cells which is consistent with previous studies that inflammatory macrophages constrain tumour growth (Sica and Mantovani, 2012, Shi and Shiao, 2018, Ostuni et al., 2015).

EVs produced by apoptotic tumour cells were further investigated as the candidate mechanism for apoptotic BL2 cells modulating macrophage phenotype and the tumour microenvironment. An optimised gentle method developed by Dr Maggie Paterson in our group was used to generate intact EVs since their functional integrity was imperative. Apoptotic BL2 cells produce more EVs with different size distribution compared with BL2-bcl2 cells. This suggests that altered EVs were produced by apoptotic BL2 cells compared with non-apoptotic cells. Using a zebrafish larval yolk sack

angiogenesis assay, I provide the first in vivo evidence that Apo-EVs are pro-angiogenic. Further analysis of the secretome from apoptotic BL2 cells as well as their Apo-EVs indicates that soluble protein component(s) in both mediate the pro-angiogenic function. To see whether the Apo-EVs polarise macrophages, macrophage reporter fish Tg(*mpeg1::mCherry*) with TNFα reporter Tg(*tnfα::eGFP*) were employed. I show that Apo-EVs modulated macrophages differently compared with non-Apo-EVs. Specifically, Apo-EVs promote macrophage activation but not TNFα expression *in vivo*.

6.2 Zebrafish as a model to study cancer of immune cell origin

The discussion here will focus on haemopoietic malignancies which are established by either transgenic technology or transplantation.

Many transgenic tumour models in zebrafish induce tumours in liver, skin or the nervous system (Zhao et al., 2015, Mirbahai et al., 2011, Mizgirev and Revskoy, 2010, Shepard et al., 2005, Storer and Zon, 2010, Phelps et al., 2009, Shin et al., 2012, Neumann et al., 2009, Santhakumar et al., 2012). The most well studied transgenic zebrafish model for malignancy in immune system is T-cell leukaemia which is also the first cancer model induced by transgenic technology in zebrafish. It was generated by overexpression of *myc* under the control of zebrafish *rag2* promoter (Langenau et al., 2003, Langenau et al., 2005).

T cell development starts relatively early in zebrafish with the general T cell marker lck starting to be expressed from around 4 dpf (Langenau et al., 2004). The superficial bilateral location of the thymus also makes direct observation of T cell ontogeny and pathogenesis relatively easy (Langenau et al., 2004). However, the study of B cells is more problematic, as B cells are produced and mature in head kidney and firstly observed in Tg(*IgM1::eGFP*) at about 20 days post fertilization when the fish body is no longer transparent, making it difficult to access via conventional microscopy

techniques (Page et al., 2013). A recent study has shown that the previously widely recognised T cell leukaemia model, Tg(*rag2::hmyc*) is in fact a combination of B and T cell acute lymphoblastic leukaemias (Borga et al., 2018). The existence of pre-B cell malignancy in this model was for a long time ignored partially because the kidney of zebrafish lies deeply in the fish body. These factors contributed to the failure of generating a transgenic B cell lymphoma model in zebrafish during the current project (discussed further below).

6.2.1 B cell malignancy driven by *myc* in zebrafish

Initially the study of *cmyc* focused on its roles in favouring malignancy including promoting cell-cycle progression and in blocking terminal differentiation (Nesbit et al., 1999, Vita and Henriksson, 2006). More recently, the dual role of *cmyc* on both cell-cycle progression and apoptosis has been well established (Uribesalgo et al., 2012, Vita and Henriksson, 2006). Askew, Cleveland, and colleagues used an IL-3-dependent myeloid cell line and showed that the constitutive expression of *myc* can cause apoptosis (Askew et al., 1991). This study also indicated that the absolute levels or perhaps kinetic pattern of *myc* expression appear to be decisive in determining the cellular response to *myc* (Askew et al., 1991). Furthermore, cells at adequate concentrations of growth factors respond to heightened *myc* by increased proliferation whereas when these growth factors are limiting cells seem to respond to *myc* with enhanced apoptosis (Askew et al., 1991). *Myc* is seen to increase the sensitivity to apoptosis in premalignant cells, but not after malignant transformation (McMahon, 2014). A number of studies have been concerned with understanding of how a cell reacts to *myc* activation and most of the mechanisms defined so far have involved the pro-apoptotic p53 pathway, the pro-survival bcl2 pathway, or both (Knezevich et al., 2005, Ozdek et al., 2004). In addition to the environmental modulation of *cmyc* function, *cmyc* activation levels is another determinant of *cmyc* function (Murphy et al., 2008). Specifically, using genetic platforms to tightly control *cmyc* levels in a rheostat-like manner, Murphy et al. showed that modest

elevation of *myc* led to enhanced transformation while robust overexpression of *myc* caused a dramatic increase in apoptosis (Murphy et al., 2008). The specific reasons why the cmyc-expressing cells died in the Tg(*IgM1::cmyc-eGFP*) were not investigated in this project. However, the expression levels of c*myc* in B cells may be one of the explanations that Tg(*IgM1::cmyc-eGFP*) did not develop cancers. Another possibility is that, as many studies suggest, the *myc* driven cell death is a default function rather than cell-cycle progression and it is only by co-operating with changes in the apoptotic machinery that *myc* is able to transform cells. In the classical Eμ-*myc* transgenic mouse model, the 6 month latency period for tumours suggests that additional genetic changes must occur subsequent to *myc* overexpression (Jacobsen et al., 1994). A later study strongly suggests that the secondary genetic change is inactivation of the p53 pathway (Eischen et al., 1999). The loss of p53 function may allow the cells to tolerate elevated *myc* without undergoing apoptosis.

Zebrafish so far is known to have three immunoglobulin heavy-chain classes, IgM, IgD and IgZ. As the name of Tg(*IgM1::cmyc-eGFP*) implied, this model only expressed *cmyc* in the major IgM-expressing B cell subset. A very recent paper published during the writing of this discussion carefully studied pre-B and pre-T cell acute lymphoblastic leukemias in zebrafish Tg(*rag2::hmyc/lck:eGFP*), where a *rag2* promoter drives human *myc* and a zebrafish *lck* promoter controls GFP expression. This study shows that *myc* may be oncogenic in only the IgZ-lineage (functionally analogous to mammalian IgA) in Tg(*rag2::hmyc/lck::eGFP*) (Borga et al., 2018). This is supported by another study that shows that the B cell development in zebrafish does not go through a Rag^{hi} CD79+IgH-μ+ pre–B cell stage (Liu et al., 2017). The differences lie in the development of B cells, especially the IgM-lineage whose development does not have a Pre–B cell stage in zebrafish indicating that IgM1 is not the best candidate promoter to drive the oncogene for mimicking human cancers.

6.2.2 Xenograft models in zebrafish for cancer research

Zebrafish especially the embryo which has not developed a functional adaptive immune system have been widely employed as a tumour xenograft host to study angiogenesis and metastasis (Kirchberger et al., 2017).

From a review of the literature, many tumour cell types including in vitro established cell lines and primary tumour derived cells can be engrafted to zebrafish (Kirchberger et al., 2017, Veinotte et al., 2014). Surprisingly, the BL2 cells I used in this study did not engraft successfully and all injected cells died within 4dpi. A possible explanation for this could be lack of key B cell survival factors in the zebrafish larvae, as normally mature B cells do not develop until two weeks post fertilization. This hypothesis is supported by the observation that cells survive worse when fewer BL2 cells were transplanted which rules out nutrient deprivation mediated cell death, and it is known that BL2 cells produce autocrine factors that help their own growth *in vitro* (Beatty et al., 1997, Vockerodt et al., 2001). Therefore, The models established during this project can be used to identify factors that are key to the survival and growth of B lymphoma. I showed in this model that macrophages modulated by apoptotic cells can in turn facilitate BL2 cells survival, although more work needs to be done to identify identify the macrophage-mediated molecular mechanisms that support BL2 cell growth. Published data show engraftment efficiency in zebrafish embryo varies with the type of transplanted cells, and this applies not only for tumour cells, but also for normal healthy cells, further indicating the importance of essential lineage specific microenvironmental cues for cell survival in zebrafish larval xenograft models. For example, healthy human CD34+ hematopoietic stem and progenitor cells from cord blood rapidly disappear after injection into zebrafish embryos while human melanocytes survive and become distributed into their normal microenvironment in the skin (Pruvot et al., 2011, Lee et al., 2005). Therefore, zebrafish embryo is an amenable host to study tumour cell host interactions, but there are many factors that need to be taken into

account when interpreting the phenotype of certain type of tumour in this model.

For human tumours, angiogenesis occurs when tumour cells grow to a certain size and require new blood vessels to bring in more nutrients and oxygen. In zebrafish xenograft models, induction of angiogenesis is often due to the release of pro-angiogenesis factors by tumour cell lines (Nicoli et al., 2007, Zhao et al., 2016). In addition to tumour cell derived signal, the microenvironment is also important for induction of angiogenesis. In a zebrafish xenograft model exposing larvae carrying tumour cells to a hypoxic environment, enhances angiogenesis while the tumour cell size remains constant (Lee et al., 2009). The failure of BL2 cells to induce angiogenesis is probably due to their limited viability in zebrafish larvae and to not producing sufficient pro-angiogenic factors. Recent studies suggest that interactions between tumour cells and endothelial cells at early stages even without blood flow are crucial for tumour growth, thereby indicating that endothelial cells can support tumour cells in a paracrine manner (Zhao et al., 2016). Provision of a potential perivascular niche may provide a solution to aid BL2 cell survival in zebrafish.

Although the interpretation and quantification of metastasis and growth of tumours in zebrafish larvae differ in various published reports, studies with melanoma cells stand out as being the most robust in terms of tumour growth and ability to metastasise as xenografts. Successful metastasis of tumour cells in zebrafish, (metastasis here refers to cells that are injected into peripheral tissue, and by their subsequent intravasation to lymph or blood vessels followed by extravasation from the circulation to seed at a distal site) seems to imply that the tumour is able to survive and proliferate as a single cell, and not to require a critical mass to do so (Lee et al., 2005, Teng et al., 2013, Marques et al., 2009). This is consistent with the behaviour of the melanoma cells (A375) used in this project as a technical control, which demonstrated that single cell derived colonies survived and proliferated at

the CHT site. In contrast, BL2 cells did not show such single cell autonomous behaviour and remained at the injection site.

6.3 Apoptosis driven pro-tumour mechanisms

Apoptotic tumour cells have been shown to promote angiogenesis, and accumulation of TAMs in aggressive B cell lymphomas. However, how apoptotic tumour cells execute these functions is still unclear.

EVs release by apoptotic cells is well documented and have been shown to play an important role in processes including immune suppression, antitumor immunity, and autoimmunity (Caruso and Poon, 2018). Apparently, the cell origin and 'package' mechanisms of EVs are closely associated with the contents and functions of EVs. EVs released by tumour cells during apoptosis can serve as long range and long lasting signal carriers mediating the modulating function of apoptotic cells in a tumour microenvironment. Enhanced angiogenesis was also found when Apo-EVs were co-cultured with HUVECs indicating the direct interaction between Apo-EVs and endothelial cells can induce angiogenesis (unpublished work in our group). Furthermore, I also show that Apo-EVs driven angiogenesis is susceptible to standard heat treatment implying that a thermo-sensitive protein(s) from Apo-EVs are required to mediate their interaction with endothelial cells. The cell-cell interactions between tumour cells and endothelial cells have been shown to stimulate angiogenesis through the VEGFs family proteins and their associated receptors (De Palma et al., 2017). It would be interesting to test if Apo-EVs are enriched with VEGF proteins. Another possible mechanism for Apo-EVs in modulating endothelial cells is via intercellular transfer of proteins or RNAs leading to the altered recipient cells. This type of modulation mechanism for Apo-EVs was seen in an aggressive glioblastoma model where Apo-EVs affected mRNA splicing in recipient tumour cells (Pavlyukov et al., 2018).

Apoptotic tumour cells have been shown to activate macrophages to a pro-angiogenic phenotype in aggressive B cell lymphoma (Ford et al., 2015). Apo-EVs modulated macrophages to an ameboid shape, which is generally considered as an activation state (Chia et al., 2018, Nguyen-Chi et al., 2017) and most activated macrophages were did not express TNFα. Previous studies in zebrafish showed that TNFα+ macrophages express high levels of the pro-inflammatory cytokines TNFβ, IL1β and IL6 while TNFα- macrophages express high levels of TGFβ, CCR2 and CXCR4β that are considered to be a specific phenotype of the M2 subtype (Nguyen-Chi et al., 2017). Therefore the activated TNFα- macrophages induced by Apo-EVs are M2-like macrophages and this is in line with that the pro-tumour growth TAM that are generally considered to have a M2-like phenotype (Nathan, 2008, Li et al., 2018). A recent zebrafish wound angiogenesis study showed that pro-inflammatory TNFα+ macrophages are necessary for early vessel sprouting through VEGFa expression and appears to downregulate TNFα during the anastomosis and vessel maturation process (Gurevich et al., 2018). Interestingly, Apo-EVs directly act on endothelial cells potentially through providing VEGFs (discussed previously) and simutaneously Apo-EVs induce a TNFα- phenotype in recruited macrophages that could contribute to the vessel remodeling during angiogenesis.

6.4 Future work

I have shown here that Apo-EVs play significant roles in inducing angiogenesis and to modulate macrophage function. I hypothesize that Apo-EVs fulfil the angiogenesis process in a well-designed manner: the direct interaction with endothelial cells to start the angiogenesis process and the polarisation of macrophages for vessel maturation. The next step forward is to reveal how Apo-EVs interact with endothelial cells and the roles of polarised macrophages polarised by Apo-EVs.

In order to identify pathways/factors that mediate Apo-EVs function, we are performing proteomics and RNA-seq analysis of Apo-EVs. Zebrafish xenograft models established here will be used to assess the functional contribution of candidate pathways.

Apart from receptor signalling between Apo-EV and endothelial cells, another mechanism whereby Apo-EVs promote angiogenesis is by intercellular transfer. By fluorescent labelling of Apo-EVs and live imaging using my established zebrafish yolk sac angiogenesis models, it will be possible to reveal the internalisation process in real time. Single-cell RNA sequencing of the recipient endothelial cells would provide the means to a further understanding the pro-angiogenic mechanisms underlying Apo-EVs action.

The data for Apo-EVs modulation of macrophage phenotype is of interest and promising. Further studies will focus on the phenotypes and functions of activated macrophage with or without TNFα expression.

The Apo-EVs used in my study are derived from BL2 cells, it will be interesting to test whether Apo-EVs derived from other tumour cell lines or normal cells have similar function, which will shed light on how might apoptotic cell modulate its environment in general.

There are multiple factors contributing to the failure to establish a zebrafish B cell lymphoma model using IgM1 driven cmyc expression as discussed previously. We are testing whether incorporating Tg(*IgM1::cmyc-eGFP*) into a *p53-/-* background might lead to B cell malignancy. IgM1 promoter might not be ideal for driving oncogene expression in immature B cells as a different developmental trajectory of B cell lineage exists in zebrafish. Therefore I would propose to test the CD79 promoter, which is newly characterised in zebrafish as a robust B cell specific promoter (Liu et al., 2017). A mutant human *cmyc* derived from a human patient could also be

tested in combination with CD79 promoter to assess its tumourigenesis potential in B cells in zebrafish.

References

ACEHAN, D., JIANG, X. J., MORGAN, D. G., HEUSER, J. E., WANG, X. D. & AKEY, C. W. 2002. Three-dimensional structure of the apoptosome: Implications for assembly, procaspase-9 binding, and activation. *Molecular Cell,* 9**,** 423-432.

ADAMS, J. M., HARRIS, A. W., PINKERT, C. A., CORCORAN, L. M., ALEXANDER, W. S., CORY, S., PALMITER, R. D. & BRINSTER, R. L. 1985. The C-Myc Oncogene Driven by Immunoglobulin Enhancers Induces Lymphoid Malignancy in Transgenic Mice. *Nature,* 318**,** 533-538.

ADAMS, R. H. & ALITALO, K. 2007. Molecular regulation of angiogenesis and lymphangiogenesis. *Nat Rev Mol Cell Biol,* 8**,** 464-78.

AGRAWAL, G. K., JWA, N. S., LEBRUN, M. H., JOB, D. & RAKWAL, R. 2010. Plant secretome: unlocking secrets of the secreted proteins. *Proteomics,* 10**,** 799-827.

AKERS, J. C., GONDA, D., KIM, R., CARTER, B. S. & CHEN, C. C. 2013. Biogenesis of extracellular vesicles (EV): exosomes, microvesicles, retrovirus-like vesicles, and apoptotic bodies. *Journal of Neuro-Oncology,* 113**,** 1-11.

AL-RAWI, M. A., MANSEL, R. E. & JIANG, W. G. 2005. Lymphangiogenesis and its role in cancer. *Histol Histopathol,* 20**,** 283-98.

ALCAIDE, J., FUNEZ, R., RUEDA, A., PEREZ-RUIZ, E., PEREDA, T., RODRIGO, I., COVENAS, R., MUNOZ, M. & REDONDO, M. 2013. The role and prognostic value of apoptosis in colorectal carcinoma. *BMC Clin Pathol,* 13**,** 24.

ALDOSS, I. T., WEISENBURGER, D. D., FU, K., CHAN, W. C., VOSE, J. M., BIERMAN, P. J., BOCIEK, R. G. & ARMITAGE, J. O. 2008. Adult Burkitt lymphoma: advances in diagnosis and treatment. *Oncology (Williston Park),* 22**,** 1508-17.

ALIZADEH, A. A., EISEN, M. B., DAVIS, R. E., MA, C., LOSSOS, I. S., ROSENWALD, A., BOLDRICK, J. C., SABET, H., TRAN, T., YU, X., POWELL, J. I., YANG, L., MARTI, G. E., MOORE, T., HUDSON, J., JR., LU, L., LEWIS, D. B., TIBSHIRANI, R., SHERLOCK, G., CHAN, W. C., GREINER, T. C., WEISENBURGER, D. D., ARMITAGE, J. O., WARNKE, R., LEVY, R., WILSON, W., GREVER, M. R., BYRD, J. C., BOTSTEIN, D., BROWN, P. O. & STAUDT, L. M. 2000. Distinct types of diffuse large B-cell lymphoma identified by gene expression profiling. *Nature,* 403**,** 503-11.

AMATRUDA, J. F. & PATTON, E. E. 2008. Genetic models of cancer in zebrafish. *Int Rev Cell Mol Biol,* 271**,** 1-34.

AMATRUDA, J. F., SHEPARD, J. L., STERN, H. M. & ZON, L. I. 2002. Zebrafish as a cancer model system. *Cancer Cell,* 1**,** 229-31.

AMORIM, M., FERNANDES, G., OLIVEIRA, P., MARTINS-DE-SOUZA, D., DIAS-NETO, E. & NUNES, D. 2014. The overexpression of a single oncogene (ERBB2/HER2) alters the proteomic landscape of extracellular vesicles. *Proteomics,* 14**,** 1472-1479.

ARNOLD, F. 1985. Tumour angiogenesis. *Ann R Coll Surg Engl,* 67**,** 295-8.

ARUR, S., UCHE, U. E., REZAUL, K., FONG, M., SCRANTON, V., COWAN, A. E., MOHLER, W. & HAN, D. K. 2003. Annexin I is an endogenous ligand that mediates apoptotic cell engulfment. *Developmental Cell,* 4**,** 587-598.

ASHKENAZI, A. & DIXIT, V. M. 1998. Death receptors: signaling and modulation. *Science,* 281**,** 1305-8.

ASKEW, D. S., ASHMUN, R. A., SIMMONS, B. C. & CLEVELAND, J. L. 1991. Constitutive c-myc expression in an IL-3-dependent myeloid cell line suppresses cell cycle arrest and accelerates apoptosis. *Oncogene,* 6**,** 1915-22.

ATKIN-SMITH, G. K. & POON, I. K. H. 2017. Disassembly of the Dying: Mechanisms and Functions. *Trends Cell Biol,* 27**,** 151-162.

BARRES, C., BLANC, L., BETTE-BOBILLO, P., ANDRE, S., MAMOUN, R., GABIUS, H. J. & VIDAL, M. 2010. Galectin-5 is bound onto the surface of rat reticulocyte exosomes and modulates vesicle uptake by macrophages. *Blood,* 115**,** 696-705.

BARRY, M. & BLEACKLEY, R. C. 2002. Cytotoxic T lymphocytes: All roads lead to death. *Nature Reviews Immunology,* 2**,** 401-409.

BATISTA, B. S., ENG, W. S., PILOBELLO, K. T., HENDRICKS-MUNOZ, K. D. & MAHAL, L. K. 2011. Identification of a Conserved Glycan Signature for Microvesicles. *Journal of Proteome Research,* 10**,** 4624-4633.

BEATTY, P. R., KRAMS, S. M. & MARTINEZ, O. M. 1997. Involvement of IL-10 in the autonomous growth of EBV-transformed B cell lines. *J Immunol,* 158**,** 4045-51.

BEN-BATALLA, I., SCHULTZE, A., WROBLEWSKI, M., ERDMANN, R., HEUSER, M., WAIZENEGGER, J. S., RIECKEN, K., BINDER, M., SCHEWE, D., SAWALL, S., WITZKE, V., CUBAS-CORDOVA, M., JANNING, M., WELLBROCK, J., FEHSE, B., HAGEL, C., KRAUTER, J., GANSER, A., LORENS, J. B., FIEDLER, W., CARMELIET, P., PANTEL, K., BOKEMEYER, C. & LOGES, S. 2013. Axl, a prognostic and therapeutic target in acute myeloid leukemia mediates paracrine crosstalk of leukemia cells with bone marrow stroma. *Blood,* 122**,** 2443-2452.

BENARD, E. L., RACZ, P. I., ROUGEOT, J., NEZHINSKY, A. E., VERBEEK, F. J., SPAINK, H. P. & MEIJER, A. H. 2015. Macrophage-expressed perforins mpeg1 and mpeg1.2 have an anti-bacterial function in zebrafish. *J Innate Immun,* 7**,** 136-52.

BERGHMANS, S., MURPHEY, R. D., WIENHOLDS, E., NEUBERG, D., KUTOK, J. L., FLETCHER, C. D., MORRIS, J. P., LIU, T. X., SCHULTE-MERKER, S., KANKI, J. P., PLASTERK, R., ZON, L. I. & LOOK, A. T. 2005. tp53 mutant zebrafish develop malignant peripheral nerve sheath tumors. *Proc Natl Acad Sci U S A,* 102**,** 407-12.

BERMAN, J., PAYNE, E. & HALL, C. 2012. The zebrafish as a tool to study hematopoiesis, human blood diseases, and immune function. *Adv Hematol,* 2012**,** 425345.

BERN, M. M. 2017. Extracellular vesicles: how they interact with endothelium, potentially contributing to metastatic cancer cell implants. *Clin Transl Med,* 6**,** 33.

BLYTH, K., TERRY, A., OHARA, M., BAXTER, E. W., CAMPBELL, M., STEWART, M., DONEHOWER, L. A., ONIONS, D. E., NEIL, J. C. & CAMERON, E. R. 1995. Synergy between a Human C-Myc Transgene and P53 Null Genotype in Murine Thymic Lymphomas - Contrasting Effects of Homozygous and Heterozygous P53 Loss. *Oncogene,* 10**,** 1717-1723.

BORGA, C., PARK, G., FOSTER, C., BURROUGHS-GARCIA, J., MARCHESIN, M., SHAH, R., HASAN, A., AHMED, S. T., BRESOLIN, S., BATCHELOR, L., SCORDINO, T., MILES, R. R., TE KRONNIE, G., REGENS, J. L. & FRAZER, J. K. 2018. Simultaneous B and T cell acute lymphoblastic leukemias in zebrafish driven by transgenic MYC: implications for oncogenesis and lymphopoiesis. *Leukemia*.

BOURNAZOU, I., POUND, J. D., DUFFIN, R., BOURNAZOS, S., MELVILLE, L. A., BROWN, S. B., ROSSI, A. G. & GREGORY, C. D. 2009. Apoptotic human cells inhibit migration of granulocytes via release of lactoferrin. *J Clin Invest,* 119**,** 20-32.

BRODEUR, G. M., SEEGER, R. C., SCHWAB, M., VARMUS, H. E. & BISHOP, J. M. 1984. Amplification of N-Myc in Untreated Human Neuroblastomas Correlates with Advanced Disease Stage. *Science,* 224**,** 1121-1124.

BRUNNER, T., WASEM, C., TORGLER, R., CIMA, I., JAKOB, S. & CORAZZA, N. 2003. Fas (CD95/Apo-1) ligand regulation in T cell homeostasis, cell-mediated cytotoxicity and immune pathology. *Semin Immunol,* 15**,** 167-76.

BRYANT, P. J. & FRASER, S. E. 1988. Wound healing, cell communication, and DNA synthesis during imaginal disc regeneration in Drosophila. *Dev Biol,* 127**,** 197-208.

BURRI, P. H. & TAREK, M. R. 1990. A novel mechanism of capillary growth in the rat pulmonary microcirculation. *Anat Rec,* 228**,** 35-45.

CABEROY, N. B., ALVARADO, G., BIGCAS, J. L. & LI, W. 2012. Galectin-3 is a new MerTK-specific eat-me signal. *Journal of Cellular Physiology,* 227**,** 401-407.

CABEROY, N. B., ZHOU, Y. X. & LI, W. 2010. Tubby and tubby-like protein 1 are new MerTK ligands for phagocytosis. *Embo Journal,* 29**,** 3898-3910.

CADUFF, J. H., FISCHER, L. C. & BURRI, P. H. 1986. Scanning electron microscope study of the developing microvasculature in the postnatal rat lung. *Anat Rec,* 216**,** 154-64.

CALIN, G. A. & CROCE, C. M. 2007. Chromosomal rearrangements and microRNAs: a new cancer link with clinical implications. *Journal of Clinical Investigation,* 117**,** 2059-2066.

CAMARDA, R., WILLIAMS, J. & GOGA, A. 2017. In vivo Reprogramming of Cancer Metabolism by MYC. *Front Cell Dev Biol,* 5**,** 35.

CANNON, M. & CESARMAN, E. 2000. Kaposi's sarcoma-associated herpes virus and acquired immunodeficiency syndrome-related malignancy. *Semin Oncol,* 27**,** 409-19.

CAO, Y. 2005. Opinion: emerging mechanisms of tumour lymphangiogenesis and lymphatic metastasis. *Nat Rev Cancer,* 5**,** 735-43.

CARMELIET, P. & JAIN, R. K. 2000. Angiogenesis in cancer and other diseases. *Nature,* 407**,** 249-57.

CARTER, D. R. F., CLAYTON, A., DEVITT, A., HUNT, S. & LAMBERT, D. W. 2018. Extracellular vesicles in the tumour microenvironment. *Philos Trans R Soc Lond B Biol Sci,* 373.

CARUSO, S. & POON, I. K. H. 2018. Apoptotic Cell-Derived Extracellular Vesicles: More Than Just Debris. *Front Immunol,* 9**,** 1486.

CASTELLANA, D., ZOBAIRI, F., MARTINEZ, M. C., PANARO, M. A., MITOLO, V., FREYSSINET, J. M. & KUNZELMANN, C. 2009. Membrane Microvesicles as Actors in the Establishment of a Favorable Prostatic Tumoral Niche: A Role for Activated Fibroblasts and CX3CL1-CX3CR1 Axis. *Cancer Research,* 69**,** 785-793.

CAVNAR, M. J., TURCOTTE, S., KATZ, S. C., KUK, D., GONEN, M., SHIA, J. R., ALLEN, P. J., BALACHANDRAN, V. P., D'ANGELICA, M. I., KINGHAM, T. P., JARNAGIN, W. R. & DEMATTEO, R. P. 2017. Tumor-Associated Macrophage Infiltration in Colorectal Cancer Liver Metastases is Associated With Better Outcome. *Annals of Surgical Oncology,* 24**,** 1835-1842.

CHAN, F. K. & LENARDO, M. J. 2000. A crucial role for p80 TNF-R2 in amplifying p60 TNF-R1 apoptosis signals in T lymphocytes. *Eur J Immunol,* 30**,** 652-60.

CHAUDHURI, J., BASU, U., ZARRIN, A., YAN, C., FRANCO, S., PERLOT, T., VUONG, B., WANG, J., PHAN, R. T., DATTA, A., MANIS, J. & ALT, F. W. 2007. Evolution of the immunoglobulin heavy chain class switch recombination mechanism. *Adv Immunol,* 94**,** 157-214.

CHEKENI, F. B., ELLIOTT, M. R., SANDILOS, J. K., WALK, S. F., KINCHEN, J. M., LAZAROWSKI, E. R., ARMSTRONG, A. J., PENUELA, S., LAIRD, D. W., SALVESEN, G. S., ISAKSON, B. E., BAYLISS, D. A. & RAVICHANDRAN, K. S. 2010. Pannexin 1 channels mediate 'find-me' signal release and membrane permeability during apoptosis. *Nature,* 467**,** 863-U136.

CHEN, J., JETTE, C., KANKI, J. P., ASTER, J. C., LOOK, A. T. & GRIFFIN, J. D. 2007. NOTCH1-induced T-cell leukemia in transgenic zebrafish. *Leukemia,* 21**,** 462-71.

CHEN, W. X., ZHONG, S. L., JI, M. H., PAN, M., HU, Q., LV, M. M., LUO, Z., ZHAO, J. H. & TANG, J. H. 2014. MicroRNAs delivered by extracellular vesicles: an emerging resistance mechanism for breast cancer. *Tumour Biol,* 35**,** 2883-92.

CHEN, Y., CORRIDEN, R., INOUE, Y., YIP, L., HASHIGUCHI, N., ZINKERNAGEL, A., NIZET, V., INSEL, P. A. & JUNGER, W. G. 2006b. ATP release guides neutrophil chemotaxis via P2Y2 and A3 receptors. *Science,* 314**,** 1792-5.

CHENG, B., CHRISTAKOS, S. & MATTSON, M. P. 1994. Tumor necrosis factors protect neurons against metabolic-excitotoxic insults and promote maintenance of calcium homeostasis. *Neuron,* 12**,** 139-53.

CHENG, C. W., YEH, J. C., FAN, T. P., SMITH, S. K. & CHARNOCK-JONES, D. S. 2008. Wnt5a-mediated non-canonical Wnt signalling regulates human endothelial cell proliferation and migration. *Biochem Biophys Res Commun,* 365**,** 285-90.

CHI, Y., HUANG, Z., CHEN, Q., XIONG, X., CHEN, K., XU, J., ZHANG, Y. & ZHANG, W. 2018. Loss of runx1 function results in B cell immunodeficiency but not T cell in adult zebrafish. *Open Biol,* 8.

CHIA, K., MAZZOLINI, J., MIONE, M. & SIEGER, D. 2018. Tumor initiating cells induce Cxcr4-mediated infiltration of pro-tumoral macrophages into the brain. *Elife,* 7.

CHOI, D. S., PARK, J. O., JANG, S. C., YOON, Y. J., JUNG, J. W., CHOI, D. Y., KIM, J. W., KANG, J. S., PARK, J., HWANG, D., LEE, K. H., PARK, S. H., KIM, Y. K., DESIDERIO, D. M., KIM, K. P. & GHO, Y. S. 2011. Proteomic analysis of microvesicles derived from human colorectal cancer ascites. *Proteomics,* 11**,** 2745-2751.

CHOWDHURY, D. & LIEBERMAN, J. 2008. Death by a thousand cuts: granzyme pathways of programmed cell death. *Annu Rev Immunol,* 26**,** 389-420.

COFFELT, S. B., TAL, A. O., SCHOLZ, A., DE PALMA, M., PATEL, S., URBICH, C., BISWAS, S. K., MURDOCH, C., PLATE, K. H., REISS, Y. & LEWIS, C. E. 2010. Angiopoietin-2 Regulates Gene Expression in TIE2-Expressing Monocytes and Augments Their Inherent Proangiogenic Functions. *Cancer Research,* 70**,** 5270-5280.

COLEGIO, O. R., CHU, N. Q., SZABO, A. L., CHU, T., RHEBERGEN, A. M., JAIRAM, V., CYRUS, N., BROKOWSKI, C. E., EISENBARTH, S. C., PHILLIPS, G. M., CLINE, G. W., PHILLIPS, A. J. & MEDZHITOV, R. 2014. Functional polarization of tumour-associated macrophages by tumour-derived lactic acid. *Nature,* 513**,** 559-63.

COLLIER, M. E. W., MAH, P. M., XIAO, Y. P., MARAVEYAS, A. & ETTELAIE, C. 2013. Microparticle-associated tissue factor is recycled by endothelial cells resulting in enhanced surface tissue factor activity. *Thrombosis and Haemostasis,* 110**,** 966-976.

COLOMBO, M., RAPOSO, G. & THERY, C. 2014. Biogenesis, secretion, and intercellular interactions of exosomes and other extracellular vesicles. *Annu Rev Cell Dev Biol,* 30**,** 255-89.

CONDE-VANCELLS, J., RODRIGUEZ-SUAREZ, E., EMBADE, N., GIL, D., MATTHIESEN, R., VALLE, M., ELORTZA, F., LU, S. C., MATO, J. M. & FALCON-PEREZ, J. M. 2008. Characterization and comprehensive proteome profiling of exosomes secreted by hepatocytes. *J Proteome Res,* 7**,** 5157-66.

COOK, J. & HAGEMANN, T. 2013. Tumour-associated macrophages and cancer. *Curr Opin Pharmacol,* 13**,** 595-601.

COOK, R. S., JACOBSEN, K. M., WOFFORD, A. M., DERYCKERE, D., STANFORD, J., PRIETO, A. L., REDENTE, E., SANDAHL, M., HUNTER, D. M., STRUNK, K. E., GRAHAM, D. K. & EARP, H. S.,

3RD 2013. MerTK inhibition in tumor leukocytes decreases tumor growth and metastasis. *J Clin Invest,* 123**,** 3231-42.
CORKERY, D. P., DELLAIRE, G. & BERMAN, J. N. 2011. Leukaemia xenotransplantation in zebrafish--chemotherapy response assay in vivo. *Br J Haematol,* 153**,** 786-9.
CREAGH, E. M., CONROY, H. & MARTIN, S. J. 2003. Caspase-activation pathways in apoptosis and immunity. *Immunol Rev,* 193**,** 10-21.
CRUNKHORN, S. 2017. Cancer: Targeting MYC-driven translation. *Nat Rev Drug Discov,* 16**,** 456.
CZERNEK, L. & DUCHLER, M. 2017. Functions of Cancer-Derived Extracellular Vesicles in Immunosuppression. *Arch Immunol Ther Exp (Warsz),* 65**,** 311-323.
DAL PORTO, J. M., GAULD, S. B., MERRELL, K. T., MILLS, D., PUGH-BERNARD, A. E. & CAMBIER, J. 2004. B cell antigen receptor signaling 101. *Molecular Immunology,* 41**,** 599-613.
DALE, D. C., BOXER, L. & LILES, W. C. 2008. The phagocytes: neutrophils and monocytes. *Blood,* 112**,** 935-45.
DAVIS, R. E., BROWN, K. D., SIEBENLIST, U. & STAUDT, L. M. 2001. Constitutive nuclear factor kappa B activity is required for survival of activated B cell-like diffuse large B cell lymphoma cells. *Journal of Experimental Medicine,* 194**,** 1861-1874.
DE ALBORAN, I. M., O'HAGAN, R. C., GARTNER, F., MALYNN, B., DAVIDSON, L., RICKERT, R., RAJEWSKY, K., DEPINHO, R. A. & ALT, F. W. 2001. Analysis of C-MYC function in normal cells via conditional gene-targeted mutation. *Immunity,* 14**,** 45-55.
DE JONG, J. S., VAN DIEST, P. J. & BAAK, J. P. A. 2000. Number of apoptotic cells as a prognostic marker in invasive breast cancer. *British Journal of Cancer,* 82**,** 368-373.
DE PALMA, M., BIZIATO, D. & PETROVA, T. V. 2017. Microenvironmental regulation of tumour angiogenesis. *Nat Rev Cancer,* 17**,** 457-474.
DE PALMA, M., VENNERI, M. A., GALLI, R., SERGI, L. S., POLITI, L. S., SAMPAOLESI, M. & NALDINI, L. 2005. Tie2 identifies a hematopoietic monocytes required for tumor lineage of proangiogenic vessel formation and a mesenchymal population of pericyte progenitors. *Cancer Cell,* 8**,** 211-226.
DETRICH, H. W., 3RD, KIERAN, M. W., CHAN, F. Y., BARONE, L. M., YEE, K., RUNDSTADLER, J. A., PRATT, S., RANSOM, D. & ZON, L. I. 1995. Intraembryonic hematopoietic cell migration during vertebrate development. *Proc Natl Acad Sci U S A,* 92**,** 10713-7.
DEVITT, A., MOFFATT, O. D., RAYKUNDALIA, C., CAPRA, J. D., SIMMONS, D. L. & GREGORY, C. D. 1998. Human CD14 mediates recognition and phagocytosis of apoptotic cells. *Nature,* 392**,** 505-9.
DEWS, M., HOMAYOUNI, A., YU, D., MURPHY, D., SEVIGNANI, C., WENTZEL, E., FURTH, E. E., LEE, W. M., ENDERS, G. H., MENDELL, J. T. & THOMAS-TIKHONENKO, A. 2006. Augmentation of tumor angiogenesis by a Myc-activated microRNA cluster. *Nat Genet,* 38**,** 1060-5.

DI NOIA, J. M. & NEUBERGER, M. S. 2007. Molecular mechanisms of antibody somatic hypermutation. *Annu Rev Biochem,* 76**,** 1-22.

DIERLAMM, J., BAENS, M., WLODARSKA, I., STEFANOVA-OUZOUNOVA, M., HERNANDEZ, J. M., HOSSFELD, D. K., DE WOLF-PEETERS, C., HAGEMEIJER, A., VAN DEN BERGHE, H. & MARYNEN, P. 1999. The apoptosis inhibitor gene API2 and a novel 18q gene, MLT, are recurrently rearranged in the t(11;18)(q21;q21) associated with mucosa-associated lymphoid tissue lymphomas. *Blood,* 93**,** 3601-9.

DIEZ-ROUX, G. & LANG, R. A. 1997. Macrophages induce apoptosis in normal cells in vivo. *Development,* 124**,** 3633-8.

DONNOU, S., GALAND, C., TOUITOU, V., SAUTES-FRIDMAN, C., FABRY, Z. & FISSON, S. 2012. Murine models of B-cell lymphomas: promising tools for designing cancer therapies. *Adv Hematol,* 2012**,** 701704.

DOTAN, E., AGGARWAL, C. & SMITH, M. R. 2010. Impact of Rituximab (Rituxan) on the Treatment of B-Cell Non-Hodgkin's Lymphoma. *P T,* 35**,** 148-57.

EDWARDS, J. P., ZHANG, X., FRAUWIRTH, K. A. & MOSSER, D. M. 2006. Biochemical and functional characterization of three activated macrophage populations. *J Leukoc Biol,* 80**,** 1298-307.

EGLE, A., HARRIS, A. W., BATH, M. L., O'REILLY, L. & CORY, S. 2004. VavP-Bcl2 transgenic mice develop follicular lymphoma preceded by germinal center hyperplasia. *Blood,* 103**,** 2276-2283.

EISCHEN, C. M., WEBER, J. D., ROUSSEL, M. F., SHERR, C. J. & CLEVELAND, J. L. 1999. Disruption of the ARF-Mdm2-p53 tumor suppressor pathway in Myc-induced lymphomagenesis. *Genes & Development,* 13**,** 2658-2669.

EISENMAN, S. T., GIBBONS, S. J., VERHULST, P. J. & FARRUGIA, G. 2015. TNF alpha Derived From Conventionally-Activated M1 Macrophages Inhibits Survival of Mouse Interstitial Cells of Cajal. *Gastroenterology,* 148**,** S18-S18.

ELLETT, F., PASE, L., HAYMAN, J. W., ANDRIANOPOULOS, A. & LIESCHKE, G. J. 2011. mpeg1 promoter transgenes direct macrophage-lineage expression in zebrafish. *Blood,* 117**,** e49-56.

ELLIOTT, M. R., CHEKENI, F. B., TRAMPONT, P. C., LAZAROWSKI, E. R., KADL, A., WALK, S. F., PARK, D., WOODSON, R. I., OSTANKOVICH, M., SHARMA, P., LYSIAK, J. J., HARDEN, T. K., LEITINGER, N. & RAVICHANDRAN, K. S. 2009. Nucleotides released by apoptotic cells act as a find-me signal to promote phagocytic clearance. *Nature,* 461**,** 282-U165.

ELMORE, S. 2007. Apoptosis: a review of programmed cell death. *Toxicol Pathol,* 35**,** 495-516.

ELSON, A., DENG, C., CAMPOS-TORRES, J., DONEHOWER, L. A. & LEDER, P. 1995. The MMTV/c-myc transgene and p53 null alleles collaborate to induce T-cell lymphomas, but not mammary carcinomas in transgenic mice. *Oncogene,* 11**,** 181-90.

ESCREVENTE, C., KELLER, S., ALTEVOGT, P. & COSTA, J. 2011. Interaction and uptake of exosomes by ovarian cancer cells. *Bmc Cancer,* 11.

ETCHIN, J., KANKI, J. P. & LOOK, A. T. 2011. Zebrafish as a Model for the Study of Human Cancer. *Zebrafish: Disease Models and Chemical Screens, 3rd Edition,* 105**,** 309-337.

EVAN, G. I., WYLLIE, A. H., GILBERT, C. S., LITTLEWOOD, T. D., LAND, H., BROOKS, M., WATERS, C. M., PENN, L. Z. & HANCOCK, D. C. 1992. Induction of apoptosis in fibroblasts by c-myc protein. *Cell,* 69**,** 119-28.

FACCHINI, L. M. & PENN, L. Z. 1998. The molecular role of Myc in growth and transformation: recent discoveries lead to new insights. *FASEB J,* 12**,** 633-51.

FADOK, V. A., BRATTON, D. L., KONOWAL, A., FREED, P. W., WESTCOTT, J. Y. & HENSON, P. M. 1998. Macrophages that have ingested apoptotic cells in vitro inhibit proinflammatory cytokine production through autocrine/paracrine mechanisms involving TGF-beta, PGE2, and PAF. *Journal of Clinical Investigation,* 101**,** 890-898.

FAN, Z., BERESFORD, P. J., OH, D. Y., ZHANG, D. & LIEBERMAN, J. 2003. Tumor suppressor NM23-H1 is a granzyme A-activated DNase during CTL-mediated apoptosis, and the nucleosome assembly protein SET is its inhibitor. *Cell,* 112**,** 659-72.

FAVRE, C. J., MANCUSO, M., MAAS, K., MCLEAN, J. W., BALUK, P. & MCDONALD, D. M. 2003. Expression of genes involved in vascular development and angiogenesis in endothelial cells of adult lung. *Am J Physiol Heart Circ Physiol,* 285**,** H1917-38.

FELSHER, D. W. & BISHOP, J. M. 1999a. Reversible tumorigenesis by MYC in hematopoietic lineages. *Mol Cell,* 4**,** 199-207.

FELSHER, D. W. & BISHOP, J. M. 1999b. Transient excess of MYC activity can elicit genomic instability and tumorigenesis. *Proceedings of the National Academy of Sciences of the United States of America,* 96**,** 3940-3944.

FERRARA, N., GERBER, H. P. & LECOUTER, J. 2003. The biology of VEGF and its receptors. *Nat Med,* 9**,** 669-76.

FIERS, W. 1991. Tumor-Necrosis-Factor - Characterization at the Molecular, Cellular and Invivo Level. *Febs Letters,* 285**,** 199-212.

FISHER, S. G. & FISHER, R. I. 2004. The epidemiology of non-Hodgkin's lymphoma. *Oncogene,* 23**,** 6524-34.

FLOREY, O. & HASKARD, D. O. 2009. Sphingosine 1-phosphate enhances Fc gamma receptor-mediated neutrophil activation and recruitment under flow conditions. *J Immunol,* 183**,** 2330-6.

FORD, C. A., PETROVA, S., POUND, J. D., VOSS, J. J., MELVILLE, L., PATERSON, M., FARNWORTH, S. L., GALLIMORE, A. M., CUFF, S., WHEADON, H., DOBBIN, E., OGDEN, C. A., DUMITRIU, I. E., DUNBAR, D. R., MURRAY, P. G., RUCKERL, D., ALLEN, J. E., HUME, D. A., VAN ROOIJEN, N., GOODLAD, J. R., FREEMAN, T. C. & GREGORY, C. D. 2015. Oncogenic properties of apoptotic tumor cells in aggressive B cell lymphoma. *Curr Biol,* 25**,** 577-88.

FOX, S. B., GATTER, K. C. & HARRIS, A. L. 1996. Tumour angiogenesis. *J Pathol,* 179**,** 232-7.

GABARRE, J., RAPHAEL, M., LEPAGE, E., MARTIN, A., OKSENHENDLER, E., XERRI, L., TULLIEZ, M., AUDOUIN, J., COSTELLO, R., GOLFIER, J. B., SCHLAIFER, D., HEQUET, O., AZAR, N., KATLAMA, C., GISSELBRECHT, C. & GROUPE D'ETUDE DES LYMPHOMES DE, L. A. 2001. Human immunodeficiency virus-related lymphoma: relation between clinical features and histologic subtypes. *Am J Med,* 111**,** 704-11.

GABAY, M., LI, Y. L. & FELSHER, D. W. 2014. MYC Activation Is a Hallmark of Cancer Initiation and Maintenance. *Cold Spring Harbor Perspectives in Medicine,* 4.

GACCHE, R. N. & MESHRAM, R. J. 2014. Angiogenic factors as potential drug target: Efficacy and limitations of anti-angiogenic therapy. *Biochimica Et Biophysica Acta-Reviews on Cancer,* 1846**,** 161-179.

GAIDANO, G., BALLERINI, P., GONG, J. Z., INGHIRAMI, G., NERI, A., NEWCOMB, E. W., MAGRATH, I. T., KNOWLES, D. M. & DALLA-FAVERA, R. 1991. p53 mutations in human lymphoid malignancies: association with Burkitt lymphoma and chronic lymphocytic leukemia. *Proc Natl Acad Sci U S A,* 88**,** 5413-7.

GARDAI, S. J., MCPHILLIPS, K. A., FRASCH, S. C., JANSSEN, W. J., STAREFELDT, A., MURPHY-ULLRICH, J. E., BRATTON, D. L., OLDENBORG, P. A., MICHALAK, M. & HENSON, P. M. 2005. Cell-surface calreticulin initiates clearance of viable or apoptotic cells through trans-activation of LRP on the phagocyte. *Cell,* 123**,** 321-34.

GERHARDT, H., GOLDING, M., FRUTTIGER, M., RUHRBERG, C., LUNDKVIST, A., ABRAMSSON, A., JELTSCH, M., MITCHELL, C., ALITALO, K., SHIMA, D. & BETSHOLTZ, C. 2003. VEGF guides angiogenic sprouting utilizing endothelial tip cell filopodia. *J Cell Biol,* 161**,** 1163-77.

GERLACH, G. F., SCHRADER, L. N. & WINGERT, R. A. 2011. Dissection of the adult zebrafish kidney. *J Vis Exp*.

GOD, J. M. & HAQUE, A. 2010. Burkitt lymphoma: pathogenesis and immune evasion. *J Oncol,* 2010.

GOODWIN, A. M., SULLIVAN, K. M. & D'AMORE, P. A. 2006. Cultured endothelial cells display endogenous activation of the canonical Wnt signaling pathway and express multiple ligands, receptors, and secreted modulators of Wnt signaling. *Dev Dyn,* 235**,** 3110-20.

GORDON, S. 1999. Macrophage-restricted molecules: role in differentiation and activation. *Immunol Lett,* 65**,** 5-8.

GOULD, S. J. & RAPOSO, G. 2013. As we wait: coping with an imperfect nomenclature for extracellular vesicles. *J Extracell Vesicles,* 2.

GRABHER, C. & LOOK, A. T. 2006. Fishing for cancer models. *Nat Biotechnol,* 24**,** 45-6.

GREEN, D. R. 2011. Means to an End: Apoptosis and Other Cell Death Mechanisms. *Cold Spring Harbor Laboratory Press*.

GREENWALD, R. J., TUMANG, J. R., SINHA, A., CURRIER, N., CARDIFF, R. D., ROTHSTEIN, T. L., FALLER, D. V. & DENIS, G. V. 2004. E mu-BRD2 transgenic mice develop B-cell lymphoma and leukemia. *Blood,* 103**,** 1475-1484.

GREGORY, C. D., FORD, C. A. & VOSS, J. J. 2016. Microenvironmental Effects of Cell Death in Malignant Disease. *Adv Exp Med Biol,* 930**,** 51-88.

GREGORY, C. D. & PATERSON, M. 2018. An apoptosis-driven 'onco-regenerative niche': roles of tumour-associated macrophages and extracellular vesicles. *Philos Trans R Soc Lond B Biol Sci,* 373.

GREGORY, C. D. & POUND, J. D. 2010. Microenvironmental influences of apoptosis in vivo and in vitro. *Apoptosis,* 15**,** 1029-49.

GREGORY, C. D., ROSSI, A. G., BOURNAZOU, I., ZHUANG, L. & WILLEMS, J. J. 2011. Leukocyte migratory responses to apoptosis: the attraction and the distraction. *Cell Adh Migr,* 5**,** 293-7.

GREGORY, M. A. & HANN, S. R. 2000. c-Myc proteolysis by the ubiquitin-proteasome pathway: stabilization of c-Myc in Burkitt's lymphoma cells. *Mol Cell Biol,* 20**,** 2423-35.

GRIMSLEY, C. & RAVICHANDRAN, K. S. 2003. Cues for apoptotic cell engulfment: eat-me, don't eat-med and come-get-me signals. *Trends in Cell Biology,* 13**,** 648-656.

GRIVENNIKOV, S. I., GRETEN, F. R. & KARIN, M. 2010. Immunity, Inflammation, and Cancer. *Cell,* 140**,** 883-899.

GRUMONT, R. J., ROURKE, I. J. & GERONDAKIS, S. 1999. Rel-dependent induction of A1 transcription is required to protect B cells from antigen receptor ligation-induced apoptosis. *Genes & Development,* 13**,** 400-411.

GRUMONT, R. J., ROURKE, I. J., O'REILLY, L. A., STRASSER, A., MIYAKE, K., SHA, W. & GERONDAKIS, S. 1998. B lymphocytes differentially use the Rel and nuclear factor kappa B1 (NF-kappa B1) transcription factors to regulate cell cycle progression and apoptosis in quiescent and mitogen-activated cells. *Journal of Experimental Medicine,* 187**,** 663-674.

GUDE, D. R., ALVAREZ, S. E., PAUGH, S. W., MITRA, P., YU, J. D., GRIFFITHS, R., BARBOUR, S. E., MILSTIEN, S. & SPIEGEL, S. 2008. Apoptosis induces expression of sphingosine kinase 1 to release sphingosine-1-phosphate as a "come-and-get-me" signal. *Faseb Journal,* 22**,** 2629-2638.

GUMIENNY, T. L., BRUGNERA, E., TOSELLO-TRAMPONT, A. C., KINCHEN, J. M., HANEY, L. B., NISHIWAKI, K., WALK, S. F., NEMERGUT, M. E., MACARA, I. G., FRANCIS, R., SCHEDL, T., QIN, Y., VAN AELST, L., HENGARTNER, M. O. & RAVICHANDRAN, K. S. 2001. CED-12/ELMO, a novel member of the crkII/dock180/rac pathway, is required for phagocytosis and cell migration. *Cell,* 107**,** 27-41.

GUPTA, S. 2001. Molecular steps of tumor necrosis factor receptor-mediated apoptosis. *Curr Mol Med,* 1**,** 317-24.

GUREVICH, D. B., SEVERN, C. E., TWOMEY, C., GREENHOUGH, A., CASH, J., TOYE, A. M., MELLOR, H. & MARTIN, P. 2018. Live imaging of wound angiogenesis reveals macrophage orchestrated vessel sprouting and regression. *EMBO J,* 37.

GYRD-HANSEN, M., DARDING, M., MIASARI, M., SANTORO, M. M., ZENDER, L., XUE, W., TENEV, T., DA FONSECA, P. C. A., ZVELEBIL, M., BUJNICKI, J. M., LOWE, S., SILKE, J. & MEIER, P. 2008. IAPs contain an evolutionarily conserved ubiquitin-binding domain that regulates NF-kappa B as well as cell survival and oncogenesis. *Nature Cell Biology,* 10**,** 1309-U130.

GYRD-HANSEN, M. & MEIER, P. 2010. IAPs: from caspase inhibitors to modulators of NF-kappa B, inflammation and cancer. *Nature Reviews Cancer,* 10**,** 561-574.

HALDI, M., TON, C., SENG, W. L. & MCGRATH, P. 2006. Human melanoma cells transplanted into zebrafish proliferate, migrate, produce melanin, form masses and stimulate angiogenesis in zebrafish. *Angiogenesis,* 9**,** 139-51.

HALL, S. E., SAVILL, J. S., HENSON, P. M. & HASLETT, C. 1994. Apoptotic neutrophils are phagocytosed by fibroblasts with participation of the fibroblast vitronectin receptor and involvement of a mannose/fucose-specific lectin. *J Immunol,* 153**,** 3218-27.

HAN, S. S., SHAFFER, A. L., PENG, L., CHUNG, S. T., LIM, J. H., MAENG, S., KIM, J. S., MCNEIL, N., RIED, T., STAUDT, L. M. & JANZ, S. 2005. Molecular and cytological features of the mouse B-cell lymphoma line iMycEmu-1. *Mol Cancer,* 4**,** 40.

HANAHAN, D. & COUSSENS, L. M. 2012. Accessories to the crime: functions of cells recruited to the tumor microenvironment. *Cancer Cell,* 21**,** 309-22.

HANAHAN, D. & WEINBERG, R. A. 2000. The hallmarks of cancer. *Cell,* 100**,** 57-70.

HANAHAN, D. & WEINBERG, R. A. 2011. Hallmarks of cancer: the next generation. *Cell,* 144**,** 646-74.

HANAYAMA, R., TANAKA, M., MIWA, K., SHINOHARA, A., IWAMATSU, A. & NAGATA, S. 2002. Identification of a factor that links apoptotic cells to phagocytes. *Nature,* 417**,** 182-187.

HARDING, C., HEUSER, J. & STAHL, P. 1984. Endocytosis and intracellular processing of transferrin and colloidal gold-transferrin in rat reticulocytes: demonstration of a pathway for receptor shedding. *Eur J Cell Biol,* 35**,** 256-63.

HASHIMOTO, D., CHOW, A., NOIZAT, C., TEO, P., BEASLEY, M. B., LEBOEUF, M., BECKER, C. D., SEE, P., PRICE, J., LUCAS, D., GRETER, M., MORTHA, A., BOYER, S. W., FORSBERG, E. C., TANAKA, M., VAN ROOIJEN, N., GARCIA-SASTRE, A., STANLEY, E. R., GINHOUX, F., FRENETTE, P. S. & MERAD, M. 2013. Tissue-resident macrophages self-maintain locally throughout adult life with minimal contribution from circulating monocytes. *Immunity,* 38**,** 792-804.

HAYNIE, J. L. & BRYANT, P. J. 1976. Intercalary regeneration in imaginal wing disk of Drosophila melanogaster. *Nature,* 259**,** 659-62.

HE, S., LAMERS, G. E., BEENAKKER, J. W., CUI, C., GHOTRA, V. P., DANEN, E. H., MEIJER, A. H., SPAINK, H. P. & SNAAR-JAGALSKA, B. E. 2012. Neutrophil-mediated experimental metastasis is enhanced

by VEGFR inhibition in a zebrafish xenograft model. *J Pathol,* 227**,** 431-45.
HECHT, J. L. & ASTER, J. C. 2000. Molecular biology of Burkitt's lymphoma. *J Clin Oncol,* 18**,** 3707-21.
HEINZEL, S., BINH GIANG, T., KAN, A., MARCHINGO, J. M., LYE, B. K., CORCORAN, L. M. & HODGKIN, P. D. 2017. A Myc-dependent division timer complements a cell-death timer to regulate T cell and B cell responses. *Nat Immunol,* 18**,** 96-103.
HENGARTNER, M. O. 2000. The biochemistry of apoptosis. *Nature,* 407**,** 770-6.
HERBOMEL, P., THISSE, B. & THISSE, C. 1999. Ontogeny and behaviour of early macrophages in the zebrafish embryo. *Development,* 126**,** 3735-3745.
HERBOMEL, P., THISSE, B. & THISSE, C. 2001. Zebrafish early macrophages colonize cephalic mesenchyme and developing brain, retina, and epidermis through, a M-CSF receptor-dependent invasive process. *Developmental Biology,* 238**,** 274-288.
HEROLD, S., WANZEL, M., BEUGER, V., FROHME, C., BEUL, D., HILLUKKALA, T., SYVAOJA, J., SALUZ, H. P., HAENEL, F. & EILERS, M. 2002. Negative regulation of the mammalian UV response by Myc through association with Miz-1. *Molecular Cell,* 10**,** 509-521.
HIDDEMANN, W., KNEBA, M., DREYLING, M., SCHMITZ, N., LENGFELDER, E., SCHMITS, R., REISER, M., METZNER, B., HARDER, H., HEGEWISCH-BECKER, S., FISCHER, T., KROPFF, M., REIS, H. E., FREUND, M., WORMANN, B., FUCHS, R., PLANKER, M., SCHIMKE, J., EIMERMACHER, H., TRUMPER, L., ALDAOUD, A., PARWARESCH, R. & UNTERHALT, M. 2005. Frontline therapy with rituximab added to the combination of cyclophosphamide, doxorubicin, vincristine, and prednisone (CHOP) significantly improves the outcome for patients with advanced-stage follicular lymphoma compared with therapy with CHOP alone: results of a prospective randomized study of the German Low-Grade Lymphoma Study Group. *Blood,* 106**,** 3725-32.
HLUSHCHUK, R., MAKANYA, A. N. & DJONOV, V. 2011. Escape mechanisms after antiangiogenic treatment, or why are the tumors growing again? *International Journal of Developmental Biology,* 55**,** 563-567.
HOCHREITER-HUFFORD, A. & RAVICHANDRAN, K. S. 2013. Clearing the dead: apoptotic cell sensing, recognition, engulfment, and digestion. *Cold Spring Harb Perspect Biol,* 5**,** a008748.
HOEPPNER, D. J., HENGARTNER, M. O. & SCHNABEL, R. 2001. Engulfment genes cooperate with ced-3 to promote cell death in Caenorhabditis elegans. *Nature,* 412**,** 202-6.
HUANG, Q., LI, F., LIU, X., LI, W., SHI, W., LIU, F. F., O'SULLIVAN, B., HE, Z., PENG, Y., TAN, A. C., ZHOU, L., SHEN, J., HAN, G., WANG, X. J., THORBURN, J., THORBURN, A., JIMENO, A., RABEN, D., BEDFORD, J. S. & LI, C. Y. 2011. Caspase 3-mediated stimulation of

tumor cell repopulation during cancer radiotherapy. *Nat Med,* 17**,** 860-6.
ICHIM, G. & TAIT, S. W. G. 2016. A fate worse than death: apoptosis as an oncogenic process. *Nature Reviews Cancer,* 16**,** 539-548.
INAL, J. M., ANSA-ADDO, E. A., STRATTON, D., KHOLIA, S., ANTWI-BAFFOUR, S. S., JORFI, S. & LANGE, S. 2012. Microvesicles in health and disease. *Arch Immunol Ther Exp (Warsz),* 60**,** 107-21.
IORIO, M. V. & CROCE, C. M. 2012. microRNA involvement in human cancer. *Carcinogenesis,* 33**,** 1126-33.
ISOGAI, S., HORIGUCHI, M. & WEINSTEIN, B. M. 2001. The vascular anatomy of the developing zebrafish: an atlas of embryonic and early larval development. *Dev Biol,* 230**,** 278-301.
IVANOVSKI, O., KULKEAW, K., NAKAGAWA, M., SASAKI, T., MIZUOCHI, C., HORIO, Y., ISHITANI, T. & SUGIYAMA, D. 2009. Characterization of kidney marrow in zebrafish (Danio rerio) by using a new surgical technique. *Prilozi,* 30**,** 71-80.
JACOBS, J. J. L., SCHEIJEN, B., VONCKEN, J. W., KIEBOOM, K., BERNS, A. & VAN LOHUIZEN, M. 1999. Bmi-1 collaborates with c-Myc in tumorigenesis by inhibiting c-Myc-induced apoptosis via INK4a/ARF. *Genes & Development,* 13**,** 2678-2690.
JACOBSEN, K. A., PRASAD, V. S., SIDMAN, C. L. & OSMOND, D. G. 1994. Apoptosis and macrophage-mediated deletion of precursor B cells in the bone marrow of E mu-myc transgenic mice. *Blood,* 84**,** 2784-94.
JAFFE ES, H. N., STEIN H, VARDIMAN JW 2001. Pathology and Genetics of Tumours of Haematopoietic and Lymphoid Tissues. *WHO Classification of Tumours, 3rd Edition,,* 3.
JENKINS, S. J., RUCKERL, D., COOK, P. C., JONES, L. H., FINKELMAN, F. D., VAN ROOIJEN, N., MACDONALD, A. S. & ALLEN, J. E. 2011. Local Macrophage Proliferation, Rather than Recruitment from the Blood, Is a Signature of T(H)2 Inflammation. *Science,* 332**,** 1284-1288.
JIN, S. W., BEIS, D., MITCHELL, T., CHEN, J. N. & STAINIER, D. Y. 2005. Cellular and molecular analyses of vascular tube and lumen formation in zebrafish. *Development,* 132**,** 5199-209.
JUNCADELLA, I. J., KADL, A., SHARMA, A. K., SHIM, Y. M., HOCHREITER-HUFFORD, A., BORISH, L. & RAVICHANDRAN, K. S. 2013. Apoptotic cell clearance by bronchial epithelial cells critically influences airway inflammation. *Nature,* 493**,** 547-51.
JUNG, D. W., OH, E. S., PARK, S. H., CHANG, Y. T., KIM, C. H., CHOI, S. Y. & WILLIAMS, D. R. 2012. A novel zebrafish human tumor xenograft model validated for anti-cancer drug screening. *Mol Biosyst,* 8**,** 1930-9.
JUNTTILA, M. R. & DE SAUVAGE, F. J. 2013. Influence of tumour micro-environment heterogeneity on therapeutic response. *Nature,* 501**,** 346-54.
KARPERIEN, A., AHAMMER, H. & JELINEK, H. F. 2013. Quantitating the subtleties of microglial morphology with fractal analysis. *Front Cell Neurosci,* 7**,** 3.

KAWAKAMI, K. 2007. Tol2: a versatile gene transfer vector in vertebrates. *Genome Biol,* 8 Suppl 1**,** S7.
KERR, J. F. 2002. History of the events leading to the formulation of the apoptosis concept. *Toxicology,* 181-182**,** 471-4.
KERR, J. F., WYLLIE, A. H. & CURRIE, A. R. 1972. Apoptosis: a basic biological phenomenon with wide-ranging implications in tissue kinetics. *Br J Cancer,* 26**,** 239-57.
KIMMEL, C. B., BALLARD, W. W., KIMMEL, S. R., ULLMANN, B. & SCHILLING, T. F. 1995. Stages of embryonic development of the zebrafish. *Dev Dyn,* 203**,** 253-310.
KIRCHBERGER, S., STURTZEL, C., PASCOAL, S. & DISTEL, M. 2017. Quo natas, Danio?-Recent Progress in Modeling Cancer in Zebrafish. *Front Oncol,* 7**,** 186.
KISCHKEL, F. C., HELLBARDT, S., BEHRMANN, I., GERMER, M., PAWLITA, M., KRAMMER, P. H. & PETER, M. E. 1995. Cytotoxicity-Dependent Apo-1 (Fas/Cd95)-Associated Proteins Form a Death-Inducing Signaling Complex (Disc) with the Receptor. *Embo Journal,* 14**,** 5579-5588.
KITAGUCHI, T., KAWAKAMI, K. & KAWAHARA, A. 2009. Transcriptional regulation of a myeloid-lineage specific gene lysozyme C during zebrafish myelopoiesis. *Mech Dev,* 126**,** 314-23.
KLIMP, A. H., HOLLEMA, H., KEMPINGA, C., VAN DER ZEE, A. G., DE VRIES, E. G. & DAEMEN, T. 2001. Expression of cyclooxygenase-2 and inducible nitric oxide synthase in human ovarian tumors and tumor-associated macrophages. *Cancer Res,* 61**,** 7305-9.
KNEZEVICH, S., LUDKOVSKI, O., SALSKI, C., LESTOU, V., CHHANABHAI, M., LAM, W., KLASA, R., CONNORS, J. M., DYER, M. J. S., GASCOYNE, R. D. & HORSMAN, D. E. 2005. Concurrent translocation of BCL2 and MYC with a single immunoglobulin locus in high-grade B-cell lymphomas. *Leukemia,* 19**,** 659-663.
KOBARA, M., SUNAGAWA, N., ABE, M., TANAKA, N., TOBA, H., HAYASHI, H., KEIRA, N., TATSUMI, T., MATSUBARA, H. & NAKATA, T. 2008. Apoptotic myocytes generate monocyte chemoattractant protein-1 and mediate macrophage recruitment. *Journal of Applied Physiology,* 104**,** 601-609.
KONANTZ, M., BALCI, T. B., HARTWIG, U. F., DELLAIRE, G., ANDRE, M. C., BERMAN, J. N. & LENGERKE, C. 2012. Zebrafish xenografts as a tool for in vivo studies on human cancer. *Hematopoietic Stem Cells Viii,* 1266**,** 124-137.
KOSAKA, N., IGUCHI, H., HAGIWARA, K., YOSHIOKA, Y., TAKESHITA, F. & OCHIYA, T. 2013. Neutral sphingomyelinase 2 (nSMase2)-dependent exosomal transfer of angiogenic microRNAs regulate cancer cell metastasis. *J Biol Chem,* 288**,** 10849-59.
KOVALCHUK, A. L., QI, C. F., TORREY, T. A., TADDESSE-HEATH, L., FEIGENBAUM, L., PARK, S. S., GERBITZ, A., KLOBECK, G., HOERTNAGEL, K., POLACK, A., BORNKAMM, G. W., JANZ, S. & MORSE, H. C., 3RD 2000. Burkitt lymphoma in the mouse. *J Exp Med,* 192**,** 1183-90.

KREIDER, T., ANTHONY, R. M., URBAN, J. F., JR. & GAUSE, W. C. 2007. Alternatively activated macrophages in helminth infections. *Curr Opin Immunol,* 19**,** 448-53.

KUPPERS, R. 2005. Mechanisms of B-cell lymphoma pathogenesis. *Nat Rev Cancer,* 5**,** 251-62.

KUPPERS, R. & DALLA-FAVERA, R. 2001. Mechanisms of chromosomal translocations in B cell lymphomas. *Oncogene,* 20**,** 5580-94.

KUPPERS, R., KLEIN, U., HANSMANN, M. L. & RAJEWSKY, K. 1999. Cellular origin of human B-cell lymphomas. *N Engl J Med,* 341**,** 1520-9.

LAM, S. H., WU, Y. L., VEGA, V. B., MILLER, L. D., SPITSBERGEN, J., TONG, Y., ZHAN, H., GOVINDARAJAN, K. R., LEE, S., MATHAVAN, S., MURTHY, K. R., BUHLER, D. R., LIU, E. T. & GONG, Z. 2006. Conservation of gene expression signatures between zebrafish and human liver tumors and tumor progression. *Nat Biotechnol,* 24**,** 73-5.

LANG, R. A. & BISHOP, J. M. 1993. Macrophages are required for cell death and tissue remodeling in the developing mouse eye. *Cell,* 74**,** 453-62.

LANGENAU, D. M., FENG, H., BERGHMANS, S., KANKI, J. P., KUTOK, J. L. & LOOK, A. T. 2005. Cre/lox-regulated transgenic zebrafish model with conditional myc-induced T cell acute lymphoblastic leukemia. *Proc Natl Acad Sci U S A,* 102**,** 6068-73.

LANGENAU, D. M., FERRANDO, A. A., TRAVER, D., KUTOK, J. L., HEZEL, J. P., KANKI, J. P., ZON, L. I., LOOK, A. T. & TREDE, N. S. 2004. In vivo tracking of T cell development, ablation, and engraftment in transgenic zebrafish. *Proc Natl Acad Sci U S A,* 101**,** 7369-74.

LANGENAU, D. M., KEEFE, M. D., STORER, N. Y., GUYON, J. R., KUTOK, J. L., LE, X., GOESSLING, W., NEUBERG, D. S., KUNKEL, L. M. & ZON, L. I. 2007. Effects of RAS on the genesis of embryonal rhabdomyosarcoma. *Genes Dev,* 21**,** 1382-95.

LANGENAU, D. M., TRAVER, D., FERRANDO, A. A., KUTOK, J. L., ASTER, J. C., KANKI, J. P., LIN, S., PROCHOWNIK, E., TREDE, N. S., ZON, L. I. & LOOK, A. T. 2003. Myc-induced T cell leukemia in transgenic zebrafish. *Science,* 299**,** 887-90.

LAUBER, K., BOHN, E., KROBER, S. M., XIAO, Y. J., BLUMENTHAL, S. G., LINDEMANN, R. K., MARINI, P., WIEDIG, C., ZOBYWALSKI, A., BAKSH, S., XU, Y., AUTENRIETH, I. B., SCHULZE-OSTHOFF, K., BELKA, C., STUHLER, G. & WESSELBORG, S. 2003. Apoptotic cells induce migration of phagocytes via caspase-3-mediated release of a lipid attraction signal. *Cell,* 113**,** 717-30.

LAVIN, Y., MORTHA, A., RAHMAN, A. & MERAD, M. 2015. Regulation of macrophage development and function in peripheral tissues. *Nat Rev Immunol,* 15**,** 731-44.

LAWSON, N. D. & WEINSTEIN, B. M. 2002. In vivo imaging of embryonic vascular development using transgenic zebrafish. *Dev Biol,* 248**,** 307-18.

LE, X., LANGENAU, D. M., KEEFE, M. D., KUTOK, J. L., NEUBERG, D. S. & ZON, L. I. 2007. Heat shock-inducible Cre/Lox approaches to induce

diverse types of tumors and hyperplasia in transgenic zebrafish. *Proc Natl Acad Sci U S A,* 104**,** 9410-5.

LEE, L. M., SEFTOR, E. A., BONDE, G., CORNELL, R. A. & HENDRIX, M. J. 2005. The fate of human malignant melanoma cells transplanted into zebrafish embryos: assessment of migration and cell division in the absence of tumor formation. *Dev Dyn,* 233**,** 1560-70.

LEE, S. L. C., ROUHI, P., JENSEN, L. D., ZHANG, D. F., JI, H., HAUPTMANN, G., INGHAM, P. & CAO, Y. H. 2009. Hypoxia-induced pathological angiogenesis mediates tumor cell dissemination, invasion, and metastasis in a zebrafish tumor model. *Proceedings of the National Academy of Sciences of the United States of America,* 106**,** 19485-19490.

LESNIK, J., ANTES, T., KIM, J., GRINER, E., PEDRO, L. & BIOL, R. P. C. 2016. Registered report: Melanoma exosomes educate bone marrow progenitor cells toward a pro-metastatic phenotype through MET. *Elife,* 5.

LEUCCI, E., COCCO, M., ONNIS, A., DE FALCO, G., VAN CLEEF, P., BELLAN, C., VAN RIJK, A., NYAGOL, J., BYAKIKA, B., LAZZI, S., TOSI, P., VAN KRIEKEN, H. & LEONCINI, L. 2008. MYC translocation-negative classical Burkitt lymphoma cases: an alternative pathogenetic mechanism involving miRNA deregulation. *J Pathol,* 216**,** 440-50.

LEVINE, A. J. 1997. p53, the cellular gatekeeper for growth and division. *Cell,* 88**,** 323-31.

LEWIS, C. E., HARNEY, A. S. & POLLARD, J. W. 2016. The Multifaceted Role of Perivascular Macrophages in Tumors. *Cancer Cell,* 30**,** 18-25.

LEWIS, C. E., LEEK, R., HARRIS, A. & MCGEE, J. O. 1995. Cytokine regulation of angiogenesis in breast cancer: the role of tumor-associated macrophages. *J Leukoc Biol,* 57**,** 747-51.

LEWIS, C. E. & POLLARD, J. W. 2006. Distinct role of macrophages in different tumor microenvironments. *Cancer Res,* 66**,** 605-12.

LI, C., XU, M. M., WANG, K., ADLER, A. J., VELLA, A. T. & ZHOU, B. 2018. Macrophage polarization and meta-inflammation. *Transl Res,* 191**,** 29-44.

LI, J., LI, K., DONG, X., LIANG, D. & ZHAO, Q. 2014. Ncor1 and Ncor2 play essential but distinct roles in zebrafish primitive myelopoiesis. *Dev Dyn,* 243**,** 1544-53.

LI, Q. & DANG, C. V. 1999. c-Myc overexpression uncouples DNA replication from mitosis. *Mol Cell Biol,* 19**,** 5339-51.

LIEBER, M. R. 2016. Mechanisms of human lymphoid chromosomal translocations. *Nat Rev Cancer,* 16**,** 387-98.

LIEBER, M. R., YU, K. & RAGHAVAN, S. C. 2006. Roles of nonhomologous DNA end joining, V(D)J recombination, and class switch recombination in chromosomal translocations. *DNA Repair (Amst),* 5**,** 1234-45.

LIEBERMAN, J. & FAN, Z. 2003. Nuclear war: the granzyme A-bomb. *Curr Opin Immunol,* 15**,** 553-9.

LIESCHKE, G. J. & CURRIE, P. D. 2007. Animal models of human disease: zebrafish swim into view. *Nat Rev Genet,* 8**,** 353-67.

LIESCHKE, G. J., OATES, A. C., PAW, B. H., THOMPSON, M. A., HALL, N. E., WARD, A. C., HO, R. K., ZON, L. I. & LAYTON, J. E. 2002. Zebrafish SPI-1 (PU.1) marks a site of myeloid development independent of primitive erythropoiesis: implications for axial patterning. *Dev Biol,* 246**,** 274-95.

LIN, E. Y., LI, J. F., GNATOVSKIY, L., DENG, Y., ZHU, L., GRZESIK, D. A., QIAN, H., XUE, X. N. & POLLARD, J. W. 2006. Macrophages regulate the angiogenic switch in a mouse model of breast cancer. *Cancer Res,* 66**,** 11238-46.

LITTLE, G. H. & FLORES, A. 1993. Inhibition of programmed cell death by catalase and phenylalanine methyl ester. *Comp Biochem Physiol Comp Physiol,* 105**,** 79-83.

LIU, F., ZHANG, G., ZHOU, X. H., LIU, J., YUE, Y. & ZHAO, T. 2010. [Immuno-characterization of mouse model similar to human diffuse large B cell lymphoma]. *Zhongguo Shi Yan Xue Ye Xue Za Zhi,* 18**,** 655-9.

LIU, X., KIM, C. N., YANG, J., JEMMERSON, R. & WANG, X. 1996. Induction of apoptotic program in cell-free extracts: requirement for dATP and cytochrome c. *Cell,* 86**,** 147-57.

LIU, X. J., LI, Y. S., SHINTON, S. A., RHODES, J., TANG, L. J., FENG, H., JETTE, C. A., LOOK, A. T., HAYAKAWA, K. & HARDY, R. R. 2017. Zebrafish B Cell Development without a Pre-B Cell Stage, Revealed by CD79 Fluorescence Reporter Transgenes. *Journal of Immunology,* 199**,** 1706-1715.

LOGES, S., SCHMIDT, T., TJWA, M., VAN GEYTE, K., LIEVENS, D., LUTGENS, E., VANHOUTTE, D., BORGEL, D., PLAISANCE, S., HOYLAERTS, M., LUTTUN, A., DEWERCHIN, M., JONCKX, B. & CARMELIET, P. 2010. Malignant cells fuel tumor growth by educating infiltrating leukocytes to produce the mitogen Gas6. *Blood,* 115**,** 2264-2273.

LUSCHER, B. 2001. Function and regulation of the transcription factors of the Myc/Max/Mad network. *Gene,* 277**,** 1-14.

MAKANYA, A. N., HLUSHCHUK, R. & DJONOV, V. G. 2009. Intussusceptive angiogenesis and its role in vascular morphogenesis, patterning, and remodeling. *Angiogenesis,* 12**,** 113-23.

MAKRIDAKIS, M. & VLAHOU, A. 2010. Secretome proteomics for discovery of cancer biomarkers. *J Proteomics,* 73**,** 2291-305.

MANTOVANI, A., GERMANO, G., MARCHESI, F., LOCATELLI, M. & BISWAS, S. K. 2011. Cancer-promoting tumor-associated macrophages: new vistas and open questions. *Eur J Immunol,* 41**,** 2522-5.

MANTOVANI, A., SOZZANI, S., LOCATI, M., ALLAVENA, P. & SICA, A. 2002. Macrophage polarization: tumor-associated macrophages as a paradigm for polarized M2 mononuclear phagocytes. *Trends in Immunology,* 23**,** 549-555.

MAO, C., TAHLIL-BEN MALEK, O., PUEYO, M. E., STEG, P. G. & SOUBRIER, F. 2000. Differential expression of rat frizzled-related frzb-1 and frizzled receptor fz1 and fz2 genes in the rat aorta after balloon injury. *Arteriosclerosis Thrombosis and Vascular Biology,* 20**,** 43-51.

MARQUES, I. J., WEISS, F. U., VLECKEN, D. H., NITSCHE, C., BAKKERS, J., LAGENDIJK, A. K., PARTECKE, L. I., HEIDECKE, C. D., LERCH, M. M. & BAGOWSKI, C. P. 2009. Metastatic behaviour of primary human tumours in a zebrafish xenotransplantation model. *BMC Cancer,* 9**,** 128.

MARQUES-DA-SILVA, C., BURNSTOCK, G., OJCIUS, D. M. & COUTINHO-SILVA, R. 2011. Purinergic receptor agonists modulate phagocytosis and clearance of apoptotic cells in macrophages. *Immunobiology,* 216**,** 1-11.

MARTIN-SUBERO, J. I., GESK, S., HARDER, L., SONOKI, T., TUCKER, P. W., SCHLEGELBERGER, B., GROTE, W., NOVO, F. J., CALASANZ, M. J., HANSMANN, M. L., DYER, M. J. & SIEBERT, R. 2002. Recurrent involvement of the REL and BCL11A loci in classical Hodgkin lymphoma. *Blood,* 99**,** 1474-7.

MARTINEZ, F. O., HELMING, L. & GORDON, S. 2009. Alternative activation of macrophages: an immunologic functional perspective. *Annu Rev Immunol,* 27**,** 451-83.

MASCKAUCHAN, T. N., SHAWBER, C. J., FUNAHASHI, Y., LI, C. M. & KITAJEWSKI, J. 2005. Wnt/beta-catenin signaling induces proliferation, survival and interleukin-8 in human endothelial cells. *Angiogenesis,* 8**,** 43-51.

MASCKAUCHAN, T. N. H., AGALLIU, D., VORONTCHIKHINA, M., AHN, A., PARMALEE, N. L., LI, C. M., KHOO, A., TYCKO, B., BROWN, A. M. C. & KITAJEWSKI, J. 2006. Wnt5a signaling induces proliferation and survival of endothelial cells in vitro and expression of MMP-1 and Tie-2. *Molecular Biology of the Cell,* 17**,** 5163-5172.

MATHIVANAN, S., LIM, J. W. E., TAURO, B. J., JI, H., MORITZ, R. L. & SIMPSON, R. J. 2010. Proteomics Analysis of A33 Immunoaffinity-purified Exosomes Released from the Human Colon Tumor Cell Line LIM1215 Reveals a Tissue-specific Protein Signature. *Molecular & Cellular Proteomics,* 9**,** 197-208.

MATSUZAKI, J. & OCHIYA, T. 2017. Circulating microRNAs and extracellular vesicles as potential cancer biomarkers: a systematic review. *Int J Clin Oncol,* 22**,** 413-420.

MATTAROLLO, S. R., WEST, A. C., STEEGH, K., DURET, H., PAGET, C., MARTIN, B., MATTHEWS, G. M., SHORTT, J., CHESI, M., BERGSAGEL, P. L., BOTS, M., ZUBER, J., LOWE, S. W., JOHNSTONE, R. W. & SMYTH, M. J. 2012. NKT cell adjuvant-based tumor vaccine for treatment of myc oncogene-driven mouse B-cell lymphoma. *Blood,* 120**,** 3019-29.

MATTSON, M. P. 2000. Apoptosis in neurodegenerative disorders. *Nat Rev Mol Cell Biol,* 1**,** 120-9.

MCDONALD, P. P., FADOK, V. A., BRATTON, D. & HENSON, P. M. 1999. Transcriptional and translational regulation of inflammatory mediator production by endogenous TGF-beta in macrophages that have ingested apoptotic cells. *J Immunol,* 163**,** 6164-72.

MCDONNELL, C. O., HILL, A. D., MCNAMARA, D. A., WALSH, T. N. & BOUCHIER-HAYES, D. J. 2000. Tumour micrometastases: the influence of angiogenesis. *Eur J Surg Oncol,* 26**,** 105-15.

MCILWAIN, D. R., BERGER, T. & MAK, T. W. 2015. Caspase functions in cell death and disease. *Cold Spring Harb Perspect Biol,* 7.

MCMAHON, S. B. 2014. MYC and the control of apoptosis. *Cold Spring Harb Perspect Med,* 4**,** a014407.

MCWHORTER, F. Y., WANG, T., NGUYEN, P., CHUNG, T. & LIU, W. F. 2013. Modulation of macrophage phenotype by cell shape. *Proc Natl Acad Sci U S A,* 110**,** 17253-8.

MEEKER, N. D. & TREDE, N. S. 2008. Immunology and zebrafish: spawning new models of human disease. *Dev Comp Immunol,* 32**,** 745-57.

MEYER, N., KIM, S. S. & PENN, L. Z. 2006. The Oscar-worthy role of Myc in apoptosis. *Semin Cancer Biol,* 16**,** 275-87.

MEYER, N. & PENN, L. Z. 2008. Reflecting on 25 years with MYC. *Nat Rev Cancer,* 8**,** 976-90.

MIKSA, M., AMIN, D., WU, R., RAVIKUMAR, T. S. & WANG, P. 2007. Fractalkine-induced MFG-E8 leads to enhanced apoptotic cell clearance by macrophages. *Mol Med,* 13**,** 553-60.

MILNER, A. E., JOHNSON, G. D. & GREGORY, C. D. 1992. Prevention of programmed cell death in Burkitt lymphoma cell lines by bcl-2-dependent and -independent mechanisms. *Int J Cancer,* 52**,** 636-44.

MINCIACCHI, V. R., FREEMAN, M. R. & DI VIZIO, D. 2015. Extracellular vesicles in cancer: exosomes, microvesicles and the emerging role of large oncosomes. *Semin Cell Dev Biol,* 40**,** 41-51.

MIONE, M. C. & TREDE, N. S. 2010. The zebrafish as a model for cancer. *Disease Models & Mechanisms,* 3**,** 517-523.

MIRBAHAI, L., WILLIAMS, T. D., ZHAN, H., GONG, Z. & CHIPMAN, J. K. 2011. Comprehensive profiling of zebrafish hepatic proximal promoter CpG island methylation and its modification during chemical carcinogenesis. *BMC Genomics,* 12**,** 3.

MIYANISHI, M., TADA, K., KOIKE, M., UCHIYAMA, Y., KITAMURA, T. & NAGATA, S. 2007. Identification of Tim4 as a phosphatidylserine receptor. *Nature,* 450**,** 435-439.

MIZGIREV, I. & REVSKOY, S. 2010. Generation of clonal zebrafish lines and transplantable hepatic tumors. *Nat Protoc,* 5**,** 383-94.

MOLDOVEANU, T., GRACE, C. R., LLAMBI, F., NOURSE, A., FITZGERALD, P., GEHRING, K., KRIWACKI, R. W. & GREEN, D. R. 2013. BID-induced structural changes in BAK promote apoptosis. *Nat Struct Mol Biol,* 20**,** 589-97.

MOLYNEUX, E. M., ROCHFORD, R., GRIFFIN, B., NEWTON, R., JACKSON, G., MENON, G., HARRISON, C. J., ISRAELS, T. & BAILEY, S. 2012. Burkitt's lymphoma. *Lancet,* 379**,** 1234-44.

MORTON, J. P. & SANSOM, O. J. 2013. MYC-y mice: from tumour initiation to therapeutic targeting of endogenous MYC. *Mol Oncol,* 7**,** 248-58.
MOSHAL, K. S., FERRI-LAGNEAU, K. F. & LEUNG, T. 2010. Zebrafish model: worth considering in defining tumor angiogenesis. *Trends Cardiovasc Med,* 20**,** 114-9.
MOSSER, D. M. & EDWARDS, J. P. 2008. Exploring the full spectrum of macrophage activation. *Nat Rev Immunol,* 8**,** 958-69.
MURALIDHARAN-CHARI, V., CLANCY, J., PLOU, C., ROMAO, M., CHAVRIER, P., RAPOSO, G. & D'SOUZA-SCHOREY, C. 2009. ARF6-regulated shedding of tumor cell-derived plasma membrane microvesicles. *Curr Biol,* 19**,** 1875-85.
MURAYAMA, E., KISSA, K., ZAPATA, A., MORDELET, E., BRIOLAT, V., LIN, H. F., HANDIN, R. I. & HERBOMEL, P. 2006. Tracing hematopoietic precursor migration to successive hematopoietic organs during zebrafish development. *Immunity,* 25**,** 963-75.
MURPHY, D. J., JUNTTILA, M. R., POUYET, L., KARNEZIS, A., SHCHORS, K., BUI, D. A., BROWN-SWIGART, L., JOHNSON, L. & EVAN, G. I. 2008. Distinct thresholds govern Myc's biological output in vivo. *Cancer Cell,* 14**,** 447-57.
NAGATA, S. 2010. Apoptosis and autoimmune diseases. *Ann N Y Acad Sci,* 1209**,** 10-6.
NATHAN, C. 2008. Metchnikoff's Legacy in 2008. *Nat Immunol,* 9**,** 695-8.
NEILSEN, P. M., NOLL, J. E., SUETANI, R. J., SCHULZ, R. B., AL-EJEH, F., EVDOKIOU, A., LANE, D. P. & CALLEN, D. F. 2011. Mutant p53 uses p63 as a molecular chaperone to alter gene expression and induce a pro-invasive secretome. *Oncotarget,* 2**,** 1203-1217.
NESBIT, C. E., TERSAK, J. M. & PROCHOWNIK, E. V. 1999. MYC oncogenes and human neoplastic disease. *Oncogene,* 18**,** 3004-16.
NEUMANN, J. C., DOVEY, J. S., CHANDLER, G. L., CARBAJAL, L. & AMATRUDA, J. F. 2009. Identification of a heritable model of testicular germ cell tumor in the zebrafish. *Zebrafish,* 6**,** 319-27.
NEWMAN, A. C. & HUGHES, C. C. 2012. Macrophages and angiogenesis: a role for Wnt signaling. *Vasc Cell,* 4**,** 13.
NGO, C. V., GEE, M., AKHTAR, N., YU, D., VOLPERT, O., AUERBACH, R. & THOMAS-TIKHONENKO, A. 2000. An in vivo function for the transforming Myc protein: elicitation of the angiogenic phenotype. *Cell Growth Differ,* 11**,** 201-10.
NGUYEN-CHI, M., LAPLACE-BUILHE, B., TRAVNICKOVA, J., LUZ-CRAWFORD, P., TEJEDOR, G., LUTFALLA, G., KISSA, K., JORGENSEN, C. & DJOUAD, F. 2017. TNF signaling and macrophages govern fin regeneration in zebrafish larvae. *Cell Death Dis,* 8**,** e2979.
NGUYEN-CHI, M., LAPLACE-BUILHE, B., TRAVNICKOVA, J., LUZ-CRAWFORD, P., TEJEDOR, G., PHAN, Q. T., DUROUX-RICHARD, I., LEVRAUD, J. P., KISSA, K., LUTFALLA, G., JORGENSEN, C. & DJOUAD, F. 2015. Identification of polarized macrophage subsets in zebrafish. *Elife,* 4**,** e07288.

NICOLI, S., DE SENA, G. & PRESTA, M. 2009. Fibroblast growth factor 2-induced angiogenesis in zebrafish: the zebrafish yolk membrane (ZFYM) angiogenesis assay. *J Cell Mol Med,* 13**,** 2061-8.
NICOLI, S. & PRESTA, M. 2007. The zebrafish/tumor xenograft angiogenesis assay. *Nat Protoc,* 2**,** 2918-23.
NICOLI, S., RIBATTI, D., COTELLI, F. & PRESTA, M. 2007. Mammalian tumor xenografts induce neovascularization in zebrafish embryos. *Cancer Res,* 67**,** 2927-31.
NOGUERA-TROISE, I., DALY, C., PAPADOPOULOS, N. J., COETZEE, S., BOLAND, P., GALE, N. W., LIN, H. C., YANCOPOULOS, G. D. & THURSTON, G. 2006. Blockade of Dll4 inhibits tumour growth by promoting non-productive angiogenesis. *Nature,* 444**,** 1032-1037.
NOY, R. & POLLARD, J. W. 2014. Tumor-associated macrophages: from mechanisms to therapy. *Immunity,* 41**,** 49-61.
NUSSENZWEIG, A. & NUSSENZWEIG, M. C. 2010. Origin of chromosomal translocations in lymphoid cancer. *Cell,* 141**,** 27-38.
OBAYA, A. J., MATEYAK, M. K. & SEDIVY, J. M. 1999. Mysterious liaisons: the relationship between c-Myc and the cell cycle. *Oncogene,* 18**,** 2934-2941.
OEHLERS, S. H., CRONAN, M. R., SCOTT, N. R., THOMAS, M. I., OKUDA, K. S., WALTON, E. M., BEERMAN, R. W., CROSIER, P. S. & TOBIN, D. M. 2015. Interception of host angiogenic signalling limits mycobacterial growth. *Nature,* 517**,** 612-5.
OGDEN, C. A., POUND, J. D., BATTH, B. K., OWENS, S., JOHANNESSEN, I., WOOD, K. & GREGORY, C. D. 2005. Enhanced apoptotic cell clearance capacity and B cell survival factor production by IL-10-activated macrophages: implications for Burkitt's lymphoma. *J Immunol,* 174**,** 3015-23.
OLIVIER, M., EELES, R., HOLLSTEIN, M., KHAN, M. A., HARRIS, C. C. & HAINAUT, P. 2002. The IARC TP53 database: new online mutation analysis and recommendations to users. *Hum Mutat,* 19**,** 607-14.
ONDREJKA, S. L. & HSI, E. D. 2015. Pathology of B-cell lymphomas: diagnosis and biomarker discovery. *Cancer Treat Res,* 165**,** 27-50.
OSTER, S. K., HO, C. S., SOUCIE, E. L. & PENN, L. Z. 2002. The myc oncogene: MarvelouslY Complex. *Adv Cancer Res,* 84**,** 81-154.
OSTUNI, R., KRATOCHVILL, F., MURRAY, P. J. & NATOLI, G. 2015. Macrophages and cancer: from mechanisms to therapeutic implications. *Trends Immunol,* 36**,** 229-39.
OTT, G. 2017. Aggressive B-cell lymphomas in the update of the 4th edition of the World Health Organization classification of haematopoietic and lymphatic tissues: refinements of the classification, new entities and genetic findings. *Br J Haematol,* 178**,** 871-887.
OTT, G., ROSENWALD, A. & CAMPO, E. 2013. Understanding MYC-driven aggressive B-cell lymphomas: pathogenesis and classification. *Blood,* 122**,** 3884-91.
OZDEK, A., SARAC, S., AKYOL, M. U., SUNGUR, A. & YILMAZ, T. 2004. c-myc and bcl-2 Expression in supraglottic squamous cell carcinoma of the larynx. *Otolaryngol Head Neck Surg,* 131**,** 77-83.

PAGE, D. M., WITTAMER, V., BERTRAND, J. Y., LEWIS, K. L., PRATT, D. N., DELGADO, N., SCHALE, S. E., MCGUE, C., JACOBSEN, B. H., DOTY, A., PAO, Y., YANG, H., CHI, N. C., MAGOR, B. G. & TRAVER, D. 2013. An evolutionarily conserved program of B-cell development and activation in zebrafish. *Blood,* 122**,** e1-11.

PAIK, E. J. & ZON, L. I. 2010. Hematopoietic development in the zebrafish. *Int J Dev Biol,* 54**,** 1127-37.

PALTRIDGE, J. L., BELLE, L. & KHEW-GOODALL, Y. 2013. The secretome in cancer progression. *Biochim Biophys Acta,* 1834**,** 2233-41.

PAN, B. T., TENG, K., WU, C., ADAM, M. & JOHNSTONE, R. M. 1985. Electron microscopic evidence for externalization of the transferrin receptor in vesicular form in sheep reticulocytes. *J Cell Biol,* 101**,** 942-8.

PAOLINO, M., CHOIDAS, A., WALLNER, S., PRANJIC, B., URIBESALGO, I., LOESER, S., JAMIESON, A. M., LANGDON, W. Y., IKEDA, F., FEDEDA, J. P., CRONIN, S. J., NITSCH, R., SCHULTZ-FADEMRECHT, C., EICKHOFF, J., MENNINGER, S., UNGER, A., TORKA, R., GRUBER, T., HINTERLEITNER, R., BAIER, G., WOLF, D., ULLRICH, A., KLEBL, B. M. & PENNINGER, J. M. 2014. The E3 ligase Cbl-b and TAM receptors regulate cancer metastasis via natural killer cells. *Nature,* 507**,** 508-+.

PAOLINO, M. & PENNINGER, J. M. 2016. The Role of TAM Family Receptors in Immune Cell Function: Implications for Cancer Therapy. *Cancers (Basel),* 8.

PAP, E., PALLINGER, E., PASZTOI, M. & FALUS, A. 2009. Highlights of a new type of intercellular communication: microvesicle-based information transfer. *Inflamm Res,* 58**,** 1-8.

PARAMESWARAN, N. & PATIAL, S. 2010. Tumor necrosis factor-alpha signaling in macrophages. *Crit Rev Eukaryot Gene Expr,* 20**,** 87-103.

PARK, D., TOSELLO-TRAMPONT, A. C., ELLIOTT, M. R., LU, M. J., HANEY, L. B., MA, Z., KLIBANOV, A. L., MANDELL, J. W. & RAVICHANDRAN, K. S. 2007. BAI1 is an engulfment receptor for apoptotic cells upstream of the ELMO/Dock180/Rac module. *Nature,* 450**,** 430-U10.

PARK, S. W., DAVISON, J. M., RHEE, J., HRUBAN, R. H., MAITRA, A. & LEACH, S. D. 2008a. Oncogenic KRAS induces progenitor cell expansion and malignant transformation in zebrafish exocrine pancreas. *Gastroenterology,* 134**,** 2080-2090.

PARK, S. Y., JUNG, M. Y., KIM, H. J., LEE, S. J., KIM, S. Y., LEE, B. H., KWON, T. H., PARK, R. W. & KIM, I. S. 2008b. Rapid cell corpse clearance by stabilin-2, a membrane phosphatidylserine receptor. *Cell Death Differ,* 15**,** 192-201.

PAROLINI, I., FEDERICI, C., RAGGI, C., LUGINI, L., PALLESCHI, S., DE MILITO, A., COSCIA, C., IESSI, E., LOGOZZI, M., MOLINARI, A., COLONE, M., TATTI, M., SARGIACOMO, M. & FAIS, S. 2009. Microenvironmental pH Is a Key Factor for Exosome Traffic in Tumor Cells. *Journal of Biological Chemistry,* 284**,** 34211-34222.

PATIENCE, L. 2016. *Apoptosis-Driven Microenvironmental Conditioning by Microvesicles in Non-Hodgkin Lymphoma.* PhD, The University of Edinburgh.

PATTON, E. E., WIDLUND, H. R., KUTOK, J. L., KOPANI, K. R., AMATRUDA, J. F., MURPHEY, R. D., BERGHMANS, S., MAYHALL, E. A., TRAVER, D., FLETCHER, C. D., ASTER, J. C., GRANTER, S. R., LOOK, A. T., LEE, C., FISHER, D. E. & ZON, L. I. 2005. BRAF mutations are sufficient to promote nevi formation and cooperate with p53 in the genesis of melanoma. *Curr Biol,* 15**,** 249-54.

PAVLYUKOV, M. S., YU, H., BASTOLA, S., MINATA, M., SHENDER, V. O., LEE, Y., ZHANG, S., WANG, J., KOMAROVA, S., WANG, J., YAMAGUCHI, S., ALSHEIKH, H. A., SHI, J., CHEN, D., MOHYELDIN, A., KIM, S. H., SHIN, Y. J., ANUFRIEVA, K., EVTUSHENKO, E. G., ANTIPOVA, N. V., ARAPIDI, G. P., GOVORUN, V., PESTOV, N. B., SHAKHPARONOV, M. I., LEE, L. J., NAM, D. H. & NAKANO, I. 2018. Apoptotic Cell-Derived Extracellular Vesicles Promote Malignancy of Glioblastoma Via Intercellular Transfer of Splicing Factors. *Cancer Cell,* 34**,** 119-135 e10.

PEINADO, H., ALECKOVIC, M., LAVOTSHKIN, S., MATEI, I., COSTA-SILVA, B., MORENO-BUENO, G., HERGUETA-REDONDO, M., WILLIAMS, C., GARCIA-SANTOS, G., GHAJAR, C. M., NITADORI-HOSHINO, A., HOFFMAN, C., BADAL, K., GARCIA, B. A., CALLAHAN, M. K., YUAN, J. D., MARTINS, V. R., SKOG, J., KAPLAN, R. N., BRADY, M. S., WOLCHOK, J. D., CHAPMAN, P. B., KANG, Y. B., BROMBERG, J. & LYDEN, D. 2012. Melanoma exosomes educate bone marrow progenitor cells toward a pro-metastatic phenotype through MET. *Nature Medicine,* 18**,** 883-+.

PELENGARIS, S., KHAN, M. & EVAN, G. 2002a. c-MYC: More than just a matter of life and death. *Nature Reviews Cancer,* 2**,** 764-776.

PELENGARIS, S., KHAN, M. & EVAN, G. I. 2002b. Suppression of Myc-induced apoptosis in beta cells exposes multiple oncogenic properties of Myc and triggers carcinogenic progression. *Cell,* 109**,** 321-34.

PETER, C., WAIBEL, M., RADU, C. G., YANG, L. V., WITTE, O. N., SCHULZE-OSTHOFF, K., WESSELBORG, S. & LAUBER, K. 2008. Migration to apoptotic "Find-me" signals is mediated via the phagocyte receptor G2A. *Journal of Biological Chemistry,* 283**,** 5296-5305.

PHELPS, R. A., CHIDESTER, S., DEHGHANIZADEH, S., PHELPS, J., SANDOVAL, I. T., RAI, K., BROADBENT, T., SARKAR, S., BURT, R. W. & JONES, D. A. 2009. A two-step model for colon adenoma initiation and progression caused by APC loss. *Cell,* 137**,** 623-34.

PRUVOT, B., JACQUEL, A., DROIN, N., AUBERGER, P., BOUSCARY, D., TAMBURINI, J., MULLER, M., FONTENAY, M., CHLUBA, J. & SOLARY, E. 2011. Leukemic cell xenograft in zebrafish embryo for investigating drug efficacy. *Haematologica,* 96**,** 612-6.

QIAN, B. Z. & POLLARD, J. W. 2010. Macrophage diversity enhances tumor progression and metastasis. *Cell,* 141**,** 39-51.

QIAN, B. Z., ZHANG, H., LI, J. F., HE, T. F., YEO, E. J., SOONG, D. Y. H., CARRAGHER, N. O., MUNRO, A., CHANG, A., BRESNICK, A. R.,

LANG, R. A. & POLLARD, J. W. 2015. FLT1 signaling in metastasis-associated macrophages activates an inflammatory signature that promotes breast cancer metastasis. *Journal of Experimental Medicine,* 212**,** 1433-1448.

RAK, J. 2013. Extracellular vesicles - biomarkers and effectors of the cellular interactome in cancer. *Front Pharmacol,* 4**,** 21.

RAKHRA, K., BACHIREDDY, P., ZABUAWALA, T., ZEISER, R., XU, L., KOPELMAN, A., FAN, A. C., YANG, Q., BRAUNSTEIN, L., CROSBY, E., RYEOM, S. & FELSHER, D. W. 2010. CD4(+) T cells contribute to the remodeling of the microenvironment required for sustained tumor regression upon oncogene inactivation. *Cancer Cell,* 18**,** 485-98.

RAPOSO, G., NIJMAN, H. W., STOORVOGEL, W., LIEJENDEKKER, R., HARDING, C. V., MELIEF, C. J. & GEUZE, H. J. 1996. B lymphocytes secrete antigen-presenting vesicles. *J Exp Med,* 183**,** 1161-72.

RAPOSO, G. & STOORVOGEL, W. 2013. Extracellular vesicles: Exosomes, microvesicles, and friends. *Journal of Cell Biology,* 200**,** 373-383.

REDDIEN, P. W., CAMERON, S. & HORVITZ, H. R. 2001. Phagocytosis promotes programmed cell death in C. elegans. *Nature,* 412**,** 198-202.

REDZIC, J. S., KENDRICK, A. A., BAHMED, K., DAHL, K. D., PEARSON, C. G., ROBINSON, W. A., ROBINSON, S. E., GRANER, M. W. & EISENMESSER, E. Z. 2013. Extracellular vesicles secreted from cancer cell lines stimulate secretion of MMP-9, IL-6, TGF-beta1 and EMMPRIN. *PLoS One,* 8**,** e71225.

RENSHAW, S. A. & INGHAM, P. W. 2010. Zebrafish models of the immune response: taking it on the ChIn. *BMC Biol,* 8**,** 148.

RIBATTI, D. & CRIVELLATO, E. 2009. Immune cells and angiogenesis. *J Cell Mol Med,* 13**,** 2822-33.

RIBATTI, D. & CRIVELLATO, E. 2012. Mast cells, angiogenesis, and tumour growth. *Biochim Biophys Acta,* 1822**,** 2-8.

RIEDL, S. J. & SHI, Y. 2004. Molecular mechanisms of caspase regulation during apoptosis. *Nat Rev Mol Cell Biol,* 5**,** 897-907.

ROBBIANI, D. F., BOTHMER, A., CALLEN, E., REINA-SAN-MARTIN, B., DORSETT, Y., DIFILIPPANTONIO, S., BOLLAND, D. J., CHEN, H. T., CORCORAN, A. E., NUSSENZWEIG, A. & NUSSENZWEIG, M. C. 2008. AID Is Required for the Chromosomal Breaks in c-myc that Lead to c-myc/IgH Translocations. *Cell,* 135**,** 1028-1038.

ROBBIANI, D. F., BUNTING, S., FELDHAHN, N., BOTHMER, A., CAMPS, J., DEROUBAIX, S., MCBRIDE, K. M., KLEIN, I. A., STONE, G., EISENREICH, T. R., RIED, T., NUSSENZWEIG, A. & NUSSENZWEIG, M. C. 2009. AID Produces DNA Double-Strand Breaks in Non-Ig Genes and Mature B Cell Lymphomas with Reciprocal Chromosome Translocations. *Molecular Cell,* 36**,** 631-641.

ROONEY, C. M., ROWE, M., WALLACE, L. E. & RICKINSON, A. B. 1985. Epstein-Barr virus-positive Burkitt's lymphoma cells not recognized by virus-specific T-cell surveillance. *Nature,* 317**,** 629-31.

ROSENWALD, A., WRIGHT, G., CHAN, W. C., CONNORS, J. M., CAMPO, E., FISHER, R. I., GASCOYNE, R. D., MULLER-HERMELINK, H. K., SMELAND, E. B., STAUDT, L. M. & PR, L. L. M. P. 2002. The use of

molecular profiling to predict survival after chemotherapy for diffuse large-B-cell lymphoma. *New England Journal of Medicine,* 346**,** 1937-1947.

ROTHLIN, C. V., CARRERA-SILVA, E. A., BOSURGI, L. & GHOSH, S. 2015. TAM receptor signaling in immune homeostasis. *Annu Rev Immunol,* 33**,** 355-91.

ROTHLIN, C. V., GHOSH, S., ZUNIGA, E. I., OLDSTONE, M. B. A. & LEMKE, G. 2007. TAM receptors are pleiotropic inhibitors of the innate immune response. *Cell,* 131**,** 1124-1136.

ROUSSEL, M. F., CLEVELAND, J. L., SHURTLEFF, S. A. & SHERR, C. J. 1991. Myc rescue of a mutant CSF-1 receptor impaired in mitogenic signalling. *Nature,* 353**,** 361-3.

ROWLEY, R. B., BURKHARDT, A. L., CHAO, H. G., MATSUEDA, G. R. & BOLEN, J. B. 1995. Syk Protein-Tyrosine Kinase Is Regulated by Tyrosine-Phosphorylated Ig-Alpha Ig-Beta Immunoreceptor Tyrosine Activation Motif Binding and Autophosphorylation. *Journal of Biological Chemistry,* 270**,** 11590-11594.

RUFFELL, B. & COUSSENS, L. M. 2015. Macrophages and therapeutic resistance in cancer. *Cancer Cell,* 27**,** 462-72.

RUSSELL, J. H. & LEY, T. J. 2002. Lymphocyte-mediated cytotoxicity. *Annu Rev Immunol,* 20**,** 323-70.

SABAAWY, H. E., AZUMA, M., EMBREE, L. J., TSAI, H. J., STAROST, M. F. & HICKSTEIN, D. D. 2006. TEL-AML1 transgenic zebrafish model of precursor B cell acute lymphoblastic leukemia. *Proc Natl Acad Sci U S A,* 103**,** 15166-71.

SACCO, A., ROCCARO, A. M., MA, D., SHI, J., MISHIMA, Y., MOSCHETTA, M., CHIARINI, M., MUNSHI, N., HANDIN, R. I. & GHOBRIAL, I. M. 2016. Cancer Cell Dissemination and Homing to the Bone Marrow in a Zebrafish Model. *Cancer Res,* 76**,** 463-71.

SAKAHIRA, H., ENARI, M. & NAGATA, S. 1998. Cleavage of CAD inhibitor in CAD activation and DNA degradation during apoptosis. *Nature,* 391**,** 96-9.

SAKAHIRA, H., ENARI, M. & NAGATA, S. 2015. Corrigendum: Cleavage of CAD inhibitor in CAD activation and DNA degradation during apoptosis. *Nature,* 526**,** 728.

SAMUEL, P., FABBRI, M. & CARTER, D. R. F. 2017. Mechanisms of Drug Resistance in Cancer: The Role of Extracellular Vesicles. *Proteomics*.

SANDER, S., CALADO, D. P., SRINIVASAN, L., KOCHERT, K., ZHANG, B. C., ROSOLOWSKI, M., RODIG, S. J., HOLZMANN, K., STILGENBAUER, S., SIEBERT, R., BULLINGER, L. & RAJEWSKY, K. 2012. Synergy between PI3K Signaling and MYC in Burkitt Lymphomagenesis. *Cancer Cell,* 22**,** 167-179.

SANTHAKUMAR, K., JUDSON, E. C., ELKS, P. M., MCKEE, S., ELWORTHY, S., VAN ROOIJEN, E., WALMSLEY, S. S., RENSHAW, S. A., CROSS, S. S. & VAN EEDEN, F. J. 2012. A zebrafish model to study and therapeutically manipulate hypoxia signaling in tumorigenesis. *Cancer Res,* 72**,** 4017-27.

SAVILL, J., DRANSFIELD, I., GREGORY, C. & HASLETT, C. 2002. A blast from the past: clearance of apoptotic cells regulates immune responses. *Nat Rev Immunol,* 2**,** 965-75.
SCHARTL, M. 2014. Beyond the zebrafish: diverse fish species for modeling human disease. *Dis Model Mech,* 7**,** 181-92.
SCHLEGEL, R. A., KRAHLING, S., CALLAHAN, M. K. & WILLIAMSON, P. 1999. CD14 is a component of multiple recognition systems used by macrophages to phagocytose apoptotic lymphocytes. *Cell Death and Differentiation,* 6**,** 583-592.
SCHMIDT, E. V. 2004. The role of c-myc in regulation of translation initiation. *Oncogene,* 23**,** 3217-21.
SCHRIJVERS, D. M., DE MEYER, G. R., KOCKX, M. M., HERMAN, A. G. & MARTINET, W. 2005. Phagocytosis of apoptotic cells by macrophages is impaired in atherosclerosis. *Arterioscler Thromb Vasc Biol,* 25**,** 1256-61.
SCHUERMANN, A., HELKER, C. S. & HERZOG, W. 2014. Angiogenesis in zebrafish. *Semin Cell Dev Biol,* 31**,** 106-14.
SHAFFER, A. L., 3RD, YOUNG, R. M. & STAUDT, L. M. 2012. Pathogenesis of human B cell lymphomas. *Annu Rev Immunol,* 30**,** 565-610.
SHAFFER, A. L., ROSENWALD, A. & STAUDT, L. M. 2002. Lymphoid malignancies: The dark side of B-cell differentiation. *Nature Reviews Immunology,* 2**,** 920-932.
SHAO, H., IM, H., CASTRO, C. M., BREAKEFIELD, X., WEISSLEDER, R. & LEE, H. 2018. New Technologies for Analysis of Extracellular Vesicles. *Chem Rev,* 118**,** 1917-1950.
SHELDON, H., HEIKAMP, E., TURLEY, H., DRAGOVIC, R., THOMAS, P., OON, C. E., LEEK, R., EDELMANN, M., KESSLER, B., SAINSON, R. C. A., SARGENT, I., LI, J. L. & HARRIS, A. L. 2010. New mechanism for Notch signaling to endothelium at a distance by Delta-like 4 incorporation into exosomes. *Blood,* 116**,** 2385-2394.
SHEN, L. J., CHEN, F. Y., ZHANG, Y., CAO, L. F., KUANG, Y., ZHONG, M., WANG, T. & ZHONG, H. 2013. MYCN Transgenic Zebrafish Model with the Characterization of Acute Myeloid Leukemia and Altered Hematopoiesis. *Plos One,* 8.
SHEPARD, J. L., AMATRUDA, J. F., STERN, H. M., SUBRAMANIAN, A., FINKELSTEIN, D., ZIAI, J., FINLEY, K. R., PFAFF, K. L., HERSEY, C., ZHOU, Y., BARUT, B., FREEDMAN, M., LEE, C., SPITSBERGEN, J., NEUBERG, D., WEBER, G., GOLUB, T. R., GLICKMAN, J. N., KUTOK, J. L., ASTER, J. C. & ZON, L. I. 2005. A zebrafish bmyb mutation causes genome instability and increased cancer susceptibility. *Proc Natl Acad Sci U S A,* 102**,** 13194-9.
SHERR, C. J. 2004. Principles of tumor suppression. *Cell,* 116**,** 235-46.
SHI, X. & SHIAO, S. L. 2018. The role of macrophage phenotype in regulating the response to radiation therapy. *Transl Res,* 191**,** 64-80.
SHI, Y., GLYNN, J. M., GUILBERT, L. J., COTTER, T. G., BISSONNETTE, R. P. & GREEN, D. R. 1992. Role for c-myc in activation-induced apoptotic cell death in T cell hybridomas. *Science,* 257**,** 212-4.

SHIN, J., PADMANABHAN, A., DE GROH, E. D., LEE, J. S., HAIDAR, S., DAHLBERG, S., GUO, F., HE, S. N., WOLMAN, M. A., GRANATO, M., LAWSON, N. D., WOLFE, S. A., KIM, S. H., SOLNICA-KREZEL, L., KANKI, J. P., LIGON, K. L., EPSTEIN, J. A. & LOOK, A. T. 2012. Zebrafish neurofibromatosis type 1 genes have redundant functions in tumorigenesis and embryonic development. *Disease Models & Mechanisms,* 5**,** 881-894.

SHINOHARA, H., KURANAGA, Y., KUMAZAKI, M., SUGITO, N., YOSHIKAWA, Y., TAKAI, T., TANIGUCHI, K., ITO, Y. & AKAO, Y. 2017. Regulated Polarization of Tumor-Associated Macrophages by miR-145 via Colorectal Cancer-Derived Extracellular Vesicles. *J Immunol,* 199**,** 1505-1515.

SICA, A., LARGHI, P., MANCINO, A., RUBINO, L., PORTA, C., TOTARO, M. G., RIMOLDI, M., BISWAS, S. K., ALLAVENA, P. & MANTOVANI, A. 2008. Macrophage polarization in tumour progression. *Semin Cancer Biol,* 18**,** 349-55.

SICA, A. & MANTOVANI, A. 2012. Macrophage plasticity and polarization: in vivo veritas. *J Clin Invest,* 122**,** 787-95.

SKOG, J., WURDINGER, T., VAN RIJN, S., MEIJER, D. H., GAINCHE, L., SENA-ESTEVES, M., CURRY, W. T., CARTER, B. S., KRICHEVSKY, A. M. & BREAKEFIELD, X. O. 2008. Glioblastoma microvesicles transport RNA and proteins that promote tumour growth and provide diagnostic biomarkers. *Nature Cell Biology,* 10**,** 1470-U209.

SOEKMADJI, C., CORCORAN, N. M., OLEINIKOVA, I., JOVANOVIC, L., AUSTRALIAN PROSTATE CANCER COLLABORATION, B., RAMM, G. A., NELSON, C. C., JENSTER, G. & RUSSELL, P. J. 2017a. Extracellular vesicles for personalized therapy decision support in advanced metastatic cancers and its potential impact for prostate cancer. *Prostate,* 77**,** 1416-1423.

SOEKMADJI, C., RICHES, J. D., RUSSELL, P. J., RUELCKE, J. E., MCPHERSON, S., WANG, C., HOVENS, C. M., CORCORAN, N. M., AUSTRALIAN PROSTATE CANCER COLLABORATION, B., HILL, M. M. & NELSON, C. C. 2017b. Modulation of paracrine signaling by CD9 positive small extracellular vesicles mediates cellular growth of androgen deprived prostate cancer. *Oncotarget,* 8**,** 52237-52255.

SONG, Y., YU, X., ZANG, Z. & ZHAO, G. 2017. Circulating or tissue microRNAs and extracellular vesicles as potential lung cancer biomarkers: a systematic review. *Int J Biol Markers***,** 0.

SOUCEK, L., LAWLOR, E. R., SOTO, D., SHCHORS, K., SWIGART, L. B. & EVAN, G. I. 2007. Mast cells are required for angiogenesis and macroscopic expansion of Myc-induced pancreatic islet tumors. *Nature Medicine,* 13**,** 1211-1218.

SOUCIE, E. L., ANNIS, M. G., SEDIVY, J., FILMUS, J., LEBER, B., ANDREWS, D. W. & PENN, L. Z. 2001. Myc potentiates apoptosis by stimulating Bax activity at the mitochondria. *Molecular and Cellular Biology,* 21**,** 4725-4736.

STALLER, P., PEUKERT, K., KIERMAIER, A., SEOANE, J., LUKAS, J., KARSUNKY, H., MOROY, T., BARTEK, J., MASSAGUE, J., HANEL,

F. & EILERS, M. 2001. Repression of p15(INK4b) expression by Myc through association with Miz-1. *Nature Cell Biology,* 3**,** 392-399.
STEFAN, E. & BISTER, K. 2017. MYC and RAF: Key Effectors in Cellular Signaling and Major Drivers in Human Cancer. *Curr Top Microbiol Immunol,* 407**,** 117-151.
STERN, H. M. & ZON, L. I. 2003. Cancer genetics and drug discovery in the zebrafish. *Nat Rev Cancer,* 3**,** 533-9.
STEVENSON, F. K., SAHOTA, S. S., OTTENSMEIER, C. H., ZHU, D., FORCONI, F. & HAMBLIN, T. J. 2001. The occurrence and significance of V gene mutations in B cell-derived human malignancy. *Adv Cancer Res,* 83**,** 81-116.
STITT, T. N., CONN, G., GORE, M., LAI, C., BRUNO, J., RADZIEJEWSKI, C., MATTSSON, K., FISHER, J., GIES, D. R., JONES, P. F., MASIAKOWSKI, P., RYAN, T. E., TOBKES, N. J., CHEN, D. H., DISTEFANO, P. S., LONG, G. L., BASILICO, C., GOLDFARB, M. P., LEMKE, G., GLASS, D. J. & YANCOPOULOS, G. D. 1995. The Anticoagulation Factor Protein-S and Its Relative, Gas6, Are Ligands for the Tyro 3/Axl Family of Receptor Tyrosine Kinases. *Cell,* 80**,** 661-670.
STORER, N. Y. & ZON, L. I. 2010. Zebrafish models of p53 functions. *Cold Spring Harb Perspect Biol,* 2**,** a001123.
STRASSER, A., HARRIS, A. W., BATH, M. L. & CORY, S. 1990. Novel Primitive Lymphoid Tumors Induced in Transgenic Mice by Cooperation between Myc and Bcl-2. *Nature,* 348**,** 331-333.
SUNDERKOTTER, C., GOEBELER, M., SCHULZE-OSTHOFF, K., BHARDWAJ, R. & SORG, C. 1991. Macrophage-derived angiogenesis factors. *Pharmacol Ther,* 51**,** 195-216.
SUSTER, M. L., KIKUTA, H., URASAKI, A., ASAKAWA, K. & KAWAKAMI, K. 2009. Transgenesis in zebrafish with the tol2 transposon system. *Methods Mol Biol,* 561**,** 41-63.
SWERDLOW, S. H., CAMPO, E., PILERI, S. A., HARRIS, N. L., STEIN, H., SIEBERT, R., ADVANI, R., GHIELMINI, M., SALLES, G. A., ZELENETZ, A. D. & JAFFE, E. S. 2016. The 2016 revision of the World Health Organization classification of lymphoid neoplasms. *Blood,* 127**,** 2375-90.
TAGO, K., FUNAKOSHI-TAGO, M., ITOH, H., FURUKAWA, Y., KIKUCHI, J., KATO, T., SUZUKI, K. & YANAGISAWA, K. 2015. Arf tumor suppressor disrupts the oncogenic positive feedback loop including c-Myc and DDX5. *Oncogene,* 34**,** 314-22.
TANAKA, H., MATSUMURA, I., EZOE, S., SATOH, Y., SAKAMAKI, T., ALBANESE, C., MACHII, T., PESTELL, R. G. & KANAKURA, Y. 2002. E2F1 and c-Myc potentiate apoptosis through inhibition of NF-kappa B activity that facilitates MnSOD-mediated ROS elimination. *Molecular Cell,* 9**,** 1017-1029.
TARTAGLIA, L. A., PENNICA, D. & GOEDDEL, D. V. 1993. Ligand passing: the 75-kDa tumor necrosis factor (TNF) receptor recruits TNF for signaling by the 55-kDa TNF receptor. *J Biol Chem,* 268**,** 18542-8.

TAYLOR, D. D. & GERCEL-TAYLOR, C. 2011. Exosomes/microvesicles: mediators of cancer-associated immunosuppressive microenvironments. *Semin Immunopathol,* 33**,** 441-54.

TAYLOR, R. C., CULLEN, S. P. & MARTIN, S. J. 2008. Apoptosis: controlled demolition at the cellular level. *Nature Reviews Molecular Cell Biology,* 9**,** 231-241.

TAZZYMAN, S., LEWIS, C. E. & MURDOCH, C. 2009. Neutrophils: key mediators of tumour angiogenesis. *Int J Exp Pathol,* 90**,** 222-31.

TENG, Y., XIE, X. Y., WALKER, S., WHITE, D. T., MUMM, J. S. & COWELL, J. K. 2013. Evaluating human cancer cell metastasis in zebrafish. *Bmc Cancer,* 13.

TENNANT, I., POUND, J. D., MARR, L. A., WILLEMS, J. J., PETROVA, S., FORD, C. A., PATERSON, M., DEVITT, A. & GREGORY, C. D. 2013. Innate recognition of apoptotic cells: novel apoptotic cell-associated molecular patterns revealed by crossreactivity of anti-LPS antibodies. *Cell Death Differ,* 20**,** 698-708.

THOMPSON, C. A., PURUSHOTHAMAN, A., RAMANI, V. C., VLODAVSKY, I. & SANDERSON, R. D. 2013. Heparanase regulates secretion, composition, and function of tumor cell-derived exosomes. *J Biol Chem,* 288**,** 10093-9.

TOBIA, C., DE SENA, G. & PRESTA, M. 2011. Zebrafish embryo, a tool to study tumor angiogenesis. *Int J Dev Biol,* 55**,** 505-9.

TODOROVA, D., SIMONCINI, S., LACROIX, R., SABATIER, F. & DIGNAT-GEORGE, F. 2017. Extracellular Vesicles in Angiogenesis. *Circ Res,* 120**,** 1658-1673.

TORRACA, V., MASUD, S., SPAINK, H. P. & MEIJER, A. H. 2014. Macrophage-pathogen interactions in infectious diseases: new therapeutic insights from the zebrafish host model. *Dis Model Mech,* 7**,** 785-97.

TRAPANI, J. A. & SMYTH, M. J. 2002. Functional significance of the perforin/granzyme cell death pathway. *Nat Rev Immunol,* 2**,** 735-47.

TRAVER, D. 2004. Cellular dissection of zebrafish hematopoiesis. *Methods Cell Biol,* 76**,** 127-49.

TRAVER, D., HERBOMEL, P., PATTON, E. E., MURPHEY, R. D., YODER, J. A., LITMAN, G. W., CATIC, A., AMEMIYA, C. T., ZON, L. I. & TREDE, N. S. 2003. The zebrafish as a model organism to study development of the immune system. *Adv Immunol,* 81**,** 253-330.

TREDE, N. S., LANGENAU, D. M., TRAVER, D., LOOK, A. T. & ZON, L. I. 2004. The use of zebrafish to understand immunity. *Immunity,* 20**,** 367-379.

TRICARICO, C., CLANCY, J. & D'SOUZA-SCHOREY, C. 2017. Biology and biogenesis of shed microvesicles. *Small GTPases,* 8**,** 220-232.

TRUMAN, L. A., FORD, C. A., PASIKOWSKA, M., POUND, J. D., WILKINSON, S. J., DUMITRIU, I. E., MELVILLE, L., MELROSE, L. A., OGDEN, C. A., NIBBS, R., GRAHAM, G., COMBADIERE, C. & GREGORY, C. D. 2008. CX3CL1/fractalkine is released from apoptotic lymphocytes to stimulate macrophage chemotaxis. *Blood,* 112**,** 5026-5036.

TRUMPP, A., REFAELI, Y., OSKARSSON, T., GASSER, S., MURPHY, M., MARTIN, G. R. & BISHOP, J. M. 2001. c-Myc regulates mammalian body size by controlling cell number but not cell size. *Nature,* 414**,** 768-73.

TSUJIMOTO, Y., IKEGAKI, N. & CROCE, C. M. 1987. Characterization of the Protein Product of Bcl-2, the Gene Involved in Human Follicular Lymphoma. *Oncogene,* 2**,** 3-7.

TSUTSUI, S., YASUDA, K., SUZUKI, K., TAHARA, K., HIGASHI, H. & ERA, S. 2005. Macrophage infiltration and its prognostic implications in breast cancer: the relationship with VEGF expression and microvessel density. *Oncol Rep,* 14**,** 425-31.

UCKER, D. S. & LEVINE, J. S. 2018. Exploitation of Apoptotic Regulation in Cancer. *Front Immunol,* 9**,** 241.

UMEZU, T., TADOKORO, H., AZUMA, K., YOSHIZAWA, S., OHYASHIKI, K. & OHYASHIKI, J. H. 2014. Exosomal miR-135b shed from hypoxic multiple myeloma cells enhances angiogenesis by targeting factor-inhibiting HIF-1. *Blood,* 124**,** 3748-3757.

URIBESALGO, I., BENITAH, S. A. & DI CROCE, L. 2012. From oncogene to tumor suppressor: the dual role of Myc in leukemia. *Cell Cycle,* 11**,** 1757-64.

VADER, P., BREAKEFIELD, X. O. & WOOD, M. J. 2014. Extracellular vesicles: emerging targets for cancer therapy. *Trends Mol Med,* 20**,** 385-93.

VAFA, O., WADE, M., KERN, S., BEECHE, M., PANDITA, T. K., HAMPTON, G. M. & WAHL, G. M. 2002. c-Myc can induce DNA damage, increase reactive oxygen species, and mitigate p53 function: A mechanism for oncogene-induced genetic instability. *Molecular Cell,* 9**,** 1031-1044.

VAN DER ENT, W., BURRELLO, C., TEUNISSE, A. F., KSANDER, B. R., VAN DER VELDEN, P. A., JAGER, M. J., JOCHEMSEN, A. G. & SNAAR-JAGALSKA, B. E. 2014. Modeling of human uveal melanoma in zebrafish xenograft embryos. *Invest Ophthalmol Vis Sci,* 55**,** 6612-22.

VAN NIEL, G., D'ANGELO, G. & RAPOSO, G. 2018. Shedding light on the cell biology of extracellular vesicles. *Nat Rev Mol Cell Biol,* 19**,** 213-228.

VEINOTTE, C. J., DELLAIRE, G. & BERMAN, J. N. 2014. Hooking the big one: the potential of zebrafish xenotransplantation to reform cancer drug screening in the genomic era. *Dis Model Mech,* 7**,** 745-54.

VITA, M. & HENRIKSSON, M. 2006. The Myc oncoprotein as a therapeutic target for human cancer. *Seminars in Cancer Biology,* 16**,** 318-330.

VOCKERODT, M., TESCH, H. & KUBE, D. 2001. Epstein-Barr virus latent membrane protein-1 activates CD25 expression in lymphoma cells involving the NFkappaB pathway. *Genes Immun,* 2**,** 433-41.

VOLL, R. E., HERRMANN, M., ROTH, E. A., STACH, C., KALDEN, J. R. & GIRKONTAITE, I. 1997. Immunosuppressive effects of apoptotic cells. *Nature,* 390**,** 350-1.

WAJANT, H. 2002. The Fas signaling pathway: More than a paradigm. *Science,* 296**,** 1635-1636.

WALTON, E. M., CRONAN, M. R., BEERMAN, R. W. & TOBIN, D. M. 2015. The Macrophage-Specific Promoter mfap4 Allows Live, Long-Term Analysis of Macrophage Behavior during Mycobacterial Infection in Zebrafish. *PLoS One,* 10**,** e0138949.

WANG, J., CAO, Z., ZHANG, X. M., NAKAMURA, M., SUN, M., HARTMAN, J., HARRIS, R. A., SUN, Y. & CAO, Y. 2015. Novel mechanism of macrophage-mediated metastasis revealed in a zebrafish model of tumor development. *Cancer Res,* 75**,** 306-15.

WANG, T., GILKES, D. M., TAKANO, N., XIANG, L. S., LUO, W. B., BISHOP, C. J., CHATURVEDI, P., GREEN, J. J. & SEMENZA, G. L. 2014. Hypoxia-inducible factors and RAB22A mediate formation of microvesicles that stimulate breast cancer invasion and metastasis. *Proceedings of the National Academy of Sciences of the United States of America,* 111**,** E3234-E3242.

WANG, Y., KAISER, M. S., LARSON, J. D., NASEVICIUS, A., CLARK, K. J., WADMAN, S. A., ROBERG-PEREZ, S. E., EKKER, S. C., HACKETT, P. B., MCGRAIL, M. & ESSNER, J. J. 2010. Moesin1 and Ve-cadherin are required in endothelial cells during in vivo tubulogenesis. *Development,* 137**,** 3119-28.

WATNICK, R. S. 2012. The role of the tumor microenvironment in regulating angiogenesis. *Cold Spring Harb Perspect Med,* 2**,** a006676.

WATNICK, R. S., CHENG, Y. N., RANGARAJAN, A., INCE, T. A. & WEINBERG, R. A. 2013. Ras Modulates Myc Activity to Repress Thrombospondin-1 Expression and Increase Tumor Angiogenesis (vol 3, pg 219, 2003). *Cancer Cell,* 23**,** 129-129.

WELTON, J. L., KHANNA, S., GILES, P. J., BRENNAN, P., BREWIS, I. A., STAFFURTH, J., MASON, M. D. & CLAYTON, A. 2010. Proteomics Analysis of Bladder Cancer Exosomes. *Molecular & Cellular Proteomics,* 9**,** 1324-1338.

WERTMAN, J., VEINOTTE, C. J., DELLAIRE, G. & BERMAN, J. N. 2016. The Zebrafish Xenograft Platform: Evolution of a Novel Cancer Model and Preclinical Screening Tool. *Adv Exp Med Biol,* 916**,** 289-314.

WESTERFIELD, M. 1995a. The zebrafish book. *Univ of Oregon Press, Eugene, OR*.

WESTERFIELD, M. 1995b. The Zebrafish Book. A Guide for the Laboratory Use of Zebrafish (Danio rerio), 3rd Edition.

WHITESIDE, T. L. 2005. Tumour-derived exosomes or microvesicles: another mechanism of tumour escape from the host immune system? *British Journal of Cancer,* 92**,** 209-211.

WHITMAN, S. P., KOHLSCHMIDT, J., MAHARRY, K., VOLINIA, S., MROZEK, K., NICOLET, D., SCHWIND, S., BECKER, H., METZELER, K. H., MENDLER, J. H., EISFELD, A. K., CARROLL, A. J., POWELL, B. L., CARTER, T. H., BAER, M. R., KOLITZ, J. E., PARK, I. K., STONE, R. M., CALIGIURI, M. A., MARCUCCI, G. & BLOOMFIELD, C. D. 2014. GAS6 expression identifies high-risk adult AML patients: potential implications for therapy. *Leukemia,* 28**,** 1252-1258.

WILLIAMS, C., RODRIGUEZ-BARRUECO, R., SILVA, J. M., ZHANG, W. J., HEARN, S., ELEMENTO, O., PAKNEJAD, N., MANOVA-TODOROVA, K., WELTE, K., BROMBERG, J., PEINADO, H. & LYDEN, D. 2014. Double-stranded DNA in exosomes: a novel biomarker in cancer detection. *Cell Research,* 24**,** 766-769.

WILLIAMS, C. B., YEH, E. S. & SOLOFF, A. C. 2016. Tumor-associated macrophages: unwitting accomplices in breast cancer malignancy. *NPJ Breast Cancer,* 2.

WILLMS, E., JOHANSSON, H. J., MAGER, I., LEE, Y., BLOMBERG, K. E., SADIK, M., ALAARG, A., SMITH, C. I., LEHTIO, J., EL ANDALOUSSI, S., WOOD, M. J. & VADER, P. 2016. Cells release subpopulations of exosomes with distinct molecular and biological properties. *Sci Rep,* 6**,** 22519.

WOOD, W., TURMAINE, M., WEBER, R., CAMP, V., MAKI, R. A., MCKERCHER, S. R. & MARTIN, P. 2000. Mesenchymal cells engulf and clear apoptotic footplate cells in macrophageless PU.1 null mouse embryos. *Development,* 127**,** 5245-52.

WRIGHT, D. H. 1963. Cytology and histochemistry of the Burkitt lymphoma. *Br J Cancer,* 17**,** 50-5.

WYNN, T. A., CHAWLA, A. & POLLARD, J. W. 2013. Macrophage biology in development, homeostasis and disease. *Nature,* 496**,** 445-55.

YANCOPOULOS, G. D., DAVIS, S., GALE, N. W., RUDGE, J. S., WIEGAND, S. J. & HOLASH, J. 2000. Vascular-specific growth factors and blood vessel formation. *Nature,* 407**,** 242-8.

YANG, H. W., KUTOK, J. L., LEE, N. H., PIAO, H. Y., FLETCHER, C. D., KANKI, J. P. & LOOK, A. T. 2004. Targeted expression of human MYCN selectively causes pancreatic neuroendocrine tumors in transgenic zebrafish. *Cancer Res,* 64**,** 7256-62.

YEN, J., WHITE, R. M. & STEMPLE, D. L. 2014. Zebrafish models of cancer: progress and future challenges. *Curr Opin Genet Dev,* 24**,** 38-45.

YOKOI, A., YOSHIOKA, Y., YAMAMOTO, Y., ISHIKAWA, M., IKEDA, S. I., KATO, T., KIYONO, T., TAKESHITA, F., KAJIYAMA, H., KIKKAWA, F. & OCHIYA, T. 2017. Malignant extracellular vesicles carrying MMP1 mRNA facilitate peritoneal dissemination in ovarian cancer. *Nat Commun,* 8**,** 14470.

YONEMURA, Y., ENDO, Y., TABATA, K., KAWAMURA, T., YUN, H. Y., BANDOU, E., SASAKI, T. & MIURA, M. 2005. Role of VEGF-C and VEGF-D in lymphangiogenesis in gastric cancer. *Int J Clin Oncol,* 10**,** 318-27.

YOULE, R. J. & STRASSER, A. 2008. The BCL-2 protein family: opposing activities that mediate cell death. *Nature Reviews Molecular Cell Biology,* 9**,** 47-59.

YOUNG, L. S. & RICKINSON, A. B. 2004. Epstein-Barr virus: 40 years on. *Nat Rev Cancer,* 4**,** 757-68.

YOUNG, R. M., HARDY, I. R., CLARKE, R. L., LUNDY, N., PINE, P., TURNER, B. C., POTTER, T. A. & REFAELI, Y. 2009. Mouse models of non-Hodgkin lymphoma reveal Syk as an important therapeutic target. *Blood,* 113**,** 2508-2516.

YU, X., HARRIS, S. L. & LEVINE, A. J. 2006. The regulation of exosome secretion: a novel function of the p53 protein. *Cancer Research,* 66**,** 4795-4801.

ZERVANTONAKIS, I. K., HUGHES-ALFORD, S. K., CHAREST, J. L., CONDEELIS, J. S., GERTLER, F. B. & KAMM, R. D. 2012. Three-dimensional microfluidic model for tumor cell intravasation and endothelial barrier function. *Proc Natl Acad Sci U S A,* 109**,** 13515-20.

ZHANG, Y., GOSTISSA, M., HILDEBRAND, D. G., BECKER, M. S., BOBOILA, C., CHIARLE, R., LEWIS, S. & ALT, F. W. 2010. The Role of Mechanistic Factors in Promoting Chromosomal Translocations Found in Lymphoid and Other Cancers. *Advances in Immunology, Vol 106,* 106**,** 93-133.

ZHAO, C., WANG, X., ZHAO, Y., LI, Z., LIN, S., WEI, Y. & YANG, H. 2011. A novel xenograft model in zebrafish for high-resolution investigating dynamics of neovascularization in tumors. *PLoS One,* 6**,** e21768.

ZHAO, C. J., ZHANG, W., ZHAO, Y. W., YANG, Y., LUO, H., JI, G. L., DONG, E., DENG, H. X., LIN, S., WEI, Y. Q. & YANG, H. S. 2016. Endothelial Cords Promote Tumor Initial Growth prior to Vascular Function through a Paracrine Mechanism. *Scientific Reports,* 6.

ZHAO, S., HUANG, J. & YE, J. 2015. A fresh look at zebrafish from the perspective of cancer research. *Journal of Experimental & Clinical Cancer Research,* 34.

ZHENG, Y., LIU, L., CHEN, C., MING, P., HUANG, Q., LI, C., CAO, D., XU, X. & GE, W. 2017. The extracellular vesicles secreted by lung cancer cells in radiation therapy promote endothelial cell angiogenesis by transferring miR-23a. *PeerJ,* 5**,** e3627.

ZHUANG, G., WU, X., JIANG, Z., KASMAN, I., YAO, J., GUAN, Y., OEH, J., MODRUSAN, Z., BAIS, C., SAMPATH, D. & FERRARA, N. 2012. Tumour-secreted miR-9 promotes endothelial cell migration and angiogenesis by activating the JAK-STAT pathway. *EMBO J,* 31**,** 3513-23.

ZIMMERMAN, K. & ALT, F. W. 1990. Expression and function of myc family genes. *Crit Rev Oncog,* 2**,** 75-95.

ZITVOGEL, L., REGNAULT, A., LOZIER, A., WOLFERS, J., FLAMENT, C., TENZA, D., RICCIARDI-CASTAGNOLI, P., RAPOSO, G. & AMIGORENA, S. 1998. Eradication of established murine tumors using a novel cell-free vaccine: dendritic cell-derived exosomes. *Nature Medicine,* 4**,** 594-600.

ZOMER, A., VENDRIG, T., HOPMANS, E. S., VAN EIJNDHOVEN, M., MIDDELDORP, J. M. & PEGTEL, D. M. 2010. Exosomes: Fit to deliver small RNA. *Commun Integr Biol,* 3**,** 447-50.